

**A morphometric study of skeletal and soft tissue components of
the glenohumeral joint associated with shoulder pathologies**

Milinda Catharina Vivian Krüger

Student nr : 84311089

A thesis submitted to the Department of Anatomy, School of Medicine, Faculty of Health
Sciences, University of Pretoria in fulfilment of the requirements for the degree

Of

MSc in Anatomy

Pretoria, 2018

Supervisor: Dr N Keough

Declaration

I, Milinda Catharina Vivian Krüger, declare that this thesis is my own work. It is being submitted for the degree of MSc in Anatomy at the University of Pretoria. It has not been submitted before for any other degree or examination at this or any other University.

Sign: _____

This _____ day of _____, 2018

Table of Contents

Declaration	i
Table of Contents	ii
List of Abbreviations	v
List of Figures	vi
List of Tables	viii
Acknowledgements	xi
Abstract	xii
Chapter 1: Introduction	1
Chapter 2: Literature Review	3
2.1. Anatomy of the glenohumeral joint (GHJ)	3
2.1.1. Skeletal tissue components	4
2.1.2. Soft tissue components	6
2.2. Biomechanics of the glenohumeral joint (GHJ).....	10
2.3. Glenohumeral joint (GHJ) pathologies.....	12
2.3.1. Chronic instability (dislocation).....	12
2.3.2. Osteoarthritis (OA) and osteoporosis (degenerative disease)	14
2.3.3. RC pathology (tears and degeneration).....	15
2.3.4. Frozen shoulder/Impingement syndrome/Adhesive capsulitis.....	16
2.3.5. Tendinopathy (Calcific tendinitis and calcific tendinosis).....	17
Chapter 3: Methods and Materials	19
3.1. Sample	19
<i>Cadaver sample</i>	19
<i>X-ray imaging sample</i>	20
<i>MRI imaging sample</i>	20
3.2. Methods	21
<i>Cadaver sample procedures and measurements</i>	21

<i>X-ray imaging procedure and measurements</i>	25
<i>MRI imaging procedure and measurements</i>	27
3.4. Statistical Analysis	30
3.4.1. Intra-and Interobserver error (repeatability tests)	31
Chapter 4: Results	32
4.1. Cadaver component	32
4.1.1. Normality tests	32
4.1.2. Descriptive statistics	33
<i>Acromial type</i>	33
<i>Morphometric variables</i>	33
4.1.3. Comparative statistics	34
<i>Acromial type: Contingency tables</i>	35
<i>Morphometric variables</i>	36
4.2. X-ray imaging component	38
4.2.1. Normality tests	38
4.2.2. Descriptive statistics	40
<i>Acromial type</i>	40
<i>Morphometric variables</i>	41
4.2.3. Comparative statistics	44
<i>Acromial type: Contingency tables</i>	44
<i>Morphometric variables</i>	45
4.3. MRI imaging component	48
4.3.1. Normality tests	48
4.3.2. Descriptive statistics	50
<i>Acromial type</i>	50
<i>Morphometric variables</i>	50
4.3.3. Comparative statistics	52
<i>Morphometric variables</i>	53

4.4. Intra- and Interobserver error (repeatability tests)	56
Chapter 5: Discussion	60
5.1. Acromial type (AT)	61
<i>Cadaveric component: incidence of AT</i>	61
<i>Cadaveric component: measurements relating to different AT</i>	62
<i>Imaging component: AT incidence in the X-ray and MRI sample</i>	64
5.2. Morphometric variables	66
5.3. Limitations of study	76
Chapter 6: Conclusion and Recommendations	77
References	80
Appendix A	109
Appendix B	112
Appendix C	114
Appendix D	116

List of Abbreviations

ACJ	Acromioclavicular joint
AHD	Acromial-humeral distance
AHL	Acromiohumeral ligament
ALPSA	Anterior-labroligamentous posterior sleeve avulsion lesion
AI	Acromial Index
AP	Anteroposterior
AT	Acromion type
CHL	Coracohumeral ligament
GFD	Glenoid fossa depth
GFL	Glenoid fossa length
GHJ	Glenohumeral joint
GA	Glenoacromial distance
GH	Glenohumeral distance
HHI (°)	Humeral head angle of inclination (degrees)
HHMax_dia	Maximum humeral head diameter
IGHL	Inferior glenohumeral ligament
ITGW	Intertubercular groove width
LAA (°)	Lateral acromion angle (degrees)
LHBT	Long head of the Biceps Brachii tendon
MGHL	Middle glenohumeral ligament
MRI	Magnetic Resonance Imaging
OA	Osteoarthritis
RC	Rotator Cuff
SGHL	Superior glenohumeral ligament
SS	Subscapularis
SP	Supraspinatus
TM	Teres Minor

List of Figures

Fig. 2.1. Osteological components forming the GHJ (adapted from Culham and Peat, 1993).....	4
Fig. 2.2. Lateral view of the rotator cuff orientation around the glenoid fossa (adapted from Burbank <i>et al.</i> , 2008).....	7
Fig. 2.3. Internal view of the glenoid labrum and synovial capsulolabral tissue (adapted from Wiley <i>et al.</i> , 2005).....	8
Fig. 2.4. Layout of the glenohumeral ligaments around the glenohumeral joint (adapted from O' Brien <i>et al.</i> , 1990).....	9
Fig. 2.5. Illustration of chronic dislocation (left) versus a normally articulated glenohumeral joint(right) (adapted from researcher's own X-ray study sample).....	13
Fig. 3.1. Acromial types - A = flat, B = round and C = hooked according to the Bigliani-Morrison-April scale (schematic) (adapted from Naidoo <i>et al.</i> , 2015).....	21
Fig. 3.2. Measuring the LAA-lateral acromion angle, AHD-acromial-humeral distance and GFL-glenoid fossa length in GHJ (schematic) adapted from Hanciau <i>et al.</i> , 2012).....	22
Fig. 3.3. Measuring of the AI-acromial index, GA-glenoacromial distance, GH-glenohumeral distance and HHMax_dia-maximum humeral head diameter in the GHJ (schematic) (adapted from Nyffeler <i>et al.</i> , 2006).....	23
Fig. 3.4. Measuring of the ITGW-intertubercular groove width and HHI humeral head angle of inclination on the humeral head (schematic) (adapted from Rajani and Man, 2013).....	24
Fig. 3.5. Measuring of GFD-glenoid fossa depth (schematic) (adapted from Lippitt <i>et al.</i> , 2003).....	24
Fig. 3.6. Measuring of the ACJ-acromioclavicular width in the GHJ (schematic) (adapted from Zanca, 1971).....	25
Fig. 3.7. Internal view of the RC-rotator cuff tendons and GHJ_Ligaments surrounding the glenoid fossa of the GHJ (schematic) (adapted from O' Brien <i>et al.</i> , 1990).....	28
Fig. 3.8. GHJ_C-glenohumeral joint capsule (schematic) (adapted from Moore <i>et al.</i> , 2010).....	28

Fig. 3.9. Internal view of GL-glenoid labrum in a healthy shoulder and labrum tear (schematic)
(adapted from Hata *et al.*, 1992).....29

List of Tables

Table 3.1. Demographic information for cadaver sample.....	19
Table 3.2. Demographic information for X-ray imaging sample.....	20
Table 3.3. Demographic information for MRI imaging sample.....	20
Table 4.1. Normality tests for data distribution for the measured variables (AHD, HHMax_dia, HHI, ITGW and GFD) in the cadaver sample.....	32
Table 4.2. Frequency distribution of acromial types AT present in the male and female cadaver sample.....	33
Table 4.3. Summary statistics with Mann-Whitney test of the morphometric skeletal variables (AHD, ITGW, HHI, HHMax_dia and GFD) measured in the cadaver sample.....	34
Table 4.4. Contingency table for AT occurrence between males and females in the cadaver sample.....	35
Table 4.5. Contingency table for AT occurrence between non-pathology/pathology in males and females in the cadaver sample using the Fisher's exact test.....	35
Table 4.6. Two sample t-tests/Mann-Whitney tests comparing male and female variable measurements in the cadaver sample.....	36
Table 4.7. Two sample t-test and Mann-Whitney test comparing male and female variable measurements with AT in the cadaver sample.....	37
Table 4.8. Comparative tests (t-test & Mann-Whitney) comparing variable measurements between pathological versus no-pathological shoulders in the cadaver sample.....	37
Table 4.9. Normality tests for data distribution for the measured variables (AI, GA, GH and LAA) in the X-ray sample.....	38
Table 4.10. Normality tests for data distribution for the measured variables (ACJ, AHD, GFL, HHMax_dia and HHI) in the X-ray sample.....	39
Table 4.11. Contingency table for AT between sex and side in the X-ray sample using the Fisher's exact test.....	41
Table 4.12. Summary statistics with Mann-Whitney test of morphometric skeletal variables (AI, GA, GH and LAA) measured in the X-ray sample.....	42

Table 4.13. Summary statistics with Mann-Whitney test of morphometric skeletal variables (ACJ, AHD, GFL, HHMax_dia and HHI) measured in the X-ray sample.....	43
Table 4.14. Contingency table for AT between sex and side in the X-ray sample using the Fisher's exact test.....	44
Table 4.15. Comparative tests (t-test & Mann-Whitney) comparing variable measurements between population groups and sides for AI, GA, GH and LAA in the X-ray sample.....	46
Table 4.16. Comparative tests (t-test & Mann-Whitney) comparing variable measurements between population groups and sides for ACJ, AHD, GFL, HHMax_dia and HHI in the X-ray sample.....	47
Table 4.17. Normality tests for data distribution for the measured variables (AI, GA, GH and LAA) in the MRI sample.....	49
Table 4.18. Contingency table for AT between males and the females left and right side in the MRI sample using Fisher's exact test.....	50
Table 4.19. Summary statistics with Mann-Whitney test of morphometric skeletal variables (AI, GA, GH and LAA) measured in the MRI sample.....	51
Table 4.20. Summary statistics with Mann-Whitney test of morphometric skeletal variables (ACJ, AHD, GFL, HHMax_dia and HHI) measured in the MRI sample.....	52
Table 4.21. Comparative tests (t-test & Mann-Whitney) comparing variable measurements between males and females and side for AI, GA, GH and LAA in the MRI sample.....	53
Table 4.22. Comparative tests (t-test & Mann-Whitney) comparing variable measurements between males and females and side for ACJ, AHD, GFL, HHMax_dia and HHI in the MRI sample.....	54
Table 4.23. Kruskal-wallis test comparing pathology groups 1,2,3 and 4 and variable measurements in the MRI sample.....	55
Table 4.24. Two-sample t-tests comparing the glenoid labrum (intact, fray/tear) and AI, GA, GH, LAA, ACJ, AHD and GFL in the MRI sample.....	55
Table 4.25. Kruskal-wallis test comparing the glenoid labrum (intact, fray/tear) and HHMax_dia and HHI in the MRI sample.....	56

Table 4.26. Intraclass Correlation Coefficient and confidence interval test for the intraobserver results of the X-ray sample.....	57
Table 4.27. Intraclass Correlation Coefficient and confidence interval test for the intraobserver results of the MRI sample.....	57
Table 4.28. Intraclass Correlation Coefficient and confidence interval test for the interobserver results of the X-ray sample.....	58
Table 4.29. Intraclass Correlation Coefficient and confidence interval test for the interobserver results of the MRI sample.....	59

Acknowledgements

I would like to thank my supervisor, Dr Natalie Keough for her support, time and patience throughout this project.

Grace, wisdom, insight and perseverance was granted to me by my Father in Heaven, enabling me with His Grace to reach the end of my sometimes-turbulent journey.

My sincerest thanks to Prof Suleman for taking time to go to Dr Velleman's practise to collect the data for this study.

I would like to thank Prof Lockhat and Dr Mark Velleman for the crucial part they had in the success of this study, through the data they provided, without hesitation.

I would also like to thank Ms Marinda Pretorius whose artistic input assisted me with the design of illustrations.

Thank you Mr Charl Janse van Rensburg, without your help the statistics would have remained a tsunami.

I would like to thank the National Research Foundation for the funding that I received for this project.

I sincerely thank my family and friends for their prayers, who have supported me throughout my journey and believing in the end result a never doubted in my success.

Thank you also to the Department of Anatomy at the University of Pretoria for the use of the human cadavers whose bodies I used in the dissection halls and for research. These donated bodies are one of the most selfless acts a person could bestow upon a research student to be given to work with.

I would also like to thank Neil for his kind assistance and friendly help during my dissections, and statistics "Neil, your hellos and hi there's" meant so much, thank you again.

Abstract

Morphological traits pertaining to the humerus and scapula have previously been linked to the occurrence and perhaps development of certain shoulder pathologies such as, osteoarthritis, rotator cuff impingement and chronic shoulder dislocations. Few studies have investigated these traits in a South African sample and therefore the aim of this study was to investigate the differences in various skeletal and soft tissues components of the glenohumeral joint (GHJ) in individuals with known or diagnosed shoulder pathology.

The sample included a cadaveric (n=46), X-ray (n=94) and MRI (n=46) component. In the cadaver component, only 11 presented with shoulder pathology, while all the individuals in the imaging component (X-ray and MRI) presented with known/diagnosed shoulder pathologies. Several measurements and observations were taken and included; acromial type (AT), intertubercular groove width (ITGW), glenoid fossa depth (GFD), acromial index (AI), lateral acromial angle (LAA), acromioclavicular joint distance (ACJ), acromiohumeral distance (AHD), glenoid fossa length (GFL), maximum humeral head diameter (HHMax_dia), humeral angle of inclination (HHI) and presence/absence of pathology.

The results indicated that males had a higher occurrence of AT I than AT II and the females an even ratio between AT I and AT II in the X-ray and cadaveric component, while black males in the X-rays had a higher occurrence of AT II than AT I. In both the X-ray and MRI samples, female groups showed a higher occurrence of AT I than AT II. Significant differences in morphology of the AI, ACJ, LAA, HHI and GHD were noted between the various acromial types (I, II, III). The HHMax_dia was the only morphometric variable that showed significance differences across all three samples (cadaver, X-ray and MRI). The AI, LAA, GFL showed significant morphological differences in both the X-ray and MRI groups, the HHI and ACJ only showed significant differences in the X-ray group, while the GH only showed differences in the MRI group.

The results gained in this study suggest that AT, AI, ACJ, LAA, HHMax_dia, HHI, GHD and GFL in individuals with known or diagnosed shoulder pathologies such as chronic joint instability, osteoarthritic and osteoporotic changes, rotator cuff pathologies, frozen shoulder/adhesive capsulitis and tendinopathy/calcific tendinitis, are different from no-pathology individuals and these traits may provide more insight, if studied further, into the development of shoulder pathology.

Keywords: Morphometric, Skeletal, Soft tissue, Pathologies, Glenohumeral joint

Chapter 1: Introduction

The glenohumeral joint (GHJ) is one of the most mobile joints in the human body and is actively involved in normal, everyday use, as well as in a majority of sporting activities. The smooth movement and functionality of the GHJ is dependent on a number of muscles, ligaments and bony elements synchronously working together (Schenkman and De Cartaya, 1987). Pathology, disease and trauma of the shoulder is perhaps one of the most prevalent and contentious musculoskeletal conditions impacting activities of daily life. Complications, whether soft tissue (muscle tear, inflammation, impingement) or skeletal tissue (bone spurs, degeneration), associated with this joint, often present the medical profession with the most challenges.

Compromised musculoskeletal well-being decreases quality of life and significantly adds to the physical limitations due to acute and/or chronic pain. This can result in reduced participation in recreational activities, withdrawal from usual social, community, and occupational activities, whilst increasing the burden in other health domains, including mental health well-being (Briggs *et al.*, 2016). Research has alluded to the fact that intrinsic causes such as patient age, decreased vascularisation of tissue, degeneration of the muscle with fatty deposits and, genetic predisposition as well as extrinsic causes for example, acromion morphological changes, are associated with tendon injury causing shoulder pain (Braman *et al.*, 2013; Yu *et al.*, 2013; Balke *et al.*, 2016).

The 2015 global burden of disease report from the World Health Organisation (WHO), which included 183 WHO member states, Asia and the West Bank, estimated that 42.2% of developed and developing nations live with the burden of musculoskeletal disease (Mathers *et al.*, 2017). Evidence suggests that shoulder pathologies may have a direct effect on worker productivity, thus causing monetary loss for companies about time off work and ultimately placing strain on the economy (Gemne *et al.*, 1987; Bodin *et al.*, 2016). An estimated 20% of the dental profession in North India, 5 million of the work population in the United States of America, 70% of the occupational groups in Germany and, 17.3 million of the work population in France suffer from a musculoskeletal condition, many of those associated with the shoulder (Gemne *et al.*, 1987; Kumar *et al.*, 2013; Palazzo *et al.*, 2014). These workers often visit medical specialists to establish the source of their shoulder discomfort, leading to time off work and medical costs incurred. During these medical consultations, the common denominator for most shoulder problems is pain and movement limitations. This guides the orthopaedic

surgeon/medical specialist to diagnose and pursue the disease aetiology of possible conditions which could be considered as problematic (Guyver *et al.*, 2014).

During the process of identifying these conditions, diagnostic equipment such as X-rays, CT-scans and MRI images are often used. These diagnostic tools guide the specialist/orthopaedic surgeon to establish a pathoanatomic diagnosis, treatment regime and rehabilitation (Hodler *et al.*, 1991; Aragão *et al.*, 2014; McClure and Michener, 2015). The choice of diagnostic tool is usually dependent on the clinical presentation but often, the first choice is a plain X-ray image of the affected shoulder. X-ray images provide insight into the skeletal components of the GHJ such as the acromion, humeral head position, and the scapula, which could all be linked to GHJ pathology such as, bone spurs or degeneration causing pain and movement restriction (Michener *et al.*, 2003; Aragão *et al.*, 2014). MRI images provide additional and in-depth soft tissue component evaluation. MRI images assist the medical specialist in evaluating the soft tissue component of GHJ pathology such as tears, capsulitis or tendinitis/tendinosis causing decreased range of motion (ROM) and pain.

Most studies investigating shoulder pathologies use these imaging techniques to evaluate specific elements of the GHJ. These include pathologies of the humeral head, glenoid fossa, rotator cuff (RC) and tendons (Montsat and Bonneville, 2012; Yu *et al.*, 2013; Kim *et al.*, 2012). Over the past couple of years, studies have associated certain morphometric skeletal (Michener *et al.*, 2003; Cadet *et al.*, 2008; Imhoff *et al.*, 2010; Urita *et al.*, 2016) and soft tissue components (Habermeyer *et al.*, 2004; Choi *et al.*, 2015) to existing or underlying pathological conditions. However, to the author's knowledge no studies have researched these morphometric components of the GHJ associated with shoulder pathologies in South African populations.

Therefore, the aim of this study was to investigate the association of the humeral and scapula morphology of the GHJ as well as the soft tissue elements relating to the stabilization of the joint with commonly diagnosed shoulder pathologies using MRI scans. X-ray images from pathological shoulders as well as cadaveric shoulders were also measured and compared to what the current normal standards are for certain measurements.

Chapter 2: Literature Review

The aim of this study was to evaluate the differences in various skeletal and soft tissues components of the glenohumeral joint (GHJ) in individuals with known or identified shoulder pathology. This review outlines the skeletal and soft tissue components of the GHJ in order to create an understanding of the basic anatomy and interactive functionality these components have. The skeletal and soft tissue components of the GHJ work synchronously together to form a highly functional, complex and mobile joint (Basmajian, 1982; Culham and Peat, 1993).

AIM: To evaluate and classify the skeletal and soft tissue morphology of the glenohumeral joint (GHJ) of individuals who present with commonly diagnosed shoulder pathologies.

RESEARCH OBJECTIVES: The research objectives of this study were to:

- Measure humeral and scapula dimensions on both X-ray images from patients with known glenohumeral pathologies;
- Measure soft tissue dimensions on MRI images from patients with known glenohumeral pathologies;
- Evaluate shoulder pathology and measure humeral and scapula dimensions in 26 embalmed, human cadaveric specimens in order to establish the association between commonly diagnosed shoulder pathologies and bony morphology.

2.1. Anatomy of the glenohumeral joint (GHJ)

The humerus and scapula are the skeletal components that directly form the GHJ (Boileau and Walch, 1997) (Fig. 2.1). The humeral head articulates with the glenoid fossa of the scapula forming a synovial, ball-and-socket joint. The humeral head is twice as large as the glenoid fossa, but this is compensated for by the glenoid labrum, which is a cartilaginous structure surrounding the periphery of the fossa (Wilk *et al.*, 1997). The GHJ is also kept in place through directional forces created between both the dynamic stabilizers (muscles) of the joint as well as the static stabilizers (ligaments/tendons) (Wilk *et al.*, 1997; Terry and Chopp, 2000; An, 2002).

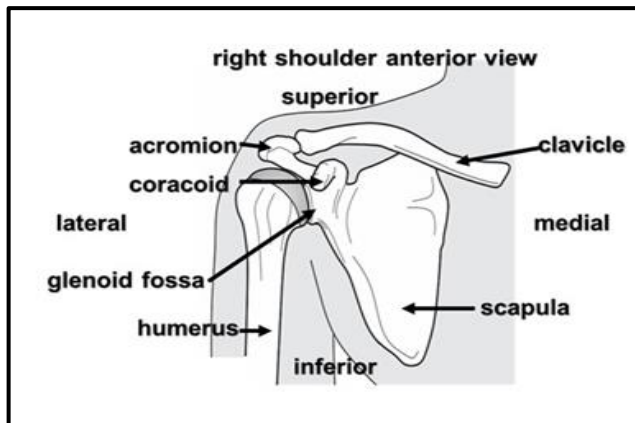


Fig. 2.1. Osteological components forming the GHJ (adapted from Culham and Peat, 1993)

2.1.1. Skeletal tissue components

Proximal humerus

The head of the humerus is directed medially, superiorly and is tilted slightly posterior at an angle of between 26 and 31 degrees (O'Connell *et al.*, 1990). The articular surface of the humeral head is spherical in shape and smooth. A rough area just lateral to, and surrounding the periphery of the articular surface, is known as the anatomical neck. The anatomical neck is an important area for attachment of the joint capsule and rotator cuff (RC) unit of the GHJ (Boileau and Walch, 1997).

The greater and lesser tubercles, as well as the intertubercular groove, are located on the proximal aspect of the humerus. The larger, greater tubercle, is rounded and serves as an attachment site for a majority of the RC muscle unit. It is positioned more lateral than the lesser tubercle, which is located on the anteromedial aspect of the humeral head and serves as the attachment for subscapularis (O'Connell *et al.*, 1990). The intertubercular groove separates the two tuberculi and becomes shallower and wider as it continues downwards onto the humeral shaft. This groove houses the long head of the biceps tendon (LHBT) as it courses from its origin on the supraglenoid tubercle and glenoid labrum to its muscular belly in the arm (O'Connell *et al.*, 1990; Marieb *et al.*, 2014). The transverse humeral ligament forms a superior arch between the two tuberculi and serves to keep the LHBT within the intertubercular groove (Brodie, 1890), as does the extensor hood created by the interdigitating fibres of supraspinatus and subscapularis (Clark *et al.*, 1992; Vosloo *et al.*, 2017). The second neck of the proximal humerus is the surgical neck, and is situated beneath the humeral tuberculi. It is an area closely associated with the axillary nerve and both circumflex humeral arteries (Zhang *et al.*, 2013).

The surgical neck also distinguishes between the proximal part of the humerus and the beginning of the shaft; it is also a common fracture site (Marieb and Zao, 1992; Tischer *et al.*, 2011).

The head of the humerus and the shaft are not aligned in the same longitudinal axis, but are positioned in a manner that creates what is known as the angle of inclination. The importance of the angle of inclination lies with the fact that it provides the GHJ with anterior stability. This stability occurs because the humeral head articulates with the upper part of the glenoid fossa creating stability in the GHJ during movement (Oh *et al.*, 2014). Normal ranges for the angle of inclination are between 130 and 150 degrees with the humeral shaft (Sarrafian, 1983; Iannotti *et al.*, 1992; Halder *et al.*, 2000).

Scapula

The scapula is a thin, flat bone held in close proximity to the thoracic wall by various muscular attachments (Peat, 1986). Three fossae and three borders provide attachment for these muscles and they include the 1) supraspinous; 2) infraspinous and 3) subscapular fossae as well as the 1) superior; 2) lateral and 3) medial borders (Bdaiwi, 2014). On the posterior surface a large slanted spinous process divides the scapular area into two fossae. The lateral end of this process forms the acromion. Scapular connections form between the clavicle, at the acromion process, and the humeral head at the glenoid fossa. This anatomical alignment forms the GHJ and is located between the humerus and the glenoid fossa (Bdaiwi, 2014; Marieb *et al.*, 2014).

The acromion is a bony spinous continuation of the scapular spine, and extends laterally over the glenoid fossa. The acromion process differs in size and shape and these differences have been classified accordingly; Type I - flat under surface; Type II - round under surface; Type III - acquired hooked under surface (Bigliani *et al.*, 1986). The acromion plays a functional role in GHJ stability because the deltoid lateral muscle fibers (acromial fibers) originates from the lateral margin of the acromion; the subacromial space provides sufficient freedom for the humeral head to glide during movement; the lateral acromion angle (LAA) and the glenoid angle (GA) affords stability to the humeral head in the GHJ (Mullaji *et al.*, 1994; Nakata *et al.*, 2011; El-Din and Ali, 2015; Saha and Vasudeva, 2017).

The lateral border of the scapula has been adapted to form the glenoid fossa. The bony fossa is shallow and curved with a concave articular surface. Both the long head of triceps brachii and the LHBT have attachments to the rim of the glenoid fossa (supra- and infraglenoid tubercles) and glenoid labrum (Culham and Peat, 1993). The fossa offers only a small

contribution to GHJ stability and makes up only one third of the articulation area. The articulation area has a cartilage floor that covers the fossa and this deepens in the middle offering increased stability. Additional and assistive stability is further provided by the soft tissue labrum (glenoid labrum) that fuses to the fossa rim. These soft tissue components enlarge the shallow fossa so that the humeral head can move smoothly and stably within the joint complex (Mullaji *et al.*, 1994; Nakata *et al.*, 2011).

The superior border of the fossa is tilted 40 and 120 degrees towards the scapular plane while the inferior border is tilted towards the coracoid process. This anatomical feature contributes to the scapulohumeral rhythm, allowing a wide range of motion in the coronal, sagittal and scapular planes (Amabile *et al.*, 2016). Therefore, movements such as flexion, abduction, adduction, circumduction and arm extension are possible (Mullaji *et al.*, 1994; Paine and Voight, 2013). Functions of the scapula are to connect the arm to the axial skeleton via the clavicle, assist the arm during movement by moving upwards and sliding away from the spine and the muscles of the scapula position the glenoid in the most favourable position for smooth GHJ movement and absorbs extra directional force stress burdens placed on the GHJ during movement (Paine and Voight, 2013).

2.1.2. Soft tissue components

The soft tissue components are attached to the scapula and humerus. They facilitate movement of the upper limb, provide important stabilisation to the GHJ and, essentially connect the skeletal components with each other (Basmajian and Bazant 1959; Culham and Peat 1993).

Rotator cuff muscles (RC)

The RC muscles extend from the scapula towards the humerus where they insert onto the tuberculi (Fig. 2.2). Their primary function is to stabilise the GHJ during movement (Hess *et al.*, 2000). This group of muscles include the subscapularis (SC), infraspinatus (IS), teres minor (TM) and supraspinatus (SS). These muscles, with their tendons, form a cuff-like structure that firmly attaches to the humeral tubercles. (Alilet *et al.*, 2016). The tendons form broad layers before inserting onto the humeral head. These broad layers function as a strengthening force in the GHJ and the SC together with the SS tendon provides a cover for the LHBT at the entrance of the intertubercular groove (Pandey and Willems, 2015).

During shoulder movement stability is provided by the RC muscles through firm medial compression of the humeral head against the glenoid fossa and the glenoid labrum (Phadke *et al.*, 2009). The RC functions as a unit where the SC, IS and TM allow a small offset (1 mm to 2 mm) of superior conversion of the humeral head by balancing the deltoid muscle vector force (Phadke *et al.*, 2009), whilst simultaneously the IS and TM externally rotates the humeral head during arm elevation (Phadke *et al.*, 2009). During the initial stages of abduction, SS initiates the movement for the first 15 degrees and then acts as an accessory elevator to the deltoid muscle to produce a slight shoulder abduction force with elevation of the arm (Poppen and Walker, 1978; Otis *et al.*, 1994; Ackland *et al.*, 2008; Reed *et al.*, 2013). The SS also functions effectively as a GHJ compressor during arm elevation and not as a GHJ depressor which adheres to the RC synergy (Nicholson *et al.*, 1996). The SS is implicated in pathologies such as subacromial impingement syndrome associated with its anatomical position underneath the acromion (Nicholson *et al.*, 1996).

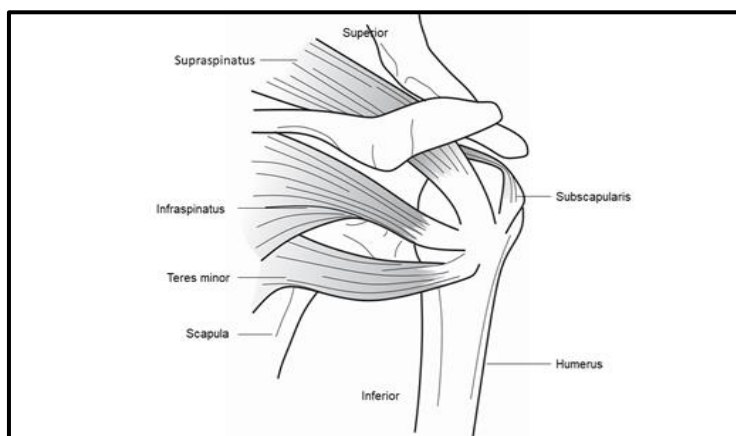


Fig. 2.2. Lateral view of the rotator cuff orientation around the glenoid fossa (adapted from Burbank *et al.*, 2008)

The long head of the biceps brachii tendon (LHBT)

The double headed biceps muscle has strong connective tissue tendons at the insertional as well as origin sites. The two heads include the long head of biceps brachii and the short head of biceps brachii (Edelson *et al.*, 1991; Nakata *et al.*, 2011). The LHBT originates from the supraglenoid tubercle and superior aspect of the glenoid labrum. The LHBT arches over the humeral head and exits the joint capsule to follow the path of the intertubercular groove downwards towards the muscle belly. The LHBT is stabilised in the intertubercular groove by a capsuloligamentous complex, the biceps pulley system (Nakata *et al.*, 2011). This pulley is formed by the middle portion of the CHL, SGHL and the SS tendon and these stabilise the

tendon in its path (Nakata *et al.*, 2011; Choi *et al.*, 2015). This pulley system is present between the front edge of the SC tendon and the upper edge of the SS tendon (Nakata *et al.*, 2011).

The LHBT arch acts to depress the humeral head in the GHJ and to prevent it from dislocating during arm movements, especially abduction, while the groove's primary function is to guide and protect the LHBT (Edelson *et al.*, 1991; Vangsness *et al.*, 1994; Chung and Steinbach, 2008; Nakata *et al.*, 2011). The main function of the LHBT is to provide static stabilisation and protection of the GHJ. The LHBT achieves this stabilisation by lessening the stress placed on other soft tissue components such as the inferior glenohumeral ligament (IGHL) during active rotation of the arm.

Glenoid labrum

The glenoid labrum functions as a soft tissue static stabiliser and prevents the humeral head from over rolling during arm movement (Cooper *et al.*, 1992). The labrum is an ovoid disc made up of dense fibrous cartilage similar to the knee meniscus, and it covers the shallow articulation glenoid fossa of the scapula (Moseley and Overgaard 1962; Shuman *et al.*, 1983; Cooper *et al.*, 1992; Huber and Putz 1997) (Fig. 2.3). The collagen fibrils and hyaline cartilage intertwine and form a smooth articulation area for the bony fossa and its edges (Nishida *et al.*, 1996). The labrum stretches over the edges or rim of the fossa to increase the size of the articulation area, especially the depth. In the middle of the labrum it deepens significantly forming a cup-like appearance. This deep area is of biomechanical importance because it creates a suction effect or a lock effect with the articulation with the humeral head, preventing uncoordinated movement within the GHJ, thereby increasing GHJ stability (Tischer *et al.*, 2011). It also it contributes to stabilising the LHBT anchor (Cooper *et al.*, 1992).

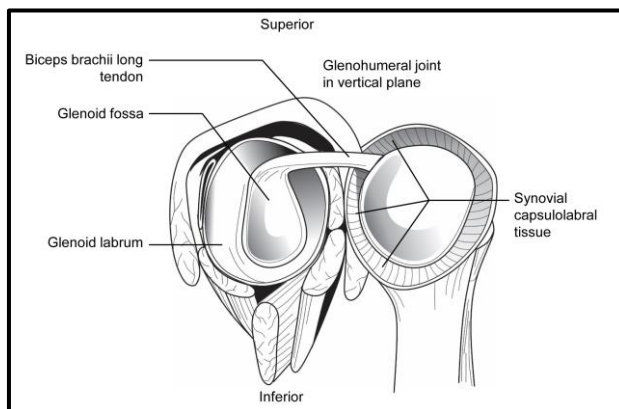


Fig. 2.3. Internal view of the glenoid labrum and synovial capsulolabral tissue (adapted from Wiley *et al.*, 2005)

Glenohumeral Joint (GHJ) capsule

The GHJ capsule consists of two soft tissue layers, a loose fibrous outer layer and an inner layer lined with a synovial membrane. The synovial membrane provides lubrication and suppleness to the capsule. The capsule stretches outwards over the GHJ and forms a soft tissue covering. The capsule extends out laterally from the rim of the glenoid fossa to the anatomical neck of the humeral head (Itoi *et al.*, 1993). The anterior side of the capsule is thicker than the posterior side. In a neutral arm position, a pouch is formed in the area between the humeral head and scapula known as the axillary recess (Carmichael and Hart, 1985). During elevation and rotation of the arm the axillary recess extends to provide increased rotational movement (Carmichael and Hart, 1985; Omoumi *et al.*, 2011). The joint capsule is not a very stable structure and therefore needs reinforcement which is provided through the combined strength of the RC muscles, the CHL and GHL soft tissue components as well as the anatomical features of the glenoid fossa (Carmichael and Hart, 1985; Massengill *et al.*, 1994).

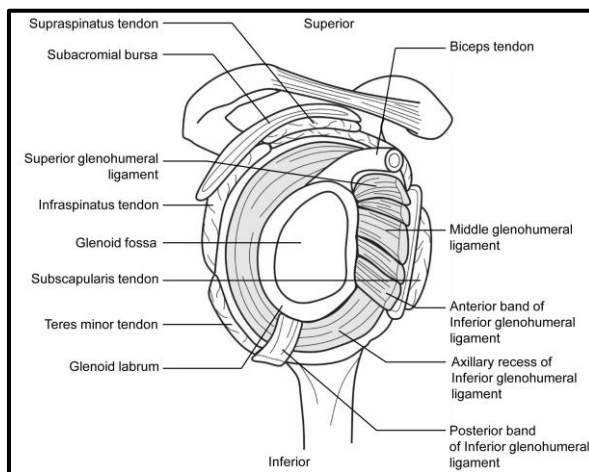


Fig. 2.4. Layout of the glenohumeral ligaments around the glenohumeral joint (adapted from O' Brien *et al.*, 1990)

Glenohumeral ligaments (GHL)

The GHLs are three ligaments that provide static stability to the GHJ. The ligaments are continuations of the capsular soft tissue components. The ligaments follow the same attachments as the joint capsule in the anterior part of the GHJ and thereby also strengthen the capsule (Yang *et al.*, 2009). The ligaments are arranged according to their anatomical position between the glenoid and the humerus: superior, middle and inferior. These are referred to as the superior glenohumeral ligament (SGHL), middle glenohumeral ligament (MGHL) and the

inferior glenohumeral ligament (IGHL) (Edelson *et al.*, 1991) (Fig. 2.4). The CHL is also considered a GHL and plays a role in the reinforcement for the superior part of the joint capsule by depicting a Z-pattern (Edelson *et al.*, 1991; Brown *et al.*, 2004; Omoumi *et al.*, 2011). The ligament that provides primary stability for the GHJ is the IGHL. The IGHL has an anterior and a posterior band and is referred to as a complex. These two bands with the axillary recess provide sturdy joint stability (Omoumi *et al.*, 2011; Shahabpour *et al.*, 2017).

2.2. Biomechanics of the glenohumeral joint (GHJ)

The position of the humerus, clavicle and the scapula in relation to the thorax allows for coordinated biomechanical functionality (Grewal, 2011). Proper and efficient biomechanical functionality is necessary to sustain structural loads often associated with demanding workplace environments such as the use of heavy machinery with repetitive and continuous movements or even being in a non-anatomical position for an extended period of time such as in Dentistry (Grewal, 2011).

The shoulder's ability to perform various degrees of motion is due to the skeletal and soft tissue components that respond to mechanical stimuli and adjust accordingly (Lugo *et al.*, 2008). Biomechanics of the GHJ entails the forces exerted by soft tissues such as the RC unit, glenoid labrum and the capsule and the effect of gravity on the skeletal components such as the humerus and scapula (Amabile *et al.*, 2016). The anatomy of the scapula is relevant since the direction of the forces transmitted across the GHJ originates from the scapula (De Duca *et al.*, 1973). The scapula, knee, spine and ankle joints share a unique skeletal feature in that the joint positions are a set of sequential rotations about three axes that are anatomically aligned (Wei-Xun and Chun-Tu 1993; Wu *et al.*, 2005). Scapular anatomy within its approximation to the thoracic alignment is unique in the sense that the three scapular rotations are able to exceed 50 degrees, but within the boundaries of 90 degrees (McQuade *et al.*, 1995; de Groot, 1997). These scapular rotations allow the humerus to articulate in directions such as lateral rotation, retraction and posterior tilting, within the boundaries of 90 degrees, whilst the humerus head remains secure within the GHJ (Harryman *et al.*, 1990; van der Helm, 1996).

Articulative motion and anatomical structural angles such as the humeral head angle of inclination together with humeral head diameter creates directional forces between muscles and the skeleton (Saha, 1971). This biomechanical arrangement orchestrates alignment and coordination in sequence to ensure upper limb muscle movement. (Saha, 1971; Poppen and

Walker 1978; Cooper *et al.*, 1992; Yang *et al.*, 2009; Dunham *et al.*, 2012). The anatomical arrangement of the skeletal and soft tissue does however create a balance via existing forces such as pull-out, compression and integration, which actively coordinate the soft tissues such as the ACL, ACJ, IGHLC, and RC to provide functional movement and stabilisation to the GHJ (O'Connell *et al.*, 1990; Vangsness *et al.*, 1994; Tischer *et al.*, 2011). GHJ movements such as abduction and adduction and external rotation are interdependent on these skeletal and soft tissue components to function optimally (Gerber *et al.*, 1985; Warth *et al.*, 2013; Yu *et al.*, 2013). A negative intraarticular pressure exists within the GH articulation component. This pressure is a suction pressure that facilitates stability during the movement of the humeral head (Halder *et al.*, 2000). The glenoid labrum acts as a static stabiliser of the GHJ (Kanatli *et al.*, 2010). Therefore, the intraarticular pressure functions to ensure smooth and stable articulative motion (Lugo *et al.*, 2008).

Scapular kinematic alterations are associated with shoulder pathologies such as, humeral head instability, RC tears, and impingement syndrome (Tate *et al.*, 2009). Impingement syndrome, for example, causes altered compensatory angular rotations of the scapula such as greater superior rotation during flexion; greater posterior tilt and greater upward rotation, increasing the subacromial space to accommodate the RC complex (McClure *et al.*, 2006). The RC is a complex musculotendinous structure which functions as a unit in the GHJ (De Franco and Cole, 2009). This unit is a fine biomechanical muscle system that provides dynamic stability to the humerus head during arm movement, keeping the humeral head centralised during articulation in the GHJ (Halder *et al.*, 2000) and function as cotensioners for the capsular ligaments i.e. IGHLC (Lugo *et al.*, 2008); creates a compressive force across the GHL to maintain the consistent contact between the humeral head and glenoid fossa (Lugo *et al.*, 2008); decreases shear forces during humeral head stabilisation; facilitates antishear in the GHJ due to organised muscular contraction; functions with the deltoid to generate a sinuous trajectory of the humerus during all phases of GH elevation (Inman *et al.*, 1944; McMahan *et al.*, 1995; Alpert *et al.*, 2000) and provides passive stability due to their location and orientation around the GHJ (Lugo *et al.*, 2008). The dual stabilisation that is created by the RC counters the forces applied through the GHJ at different positions in the motion arc (Halder *et al.*, 2000; Lugo *et al.*, 2008).

The biomechanics of the GHJ is multifaceted (as described above) and designed to stabilise the GHJ in a coordinated intrinsic manner (Michener *et al.*, 2003). When this

coordinated mechanism is disturbed due to disease of its skeletal-and/or soft tissue components, associated pathology can develop in the GHJ (Michener *et al.*, 2003).

2.3. Glenohumeral joint (GHJ) pathologies

The study of joint pathology is the science whereby causes and effects of structural abnormalities produced by disease due to either acute or chronic factors are investigated (McClure and Michener, 2015). In the healthy GHJ a synergistic relationship exists between skeletal and soft tissue components (Ruckstuhl-Knüsel, 2008). However, factors such as biomechanical composition, inheritability, lifestyle, ageing, and environment may contribute to several dysfunctions, such as osteoarthritis, frozen shoulder, dislocations and calcifications of the healthy GHJ (Pandey and Willems, 2015). These factors expose the healthy skeletal and soft tissue components to functional and structural changes such as erosion, tears, inflammation, degeneration and bone lesions (Ruckstuhl-Knüsel, 2008; Pandey and Willems, 2015). GHJ pathology contributes to loss of functional everyday living as well as high pain levels (McClure and Michener, 2015). Several authors have investigated osteoarthritis, enthesophytes, adhesive capsulitis (frozen shoulder), tendinopathy, bursitis, osteophytes and RC tears as GHJ pathologies (Ruckstuhl-Knüsel, 2008; Singh *et al.*, 2013; Aragão *et al.*, 2014; Henderson *et al.*, 2015) and have found that if RC tears or tendinopathy occur first, instability and SS impingement is due to glenohumeral cartilage loss as well as acromion curvature deviance which is associated with SS tendon impingement independent of the ageing process.

2.3.1. Chronic instability (dislocation)

A shoulder dislocation less than one month old was suggested by Souchon, (1891) not to be chronic but recent, whilst others (Schulz *et al.*, 1969) argued that a time lapse of more than twenty-four hours should be considered a chronic dislocation (Goga, 2003). Chronic dislocation is associated with instability, which is caused by an overly lax and stretched GHJ capsule (Bencardino *et al.*, 2013). This unsupportive GHJ capsule causes multidirectional instability often associated with Hill-Sachs defects (humeral head cortical erosion) and glenoid rim erosion, causing shoulder clicking, or popping sounds, within the GHJ during movement (Bencardino *et al.*, 2013). Chronic dislocation is also associated with an anatomical anomaly

such as a flattened glenoid fossa in the anterior to posterior and superior to inferior directions (decreased depth) (von Eisenhart-Rothe *et al.*, 2010; Peltz *et al.*, 2015) (Fig. 2.5). A flattened fossa anatomically compromises the glenoid and is also associated with multidirectional GHJ instability (von Eisenhart-Rothe *et al.*, 2010; Peltz *et al.*, 2015). During contact sport activities or high impact injuries, sudden impact forces on the RC, pulls the muscles into different directions which can cause GHJ dislocation (Imhoff *et al.*, 2010; Peltz *et al.*, 2015).

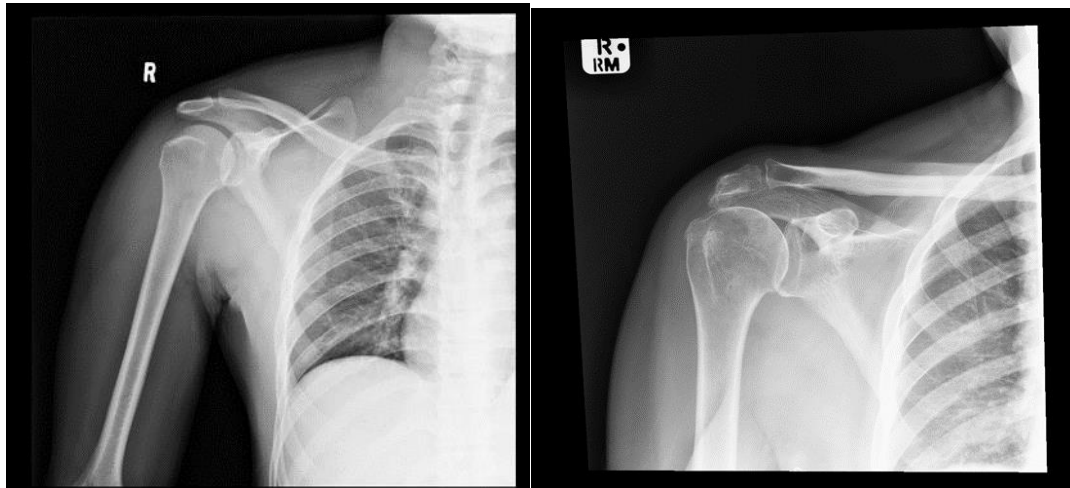


Fig. 2.5. Illustration of chronic dislocation (left) versus a normally articulated glenohumeral joint (right) (adapted from researchers' own X-ray study sample)

Chronic instability of the GHJ is prevented by dynamic (RC) and static (glenoid labrum, ligaments and LHBT) stabilisers (Wilk *et al.*, 1997; Bencardino *et al.*, 2013). These stabilisers in coordination with each other maintain a precise rotation of the humeral head over the center of the glenoid fossa (Bencardino *et al.*, 2013). However, when there is over joint play of the capsular ligaments, during midrange glenohumeral movement, the glenoid fossa concavity compression provides stability to the GHJ (Gerber and Nyffeler, 2002; Bencardino *et al.*, 2013). Stability of the GHJ is compromised by hyper flaccidness and over stretching of the GHJ capsule (Smith and Brunolli, 1989; Bencardino *et al.*, 2013). A distorted, inflamed GHJ capsule is associated with pathological involuntary dislocation of the humeral head (Hayes *et al.*, 2002). The GHJ capsule provides some humeral head support during GHJ movement (Hayes *et al.*, 2002; Ranjan and Antao, 2002). A chronic tendency of the humeral head to dislocate can be caused by movements such as hyper-abduction when the humeral head translates in a lower grade out of the glenoid fossa with some support provided by the GHJ capsule (Terry and Chopp, 2000).

Glenoid labral lesions associated with chronic GHJ instability include Bankart, SLAP, and ALPSA lesions (Hecker *et al.*, 1993; Tischer *et al.*, 2011; Bencardino *et al.*, 2013; Wilk *et al.*, 2013). The Bankart lesion is an anterior-inferior labrum separation from the glenoid, the SLAP lesion is a superior labrum anterior to posterior separation from the glenoid and the ALPSA lesion is an anterior labral periosteal sleeve avulsion (Hecker *et al.*, 1993; Tischer *et al.*, 2011; Carrazzone *et al.*, 2012; Bencardino *et al.*, 2013). The glenoid labrum is vital in GHJ stability during humeral movement and therefore, chronic glenoid labrum pathology, is associated with humeral head dislocation (Yiannakopoulos *et al.*, 2007). Humeral head defects associated with chronic GHJ instability include typical secondary Hill-Sachs lesions (Tischer *et al.*, 2011). This lesion is associated with a forceful traction on the humeral head during GHJ movement, causing a posterolateral fracture, which destabilises the humeral head at the anteroinferior glenoid fossa rim (Tischer *et al.*, 2011; Wilk *et al.*, 2013).

2.3.2. Osteoarthritis (OA) and osteoporosis (degenerative disease)

There is a vast amount of literature on OA which is described as a progressive bone cartilage degenerative disease and is also referred to as wear and tear disease (Kanatli *et al.*, 2013; Yu *et al.*, 2013; Spiegl *et al.*, 2014; Huegel *et al.*, 2015; Jacxsens *et al.*, 2016; Knowles *et al.*, 2016). This disease progressively erodes the bony articulation surfaces and also occurs at the elbow, thumb, hip and knee joints (Martinoli *et al.*, 2003). This erosion results in the formation of osteochondral bodies in the GHJ (Martinoli *et al.*, 2003). As the disease progresses in the GHJ, intraarticular osteochondral bodies migrate into the joint and remain trapped in the axillary pouch and LHBT sheath (Martinoli *et al.*, 2003). These free osteochondral bodies can be associated with GHJ stiffness and inflammation as this osteoarthritic disease progresses (Martinoli *et al.*, 2003; Millett *et al.*, 2008). Progression of OA on the glenoid surface influences the articular arch of the GHJ. The glenoid labrum and fossa cartilage becomes sheared/shaved and the humeral head is subjected to this shear strain as degeneration progresses and becomes loosely compressed (Kanatli *et al.*, 2013; Yu *et al.*, 2013). This articulation stress on the humeral head is associated with morphological changes (Kanatli *et al.*, 2013; Yu *et al.*, 2013; Spiegl *et al.*, 2014; Huegel *et al.*, 2015; Jacxsens *et al.*, 2016; Knowles *et al.*, 2016).

GHJ pathology is not only associated with OA but also with osteoporosis which is a disease characterised by low bone density and microarchitectural bone matrix deterioration in the humeral head (Christodoulou and Cooper, 2003) These microarchitectural changes are

associated with a weakened bony matrix, which increases the occurrence of humeral head fractures (Christodoulou and Cooper, 2003). Osteoporotic change in the humeral head is associated with a decrease in tuberculi bone, which predisposes the RC tendons to tears (Christodoulou and Cooper, 2003; Briggs *et al.*, 2016). RC tendon tears are therefore associated with fragile humeral head attachment surfaces and intraarticular tension forces (Christodoulou and Cooper, 2003; Cadet *et al.*, 2008). Osteoporotic humeral head changes are also commonly associated with surgical neck fractures in different population groups over 40 years of age (Briggs *et al.*, 2016).

2.3.3. RC pathology (tears and degeneration)

Studies on the natural aetiology/history of RC pathology have been limited to anatomic investigations, indicating RC pathological changes (Sher *et al.*, 1995; Yamaguchi *et al.*, 2001). Asymptomatic shoulder RC pathology is seen in an ageing population where degenerative RC tears are not common prior to 40 years of age whereas partial-thickness tears are more common after 60 and full-thickness tears after 70 years of age. (Milgrom *et al.*, 1995; Yamaguchi *et al.*, 2001; Hsu and Keener, 2015). Although demographic factors such as dominant-hand, sex and activity level were investigated for correlation with pain development, none could be associated with the development of pain (Yamaguchi *et al.*, 2001).

Pain development in RC tears and degeneration is a common musculoskeletal problem associated with skeletal and soft tissue pathology (Seitz *et al.*, 2011). This pathology weakens and compromises the RC and interferes with the symbiosis that exists within the GHJ (Seitz *et al.*, 2011; Pandey and Willems, 2015). The GHJ with the RC is part of the shoulder girdle and the shoulder girdle is part of the axial skeleton, which all function in unity with each other (Peat, 1986). Shoulder pain is often associated with various RC pathology such as full-thickness, massive, partial tears and tendinopathy (Thomazeau *et al.*, 1996; Goutallier *et al.*, 2011). Full-thickness tears present as a complete rupture within the tendon due to osteological changes on the under surface of the acromion, such as either bony spurs or enthesophytes (Bigliani *et al.*, 1997). Enthesophytes (pulling osteophytes) exert a pulling force on the greater tubercle of the humerus, causing these RC tears. Continuous chafing of bony spurs against the RC during movement in the GHJ often progresses to full-thickness tears. (Gupta *et al.*, 2014). Massive tears accompanied by muscle fatty infiltration is associated with pain, with or without loss of range of motion (Denard *et al.*, 2012; Collin *et al.*, 2014). Partial-thickness tears occur on the

bursa surface of the tendon, intratendinous or at the joint which is on the side of the tendon adjacent to the joint (Fukuda, 2003).

In RC tendinopathy pathology, the process starts with tendonitis which then progresses to tendinosis associated with degeneration and partial thickness tears, and finally results in full thickness tears (Neer, 1972). Tendinosis and/or tendinitis associated with RC tears, is an inflammatory response that causes pain, swelling and loss of tensile strength (Gursel *et al.*, 2004). This loss of tensile strength impacts the RC tendons attachment around the humeral head and often functional loss is associated with inflammation of the tendons. This inflammation associated with the inflammatory pathway produces and adds to greater tension force during articulation, contributing to tears (Codman, 1931; Romeo *et al.*, 1999; Dugas *et al.*, 2002; Mehta *et al.*, 2003).

2.3.4. Frozen shoulder/Impingement syndrome/Adhesive capsulitis

The aetiology of frozen shoulder (or impingement syndrome or adhesive capsulitis) was initially unidentified but later described by Codman (1931) as a frozen/contracted shoulder displaying shoulder muscle spasm (deltoid) and stiffness of the GHJ. In later studies, Neviasser (1945) differed with this finding and concluded that the GHJ capsule appeared thickened and contracted, and during dissection it had to be peeled from the humeral head, like adhesive plaster from the skin. Hence the name, adhesive capsulitis (Neviaser, 1945). Adhesive capsulitis is associated with inflammation of the capsule (Neviaser, 1945).

In 1952, De Palma stated that this disease progression is rather associated with the inelastic and inflamed anterosuperior capsule and the CHL, restricting humeral head movement. Neer *et al.* (1992), suggested that the CHL was contracted rather than inflamed. Therefore, loss of external humeral head rotation in the GHJ is associated with a contracted CHL, that acts as a check-rein, causing loss of passive and active movement (Bunker and Anthony, 1995). Lundberg (1969), differed with these findings and concluded that the capsule morphology resembled fibromatosis, similar to Dupuytren's contracture of the hand, with concentrations of fibroblasts present. This fibromatose capsule is associated with passive and active movement restriction in the GHJ (Lundberg, 1969). Later studies referred to this GHJ pathology as impingement syndrome and concurred with these previous studies (Koester *et al.*, 2005; Lewis 2009; Heron *et al.*, 2017).

This pathology is identified by different names and is universally experienced as a painful shoulder with slow onset, associated with stiffness, difficulty sleeping on the affected side and, reduced movement during forward elevation and external rotation (Bunker and Anthony, 1995; Dias *et al.*, 2005). The slow onset of pain is primarily associated with synovitis and capsule contracture and not capsular adhesions, which tend to resolve spontaneously, by itself over a period of months (Dias *et al.*, 2005; Laubscher and Rösch, 2009). The occurrence of frozen shoulder can be primary or secondary (Hand *et al.*, 2007). A primary occurrence is associated with severe muscle spasms and stiffness (Codman, 1931; Hand *et al.*, 2007) and a secondary occurrence is associated with osteoarthritis or fractures (Hand *et al.*, 2007).

During the progression of the impingement symptoms, pain typically develops with a menacing onset over a period of weeks to months (Dias *et al.*, 2005). These symptoms are in response to proinflammatory cytokines, collagen accumulation by myofibroblast and fibroblasts and, synovial inflammation associated with capsular fibrosis which appear and resolve spontaneous over a period of months (Dias *et al.*, 2005; Ko and Wang, 2011).

2.3.5. Tendinopathy (Calcific tendinitis and calcific tendinosis)

Tendinopathy is a broad term, describing pathology in and pain, arising from a tendon but the definite cause remains uncertain (Lewis, 2009). However, certain mechanisms – intrinsic (which originates within the tendon itself, i.e. degeneration and calcification) and extrinsic (which originates outside the tendon itself, i.e. acromial irritation of the tendon) may attribute to this condition (Lewis, 2009). Tendinopathy includes but is not limited to, calcific tendinitis which is an intrinsic pathology of the GHJ associated with metabolic cellular pathways and soft tissue degeneration (ElShewy, 2016) and calcific tendinosis which is associated with deposition of hydroxyapatite (calcium builds up) (Hamada *et al.*, 2006; Lin *et al.*, 2015).

Calcific tendinitis of the shoulder is associated with decreased subcoracoacromial arch space leading to GHJ pain and disability (DePalma and Kruper, 1961; Gerber *et al.*, 1985). Calcific deposits, which are classified as Type I (acute) and Type II (chronic), increases the mechanical load across the RC tendons because of a decreased subcoracoacromial space and this is often associated with tendinopathy (Bosworth, 1941; Evolve, 2017). Calcium deposition essentially enlarges the coracoid's rounded end, precipitating entrapment of RC tendons

between the coracoid process and acromion tip which is further associated with decreased subcoracoacromial arch space (Gerber *et al.*, 1985).

The aetiology of calcific tendinosis is degenerative and metabolic, thus intrinsic mechanisms (Sansone *et al.*, 2016). Metabolic calcium and sodium channel dysfunction are associated with calcium deposition within the tendons (Evolve, 2017). This deposition often causes disproportionate mechanical load over the RC tendons leading to tendinitis (ElShewy, 2016; Sansone *et al.*, 2016).

Chapter 3: Methods and Materials

This study made use of three sample types in order to gather both skeletal-and soft tissue component data, which consisted of: 1) cadavers to gather skeletal-and soft tissue data; 2) retrospective X-ray images to gather skeletal data; and 3) retrospective MRI images to gather soft tissue data.

3.1. Sample

Cadaver sample

The sample used in this study comprised of thirteen male cadavers (n=13) where thirteen left shoulders (n=13) and thirteen right shoulders (n=13) were dissected. The sample's female cadavers were eleven (n=11), of which nine left shoulders (n=9) and nine right shoulders (n=9) were dissected. Of the remaining two female cadavers (n=2), only the one left shoulder of one female cadaver (n=1) could be dissected and one right shoulder of the other female cadaver (n=1) could be dissected. Thus, there is a cadaver sample of twenty-four cadavers, which included both male and female cadavers, (n=24). Twenty-two of the cadavers' left and right shoulders (n=22) were dissected, thus totalling to forty-four left and right cadaver shoulders (n=44). The remaining two female cadavers (n=2) alternate sides were dissected - one left shoulder, (n=1) and one right shoulder (n=1) giving a sample total of forty-six dissected male and female cadaver shoulders (n=46), which were selected from a sample of white South Africans (13 male; 11 female) (Table 3.1). Only adult cadavers (>25 years of age) were used in this study and were randomly selected, comprising of different body sizes, from the donated bodies used for undergraduate medical and dental students, and also for research within the Department of Anatomy (UP) (Ethical clearance 304/2017 – see Appendix A). Sex, age and population were recorded and not considered exclusion factors. Cadaver specimens that showed signs of surgery were excluded. The cadaveric component of this study is covered by the National Health Act, 61 of 2003.

Table 3.1. Demographic information for cadaver sample

Sample	Sample size (left and right)	Mean age (years)	95 % CI range
White female	20	68.9	61.59-76.22
White male	26	61	57.14-64.86

X-ray imaging sample

The sample for this part of the study comprised of a total of 94 X-ray images (n=94) taken from a South African sample; 42 black males, 22 black females, 17 white males and 13 white females (Ethical clearance 304/2017 – see Appendix A). X-ray images were obtained from the Department of Radiology at the Steve Biko Academic Hospital. The sample included individuals between 25 and 65 years of age with known shoulder injury or shoulder pathology (Table 3.2). Patients who underwent known shoulder surgeries were excluded. Only retrospective X-ray images were used.

Table 3.2. Demographic information for X-ray imaging sample

Sample	Sample size	Mean age (years)	95 % CI range
Black males	42	41.71	38.27-45.16
Black females	22	49.27	44.10-54.44
White males	17	41.12	35.45-46.78
White females	13	51.77	44.38-59.16

MRI imaging sample

This sample for the study comprised a total of 46 MRI images (n=46) taken from a white South African population; 26 white females and 20 white males (Table 3.3) (Ethical clearance 304/2017 – see Appendix A). MRI scans were obtained from the Department of Radiology at the Life Groenkloof Hospital (Little Company of Mary) and from the Department of Radiology at the Steve Biko Academic Hospital. The sample included individuals between 25 and 65 years of age with a known, diagnosed shoulder injury or shoulder pathology (Table 3.3). Patients who underwent previous known shoulder surgeries were excluded. Only retrospective MRI scan images were used and permission was obtained from the Chief Executive Officer of the Steve Biko Academic Hospital and the Head of Radiology.

Table 3.3. Demographic information for MRI imaging sample

Sample	Sample size	Mean age (years)	95 % CI range
White females	26	46.8	43.31-50.36
White males	20	41.2	37.57-45.88

During the MRI data collection diagnoses of pathologies were grouped to represent pathology groups within the sample. The diagnosis of GHJ pathologies were grouped into four categories according to the dominant factor within a diagnosis of the sample. The categories represent some of the common pathologies that have been discussed in Chapter 2: Literature Review, 2.3. GHJ pathologies. The groups are as follows:

Group 1: Tendinopathy of RC tendons due to calcifications and ACJ joint degeneration.

Group 2: Tears and degeneration of: glenoid labrum, GHJ ligaments and RC tendons with complications of tears and degeneration causing chronic instability and chronic dislocation of humeral head occur.

Group 3: Osteoarthritis and osteoporosis degenerative changes in acromion type.

Group 4: Adhesive capsulitis/impingement syndrome of GHJ capsule and osteoarthritic degenerative disease of glenoid fossa and humeral head within the capsule in the GHJ.

3.2. Methods

Cadaver sample procedures and measurements

The cadavers were placed in supine position. The muscles of the shoulder were exposed by removal of the skin with the underlying subcutaneous tissue. The deltoid was detached from its origin and reflected to its insertion on the humeral shaft which exposed the acromion, clavicle, humeral head and humeral shaft (Nakazawa *et al.*, 2016). Medially adjacent to the capsule axillary fold, the skin, subcutaneous fat, fascia and pectoralis muscle was dissected from the humerus to reveal the biceps (Nakazawa *et al.*, 2016). The acromion was partially cleaned of soft tissue on the superior and inferior surface.

The following observations and measurements were taken:

- Acromion type (AT): The shape of the bony inferior surface of the acromion to ascertain either a flat, round or hooked surface area to classify acromion type as Type I, II, III, according to the Bigliani-Morrison-April classification scale (Paraskevas *et al.*, 2008) (Fig. 3.1).

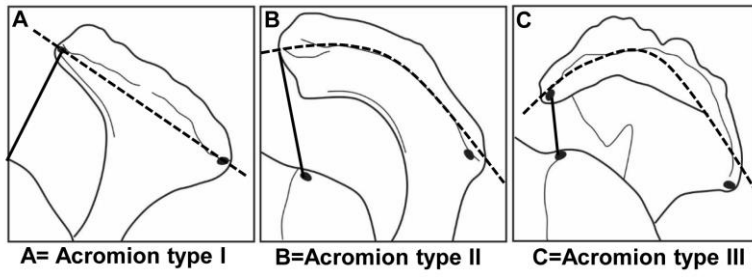


Figure 3.1. Acromial types - A = flat, B = round and C = hooked according to the Bigliani-Morrison-April scale (schematic) (adapted from Naidoo *et al.*, 2015)

- Acromial-humeral distance (AHD): Fascia and soft tissue were removed between the acromion and humeral head, anteriorly, to measure the acromial-humeral distance (AHD). The calibrated sliding calliper was placed on the bony acromion inferior edge and bony superior humeral head edge to measure this distance (Flatow *et al.*, 1994). (Fig. 3.2).

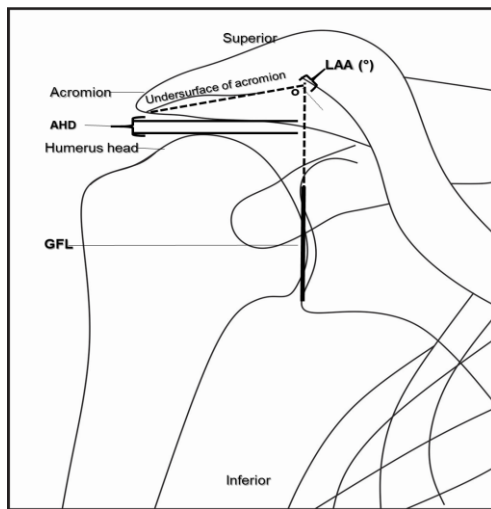


Fig. 3.2. Measuring the LAA-lateral acromion angle, AHD-acromial-humeral distance and GFL-glenoid fossa length in GHJ (schematic) (adapted from Hanciau *et al.*, 2012)

- Maximum humeral head diameter (HHMax_dia): The capsule was cut away to expose the whole humeral head. The RC muscles and the biceps brachii long head tendon were cut away until the humeral head was free to move out of the glenoid fossa and turned outwards to measure humeral head diameter with the calibrated sliding calliper (Boileau and Walch, 1997). (Fig. 3.3).

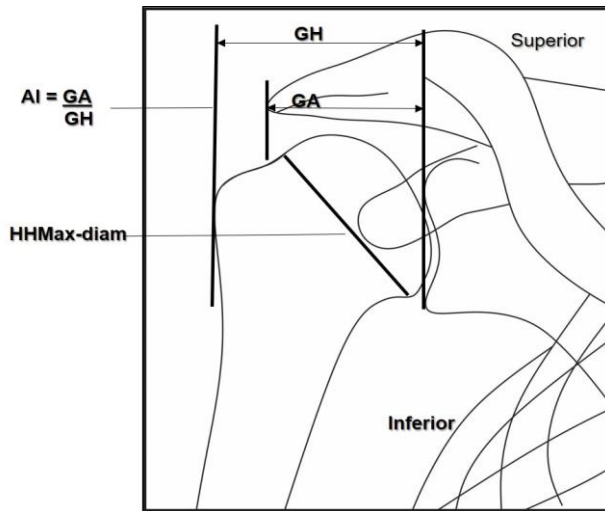


Fig. 3.3. Measuring of the AI-acromial index, GA-glenoacromial distance, GH-glenohumeral distance and HHMax_dia-maximum humeral head diameter in the GHJ (schematic) (adapted from Nyffeler *et al.*, 2006)

- Humeral head angle of inclination (HHI): An angle measured in degrees ($^{\circ}$). Two rulers were used. One was placed in the humeral head plane and one was placed in the plane of the humeral shaft. A protractor was used to measure the medial angle formed (Boileau and Walch, 1997). (Fig. 3.4).
- Intertubercular groove width (ITGW): The bicep tendon was located and cut to follow the path in the intertubercular groove. The capsule was cut away partially, from the humeral head. Intertubercular groove width was measured with a calibrated sliding calliper between the lesser and greater tuberculi of the humerus head (Chan *et al.*, 1991; Murlimanju *et al.*, 2012; Rajani and Man, 2013; Gupta *et al.*, 2014). (Fig. 3.4).

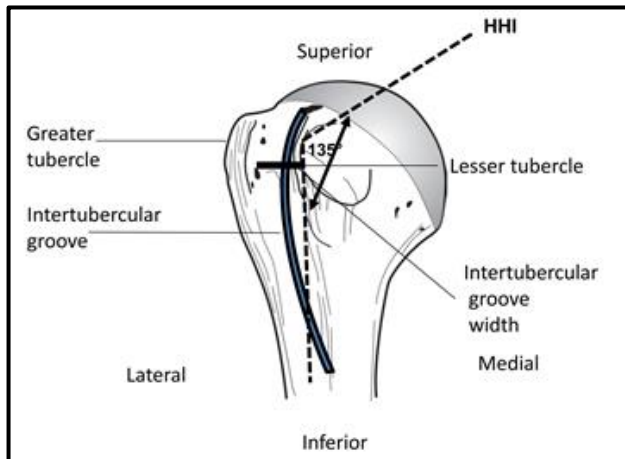


Fig. 3.4. Measuring of the ITGW-intertubercular groove width and HHI humeral head angle of inclination on the humeral head (schematic) (adapted from Rajani and Man, 2013)

- Glenoid fossa depth (GFD): A calibrated depth sliding calliper with a ruler was placed across the glenoid fossa to provide an anchor point for the depth measure instrument in order to obtain the depth measure (Howell and Galinat, 1989). (Fig. 3.5).

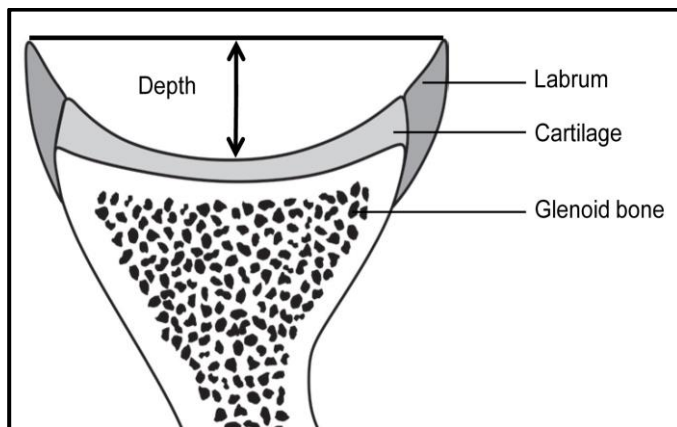


Fig. 3.5. Measuring of GFD-glenoid fossa depth (schematic) (adapted from Lippitt *et al.*, 2003)

X-ray imaging procedure and measurements

The CD with X-ray images downloaded onto it, was studied by using Agfa Impax EE CD viewer version: R20 XV SU2 HF1 on Windows 7. The following observations and measurements were taken:

- Acromion type (AT): Classification was done according to the Bigliani-Morrison-April classification scale as Type I, II and III acromion shapes (Aragão *et al.*, 2014; Paraskevas *et al.*, 2008). (Fig. 3.1).

- Acromial Index (AI): This index represents a ratio between two distances (a) and (b). The first distance (a) exists between the glenoid joint surface and the lateral border of the acromion (GA). The second distance (b) exists between the glenoid joint surface and the greater tubercle of the humeral head (GH). The AI is calculated by dividing (GA)/(GH). (Nyffeler *et al.*, 2006; Torrens *et al.*, 2007; Balke *et al.*, 2013; Gu and Yu, 2013). (Fig. 3.3).
- Glenoacromial distance (GA): The distance between the joint surface of the glenoid and the lateral border of the acromion (Hanciau *et al.*, 2012). (Fig. 3.3).
- Glenohumeral distance (GH): The distance between the glenoid and the lateral border of the greater tubercle (Hanciau *et al.*, 2012). (Fig. 3.3).
- Lateral acromion angle (LAA): This angle was measured with lines drawn on the image, between the subacromial surface and the joint surface of the glenoid (Hanciau *et al.*, 2012). The first line is a straight line that is drawn parallel on the under surface of the acromion and the second line is a straight line that is drawn from the inferior glenoid fossa rim, upwards towards the superior glenoid fossa rim, towards the acromion. At the point where the two lines intersect an angle is formed (Banas *et al.*, 1995; Nyffeler *et al.*, 2006). (Fig. 3.2).
- Acromioclavicular joint (ACJ) space: The joint was measured between the junction of the lateral clavicle and the acromion process of the scapula (Oppenheimer, 1943, Zanca, 1971; van der Helm, 1996; Buttaci *et al.*, 2004). (Fig. 3.6).

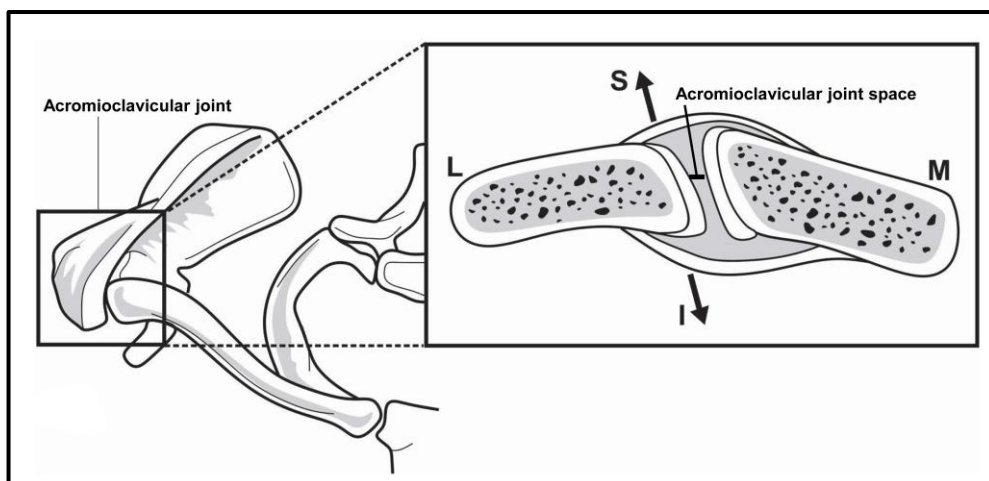


Fig. 3.6. Measuring of the ACJ-acromioclavicular space in the GHJ (schematic) (adapted from Zanca, 1971)

- Acromial-humeral distance (AHD): AHD represents the bone-to-bone distance. This distance is a space that exists between the under surface of the acromion and the humeral head. In the space between the acromion and the humeral head, soft tissue components such as the GHJ capsule, RC tendons and bursae are found. (Flatow *et al.*, 1994; Bdaiwi, 2014; França *et al.*, 2016). (Fig. 3.2).
- Glenoid fossa length (GFL): The superior to inferior length of the glenoid fossa (Lewis and Armstrong, 2011; Sarwar *et al.*, 2015; Rajendra *et al.*, 2016). (Fig 3.2).
- Maximum humeral head diameter (HHMax_dia): The distance at the anatomical neck measured from superior to inferior (Hertel *et al.*, 2002; Iyem *et al.*, 2017). (Fig. 3.3).
- Humeral head angle of inclination (HHI): An angle measured in degrees (°). This angle exists between the humerus shaft axis and the most superior articulation surface of the humeral head (Iyem *et al.*, 2017). Humeral head angle of inclination exists between the intersection of two lines. A line through the longitudinal axis of the humeral shaft (metaphyseal axis) and a line oblique from the most superior articulation point of the humeral head, connecting the two lines. An angle is formed and varies between 130 and 150 degrees and present with differences between sex groups and population groups (Hertel *et al.*, 2002; DeLude *et al.*, 2007; Matsumura *et al.*, 2016; Iyem *et al.*, 2017). (Fig. 3.4).

MRI imaging procedure and measurements

The CD with MRI scan images downloaded onto it, was studied by using a digital software programme GearViewpacsgear Osiri X launcher on Windows 7. The following observations and measurements were taken:

- Acromion type (AT): Classification was done according to the Bigliani-Morrison-April classification scale as Type I, II and III acromion shapes (Aragão *et al.*, 2014; Paraskevas *et al.*, 2008). (Fig.3.1).
- Acromial Index (AI): This index represents a ratio between two distances (a) and (b). The first distance (a) exists between the glenoid joint surface and the lateral border of the acromion (GA). The second distance (b) exists between the glenoid joint surface and the greater tubercle of the humeral head (GH). The AI is calculated by dividing (GA)/(GH). (Nyffeler *et al.*, 2006; Torrens *et al.*, 2007; Balke *et al.*, 2013; Gu and Yu, 2013). (Fig. 3.3).

- Glenoacromial distance (GA): The distance between the joint surface of the glenoid and the lateral border of the acromion (Hanciau *et al.*, 2012). (Fig. 3.3).
- Glenohumeral distance (GH): The distance between the glenoid and the lateral border of the greater tubercle (Hanciau *et al.*, 2012). (Fig. 3.3).
- Lateral acromion angle (LAA): An angle measured in degrees (°). This angle is measured with lines drawn on the image, between the subacromial surface and the joint surface of the glenoid (Banas *et al.*, 1995; Hanciau *et al.*, 2012). The first line is a straight line that is drawn parallel on the under surface of the acromion and the second line is a straight line that is drawn from the inferior glenoid fossa rim, upwards towards the superior glenoid fossa rim, towards the acromion. At the point where the two lines intersect an angle is formed (Banas *et al.*, 1995; Nyffeler *et al.*, 2006). (Fig. 3.2).
- Acromial-humeral distance (AHD): AHD represents the bone-to-bone distance. This distance is a space that exists between the under surface of the acromion and the superior humeral head surface. In the space between the acromion and the humeral head, soft tissue components such as the GHJ capsule, RC tendons and bursae are found. (Flatow *et al.*, 1994; Gu and Yu 2013; Yu *et al.*, 2013; Bdaiwi, 2014; França *et al.*, 2016). (Fig. 3.2).
- Glenoid fossa length (GFL): The superior to inferior distance of the glenoid fossa measured for length (Lewis and Armstrong, 2011; Sarwar *et al.*, 2015; Rajendra *et al.*, 2016). (Fig. 3.2).
- Maximum humeral head diameter (HHMax_diam): The distance at the anatomical neck measured from superior to inferior (Hertel *et al.*, 2002; Iyem *et al.*, 2017). (Fig. 3.3).
- Humeral head angle of inclination (HHI): An angle, measured in degrees (°). This exists between the humerus shaft axis and the most superior articulation surface of the humeral head (Iyem *et al.*, 2017). Humeral head angle of inclination exists between the intersection of two lines. A line through the longitudinal axis of the humeral shaft (metaphyseal axis) and a line oblique from the most superior articulation point of the humeral head, connecting the two lines. An angle is formed and varies between 130 to 150 degrees and present with differences between sex groups and population groups (Hertel *et al.*, 2002; DeLude *et al.*, 2007; Matsumura *et al.*, 2016; Iyem *et al.*, 2017). (Fig. 3.4).

- Acromioclavicular joint (ACJ) width: This joint was measured between the junction of the lateral clavicle and the acromion process of the scapula (van der Helm, 1996; Miyazaki *et al.*, 2014). (Fig. 3.6).
- RC tendons (RC): The SSP, IS, TM and SC were observed for pathology such as intactness, tears or avulsions (Huegel *et al.*, 2015). (Fig.3.7).

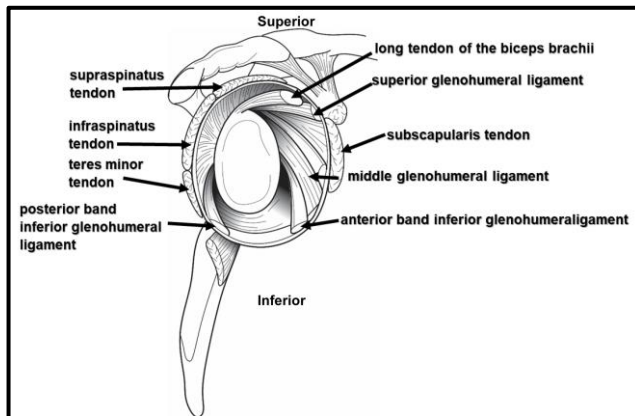


Fig. 3.7. Internal view of the RC-rotator cuff tendons and GHJ_Ligaments surrounding the glenoid fossa of the GHJ (schematic) (adapted from O' Brien *et al.*, 1990)

- Glenohumeral joint capsule (GHJ_C): The capsule was observed for pathology such as tears or impingement (Carmichael and Hart, 1985). (Fig. 3.8).

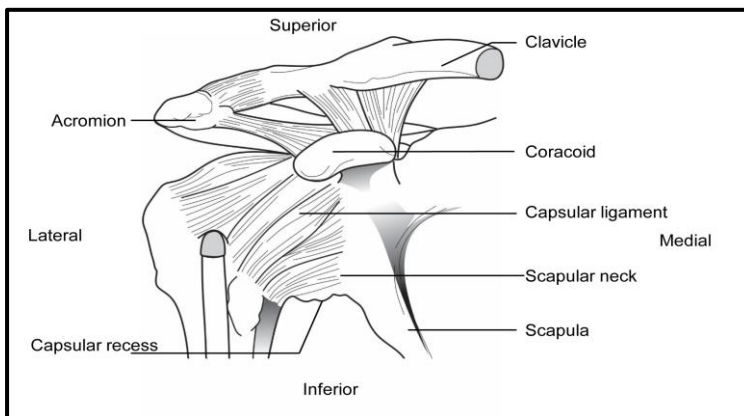


Fig. 3.8. GHJ_C-glenohumeral joint capsule (schematic) (adapted from Moore *et al.*, 2010)

- GHJ ligaments (GHJ_L): The SGHL, MGHL and IGHLC were observed for pathology such as tears, intactness and fraying (Lugo *et al.*, 2008). (Fig. 3.7).
- Glenoid labrum (GL): Existing pathology such as fraying and/or tears were observed and documented (Nishida *et al.*, 1996). (Fig. 3.9).

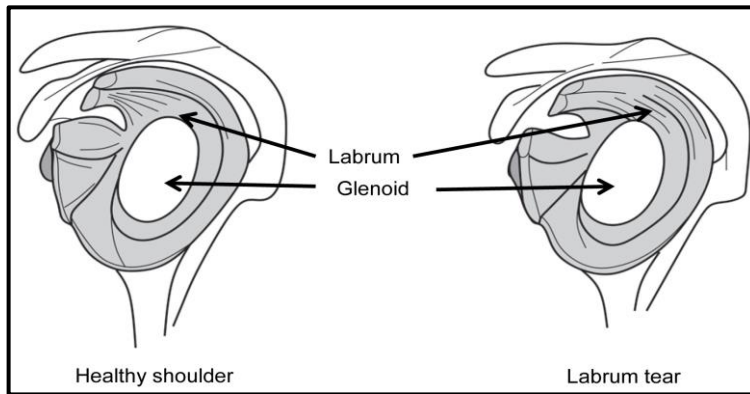


Fig. 3.9. Internal view of GL-glenoid labrum in a healthy shoulder and labrum tear (schematic) (adapted from Hata *et al.*, 1992)

3.4. Statistical Analysis

Statistical analyses for the morphometric skeletal- and soft tissue measurements were done with STATA version 14.0, statistical analysis software programme, after data was sorted on an Excel spreadsheet (Pinzon, 2016). Statistical analysis commonly assumes that a random variable (e.g. sex) is normally distributed in data (Park, 2002). This normality assumption is essential for insight into descriptive statistics, which provides important information by means of sex or age, mean, standard deviation (SD), standard error (SE) and 95% Confidence Interval of the data (Park, 2002). Deviations from normality (non-normality), render those statistical tests inaccurate, therefore it is of importance to know if data is normal or non-normal (Park, 2002). The Shapiro-Wilk W test for normality was run, which is a universal normality test, to detect all deviations from normality. A $p\text{-value} < 0.05$ for this test rejects the hypothesis of normality (Shapiro and Wilk, 1965).

Probability of relationship was analysed by means of the Fisher exact test, between two nominal variables e.g. sex and AT (Tea, 1981). The $p\text{-value}$ of 0.05, for the Fisher exact test is the probability value assigned to ascertain whether the result is greater or smaller than the $p\text{-value}$ of 0.05 (Tea, 1981; Dahiru, 2008). $P\text{-value}$ or probability value is a number between 0 and 1 and an alpha of 0.05 is used as the cut-off point for significance (Dahiru, 2008). A $p\text{-value} < 0.05$ indicated that the means of the two groups differed significantly (Dahiru, 2008).

A two-sample t-test with unequal and equal variances and Kruskal-wallis equality-of-populations rank test, were statistical tests used to compare group means (Park, 2009). The two-sample t-test was used because of the distributions of the respective variables and to test if the

means of the two respective groups are the same (Park, 2009). The two-sample t-test's, p-value or probability ($p < 0.05$), measured how probable it was that an observed difference, between two groups, were due to coincidence (Dahiru, 2008).

The Kruskal-wallis is a non-parametric test, with an assigned p-value > 0.05 , which measures effect size and tests for equality of medians in STATA (Kruskal and Wallis, 1952). Kruskal-wallis tests were used in the MRI sample for non-parametric variables (Park, 2009). These variables had distributions which were either not normally distributed or where outliers were a problem (Kruskal and Wallis, 1952). The Kruskal-wallis test only indicated that differences existed between two groups of an independent variable on a continuous dependant variable (Park, 2009). The p-value tested if the two groups had the same distribution, specifically with respect to location (median) (Park, 2009). A p-value < 0.05 indicated that the two groups differed with respect to the variable of interest (Park, 2009). The Mann-Whitney is a non-parametric test, with an assigned p-value > 0.05 , which measures effect size and tests for equality of medians in STATA (Pettitt, 1979; Conroy, 2012). The Mann-Whitney test was used because some morphometric variables in the cadaver-, X-ray and MRI samples had distributions which were either skewed or not normally distributed (Conroy, 2012).

A chi-square (r^2) value was used with the Kruskal-wallis test, to test group differences in proportions when a contingency table was created (Green and Salkind, 2008). Chi-square statistic was calculated by comparing observed rate of recurrence and expected rate of recurrence (Polit and Beck, 2012).

3.4.1. Intra-and Interobserver error (repeatability tests)

Repeatability tests were conducted to achieve the aim of intra- and interobserver error tests and to test the repeatability of the proposed method. The results are presented in Table 4.26 and Table 4.27. The primary observer and an external observer determined whether the observer is able to repeat his/her own results. The interobserver error was done and tests whether the results can be reproduced by anyone trying to make use of the proposed method.

In order to test the repeatability, 14 X-ray images and 10 MRI images (male and female) were randomly chosen from the study sample and re-analysed and compared to the original results. The time between reanalysis varied from a month to six months. The interobserver test was done by an experienced anatomist.

Chapter 4: Results

In order to evaluate the skeletal- and soft tissue components of the GHJ several statistical procedures were used. The study's sample descriptive statistics which include the mean, median, standard deviation and 95% confidence intervals were determined. Normality tests using the Shapiro-Wilk test was run to determine if the data were normally distributed. Two sample t-tests were run to investigate possible differences between all parameters by sex and population in the study sample. Raw measurements for all the data are provided in Appendices B, C and D.

4.1. Cadaver component

4.1.1. Normality tests

Table 4.1. Normality tests for data distribution for the measured variables (AHD, HHMax_dia, HHI, ITGW and GFD) in the cadaver sample

Variable	Sex	Side	N	p-value**
AHD*	M	L	13	0.1816
		R	13	0.0264
	F	L	10	0.5920
		R	10	0.8005
HHMax_dia	M	L	13	0.4460
		R	13	0.8078
	F	L	10	0.8595
		R	10	0.7638
HHI*(°)	M	L	13	0.0308
		R	13	0.0218
	F	L	10	0.0002
		R	10	0.0000
ITGW	M	L	13	0.6000
		R	13	0.0310
	F	L	10	0.7039
		R	10	0.8291
GFD	M	L	13	0.2568
		R	13	0.8865
	F	L	10	0.5585
		R	10	0.6524

*Key: N = number of individuals, M = male, F = female, L = left, R = right, AHD = acromial-humeral distance, HHMax_dia = maximum humeral head diameter, HHI = humeral head angle of inclination, ITGW = intertubercular groove width, GFD = glenoid fossa depth, *non-parametric data, **Shapiro-Wilk normality test*

In Table 4.1 it is clear that only the AHD for the male's right side ($p=0.0264$) and the HHI for both males ($p=0.0022$) and females ($p=0.0000$) did not have a normal distribution. Normal distributions are observed for all other variables measured ($p>0.05$) (Table 4.1).

4.1.2. Descriptive statistics

Acromial type

Table 4.2 shows that the male sample had a higher ratio for the occurrence of AT I than AT II compared to the female sample who showed a more even ratio of occurrence of AT I to AT II. Out of the whole sample, AT I was the most common type identified, with no difference observed between left and right distributions in the males and in the females ($p=1$; $p=0.6531$) (Table 4.2).

Table 4.2. Frequency distribution of acromial types (AT) present in the male and female cadaver sample

Sex	Side	AT I	AT II	Total	Fisher's exact p-value
Male	L	11	2	13	1
	R	11	2	13	
TOTAL		22	4	26	
Female	L	5	5	10	0.6531
	R	6	4	10	
TOTAL		11	9	20	
SAMPLE TOTAL		33	13	46	
<i>Key: L = left, R = right, AT = acromion type</i>					

Morphometric variables

Similar means were seen between males and females for all measured variables except the HHMax_dia, which was much larger in males (± 49 mm) compared to the females ($\pm 43-46$ mm) (Table 4.3). No significant differences were noted between left and right sides in each of the male and female sample group $p>0.05$ and therefore for the comparative analysis, left and right sides were pooled together for males and for females (Table 4.3).

Table 4.3. Summary statistics with Mann-Whitney test of the morphometric skeletal variables (AHD, ITGW, HHI, HHMax_dia and GFD) measured in the cadaver sample

Variable	Sex	Side	N	Mean	SE	SD	95% CI	p-value
AHD	Female	L	10	4.49	0.27	0.84	3.89-5.09	0.1678
		R	10	3.86	0.35	1.11	3.06-4.65	
	Male	L	13	4.36	0.29	1.05	3.73-5.00	0.4118*
		R	13	4.42	0.34	1.22	3.68-5.15	
ITGW	Female	L	10	6.39	0.49	1.56	5.27-7.51	0.4804
		R	10	5.86	0.53	1.69	4.66-7.07	
	Male	L	13	5.64	0.35	1.28	4.87-6.41	0.3939
		R	13	5.15	0.44	1.57	4.21-6.10	
HHI (°)	Female	L	10	132.20	1.17	3.71	129.55-134.85	0.8979*
		R	10	131.50	0.90	2.84	129.47-133.53	
	Male	L	13	130.77	0.36	1.30	129.98-131.56	0.5233*
		R	13	130.69	0.57	2.06	129.45-131.94	
HHMax_dia	Female	L	10	43.64	1.33	4.20	40.64-46.644	0.3319
		R	10	45.47	1.27	4.01	42.61-48.34	
	Male	L	13	49.64	1.17	4.22	47.09-52.19	0.8087
		R	13	49.15	1.63	5.87	4.61-52.69	
GFD	Female	L	10	4.16	0.59	1.87	2.83-5.50	0.2570
		R	10	5.58	1.06	3.36	3.18-7.98	
	Male	L	13	4.95	0.59	2.14	3.66-6.24	0.6642
		R	13	5.32	0.62	2.22	3.98-6.67	

*Key: N = number of individuals, SD = standard deviation, SE = standard error, CI = confidence interval, AHD = acromial-humeral distance, ITGW = intertubercular groove width, HHI = humeral head angle of inclination, HHMax_dia = maximum humeral head diameter, GFD-glenoid fossa depth, L = left, R = right, p-value – two-sample t-test, *Mann-Whitney p-value due to non-parametric data distribution*

4.1.3. Comparative statistics

Contingency tables were constructed to look at possible differences between, 1) AT in the male and female sample and 2) AT versus shoulders with pathologies and shoulders without pathologies.

Normal data was run through a two-sample t-test while a Mann-Whitney U test was conducted on the non-parametric data to determine if differences existed in the variable measurements (AHD, HHMax_dia, HHI, ITGW and GFD) between males and females and also if differences existed between variable measurement and the two types of acromial shapes observed in the sample.

Acromial type: Contingency tables

The results in Table 4.4 indicate that there is a significant difference in the ratio of acromial types between the male and female sample group ($p=0.046$). As mentioned in section 4.1.1, males tend to have a significantly higher occurrence of AT I than AT II, where females have a more even distribution between the two types (Table 4.2).

Table 4.4. Contingency table for AT occurrence between males and females in the cadaver sample using the Fisher's exact test

Sex	AT I	AT II	Total	Fisher's exact p-value
	N	N	N	
Female	11	9	20	0.046
Male	22	4	26	
Total	33	13	46	

Key: N = sample size, AT = acromion type

The results in Table 4.5 indicate that there is a significant difference in the ratio of AT in the non-pathology and pathology groups both in the male and female sample group as well as a significant difference between male and female groups ($p<0.05$). (Table 4.5). From this table it is clear that for AT I the chances of having pathology are minimal compared to an AT II where there is a higher percentage of pathology associated with this acromial type; this can be seen in both the female and male group ($p<0.001$).

Table 4.5. Contingency table for AT occurrence between non-pathology/pathology in males and females in the cadaver sample using the Fisher's exact test

Sex	Condition	AT I	AT II	Total	p-value	Fisher's exact p-value
		N	N	N		
Female	NP	11	2	13	<0.001	0.000
	P	0	7	7		
TOTAL		11	9	20		
Male	NP	22	0	22	<0.001	
	P	0	4	4		
TOTAL		22	4	26		
SAMPLE TOTAL		33	13	46		

Key: N = sample size, NP = non-pathology, P = pathology, AT = acromion type

Morphometric variables

Males and females showed no significant differences ($p>0.05$) between most variables measured except for the HHMax_dia ($p=0.0010$) (Table 4.6). Males showed a significantly larger humeral head diameter (49.40 ± 5.01 mm) when compared to the female sample (44.56 ± 4.10 mm) (Table 4.6).

Table 4.6. Two sample t-test/Mann-Whitney tests comparing male and female variable measurements in the cadaver sample

Variable	Sex	N	Mean	SE	SD	95% CI	p-value
AHD	Male	26	4.39	0.22	1.12	3.94-4.84	0.4921*
	Female	20	4.17	0.23	1.01	3.70-4.65	
HHMax_dia	Male	26	49.40	0.98	5.01	47.37-51.42	0.0010
	Female	20	44.56	0.92	4.10	42.64-46.48	
HHI (°)	Male	26	130.73	0.33	1.69	130.05-131.41	0.3772*
	Female	20	131.85	0.72	3.23	130.34-133.36	
ITGW	Male	26	5.40	0.28	1.42	4.82-5.97	0.1098
	Female	20	6.13	0.36	1.61	5.38-6.88	
GFD	Male	26	5.14	0.42	2.15	4.27-6.00	0.7163
	Female	20	4.87	0.61	2.74	3.59-6.16	

Key: N = number of individuals, SD = standard deviation, SE = standard error, CI = confidence interval, AHD = acromial-humeral distance, HHMax_dia = maximum humeral head diameter, HHI = humeral head angle of inclination, ITGW = intertubercular groove width, GFD = glenoid fossa depth, * Mann-Whitney test used for HHI

No differences were noted for the majority of the variables measured when grouped into acromial types (Table 4.7). The only measured variables that showed significant difference between AT I and AT II was the HHMax_dia in the male sample, and the GFD (males and females combined). With AT I specimens, the HHMax_dia in males was significantly larger (50.21 ± 4.53 mm) than the diameter observed in AT II (44.94 ± 5.88 mm). The GFD appears to be significantly deeper with an AT I (5.80 ± 2.31 mm) than an AT II (3.06 ± 1.24 mm) (Table 4.7).

No differences were noted in the majority of the measured variables when comparing the shoulders identified with pathology versus those without pathology ($p>0.05$) (Table 4.8). The only variables that showed significant differences were the HHMax_dia in the male sample, where shoulders with pathologies showed a significantly smaller diameter (44.94 ± 5.88 mm) compared to the shoulder without pathologies (50.21 ± 4.53 mm) (Table 4.8). The second variable that showed significant differences between the pathology and without pathology group was the GFD, where a significantly ($p=0.0000$) shallower depth was noted in the shoulder

with pathologies (Table 4.8).

Table 4.7. Two sample t-test and Mann-Whitney test comparing male and female variable measurements with AT in the cadaver sample

Variable	Sex	AT	N	Mean	SE	SD	95% CI	p-value
AHD	***	I	33	4.12	0.19	1.12	3.72-4.52	0.0854
		II	13	4.74	0.22	0.80	4.25-5.22	
HHMax_dia	Male	I	22	50.21	0.97	4.53	48.20-52.21	0.0500*
		II	4	44.94	2.94	5.88	35.59-54.30	
	Female	I	11	44.40	1.27	4.20	41.58-47.22	0.8554
		II	9	44.75	1.41	4.22	41.51-48.00	
HHI (°)	***	I	33	131.27	0.49	2.79	130.28-132.26	0.7459**
		II	13	131.08	0.47	1.71	130.05-132.11	
ITGW	***	I	33	5.63	0.23	1.33	5.16-6.10	0.5643
		II	13	5.92	0.56	2.01	4.71-7.14	
GFD	***	I	33	5.80	0.40	2.31	4.98-6.61	0.0002
		II	13	3.06	0.34	1.24	2.30-3.81	

*Key: N = sample number, SE = standard error, SD = standard deviation, CI = confidence interval, AHD = acromial-humeral distance, HHMax_dia = maximum humeral head diameter, ITGW = intertubercular groove width, GFD = glenoid fossa depth, * HHMax_dia showed significant difference between males and females and thus were kept separate for t-test, ** Mann-Whitney test used for HHI due to non parametric data, *** male and female sample combined due to no significant difference in measurements*

Table 4.8. Comparative tests (t-test & Mann-Whitney) comparing variable measurements between shoulders with pathology versus shoulders without pathologies in the cadaver sample

Variable	Sex	Condition	N	Mean	SE	SD	95% CI	p-value
AHD	***	NP	35	4.18	0.19	1.13	3.79-4.56	0.1782*
		P	11	4.68	0.22	0.74	4.18-5.17	
HHMax_dia**	Male	NP	22	50.21	0.97	4.53	48.20-52.21	0.0513
		P	4	44.94	2.94	5.88	35.59-54.30	
	Female	NP	13	44.01	1.10	3.98	41.60-46.41	0.4302
		P	7	45.57	1.68	4.44	41.47-49.68	
HHI (°)	***	NP	35	131.2	0.46	2.72	130.3-132.1	0.4683*
		P	11	131.3	0.54	1.79	130.1-132.5	
ITGW	***	NP	35	5.56	0.23	1.34	5.10-6.02	0.2171
		P	11	6.21	0.61	2.03	4.85-7.58	
GFD	***	NP	35	5.76	0.38	2.25	5.00-6.53	0.0000
		P	11	2.68	0.25	0.83	2.12-3.24	

*Key: N = sample number, SE = standard error, SD = standard deviation, CI = confidence interval, AHD = acromial-humeral distance, HHMax_dia = maximum humeral head diameter, ITGW = intertubercular groove width, GFD = glenoid fossa depth, HHI = humeral head angle of inclination, (°)- degrees, *Mann-Whitney test used for HHI due to non parametric data, NP=no-pathology, P=pathology **HHMax_dia showed significant difference between males and females and thus were kept separate for t-test, *** male and female sample combined due to no significant difference between groups*

4.2. X-ray imaging component

4.2.1. Normality tests

Table 4.9. Normality tests for data distribution for the measured variables (AI, GA, GH and LAA) in the X-ray sample

Variable	Sex	Side	N	p-value*
AI	BM	L	14	0.8887
		R	28	0.1103
	BF	L	12	0.8225
		R	10	0.0418
	WM	L	5	0.5838
		R	12	0.7828
	WF	L	8	0.3035
R		5	0.9414	
GA	BM	L	14	0.1996
		R	28	0.8735
	BF	L	12	0.6849
		R	10	0.6152
	WM	L	5	0.8566
		R	12	0.8787
	WF	L	8	0.7811
R		5	0.5366	
GH	BM	L	14	0.1138
		R	28	0.0252
	BF	L	12	0.4150
		R	10	0.4956
	WM	L	5	0.4204
		R	12	0.1030
	WF	L	8	0.9775
R		5	0.0367	
LAA (°)	BM	L	14	0.0055
		R	28	0.1312
	BF	L	12	0.2393
		R	10	0.2236
	WM	L	5	0.6843
		R	12	0.4220
	WF	L	8	0.8431
R		5	0.6195	
<p>Key: N = number of individuals, AI = acromial index, GA = glenoacromial distance, GH = glenohumeral distance, LAA = lateral acromial angle, (°)- degrees, BM = black male, BF = black female, WM = white male, WF = white female, L = left, R = right, *Shapiro-Wilk normality test</p>				

Table 4.10. Normality tests for data distribution for the measured variables (ACJ, AHD, GFL, HHMax_dia and HHI) in the X-ray sample

Variable	Sex	Side	N	p-value*
ACJ	BM	L	14	0.0083
		R	28	0.0467
	BF	L	12	0.4663
		R	10	0.4418
	WM	L	5	0.0287
		R	12	0.0963
WF	L	8	0.3174	
	R	5	0.7596	
AHD	BM	L	14	0.3927
		R	28	0.6703
	BF	L	12	0.4365
		R	10	0.8016
	WM	L	5	0.9287
		R	12	0.0248
WF	L	8	0.2065	
	R	5	0.6858	
GFL	BM	L	14	0.6223
		R	28	0.2634
	BF	L	12	0.1522
		R	10	0.5772
	WM	L	5	0.8740
		R	12	0.3493
WF	L	8	0.7072	
	R	5	0.2159	
HHmax_dia	BM	L	14	0.2656
		R	28	0.3149
	BF	L	12	0.0918
		R	10	0.9105
	WM	L	5	0.2384
		R	12	0.7296
WF	L	8	0.1318	
	R	5	0.1180	
HHI (°)	BM	L	14	0.8487
		R	28	0.9421
	BF	L	12	0.0068
		R	10	0.7408
	WM	L	5	0.8381
		R	12	0.5538
WF	L	8	0.1782	
	R	5	0.2692	

Key: N = number of individuals, ACJ = acromioclavicular joint, AHD = acromial-humeral distance, GFL = glenoid fossa length, HHMax_dia = maximum humeral head diameter, HHI = humeral head angle of inclination, (°)- degrees, BM = black male, BF = black female, WM = white male, WF = white female, L = left, R = right, *Shapiro-Wilk normality test

In Table 4.9 it is clear that the AI for black females' right side ($p=0.0418$); the GH for black males' right side ($p=0.0252$) and white females' right side ($p=0.0367$) as well as the LAA for black males left side ($p=0.0055$) did not have a normal distribution of data. Normal distribution was observed for all other variables measured ($p>0.05$) (Table 4.9).

In Table 4.10 it is clear that the ACJ for black males' right side ($p=0.0467$) and white males left side ($p=0.0287$); the AHD for white males' right side ($p=0.0248$) and HHI for black females left side ($p=0.0068$) did not have normal distribution. Normal distribution was observed for all other variables measured ($p>0.05$) (Table 4.10).

4.2.2. Descriptive statistics

Acromial type

Table 4.11 shows that the white male sample had a slightly higher ratio for the occurrence of AT I than AT II compared to the black male sample, who showed a higher percentage for the occurrence of AT II than AT I or AT III. The white and black female sample showed a higher ratio of occurrence of AT I compared to the occurrence of AT II (Table 4.11).

In general AT I was the most common type represented in the sample total with AT II represented as the second most common type (Table 4.11). In this sample AT I representation in the white female population was the most with black male AT I the least representative (Table 4.11). AT II was however the most representative in the black male population with AT II in white female population the least representative (Table 4.11). AT III was not present in the white population at all. No significant differences between black males and white males, and between black females and white females were noted with regard to distribution of AT ($p>0.05$).

Table 4.11. Contingency table for AT between sex and side in X-ray sample using the Fisher's exact test

Sex	Side	AT I	AT II	AT III	Total	Fisher's exact p-value
Black male	L	7	6	1	14	0.6653
	R	12	15	1	28	
TOTAL		<u>19</u>	<u>21</u>	<u>2</u>	<u>42</u>	
White male	L	2	3	0	9	0.6199
	R	7	5	0	8	
TOTAL		<u>9</u>	<u>8</u>	<u>0</u>	<u>17</u>	
Black female	L	7	4	1	12	1.0000
	R	5	4	1	10	
TOTAL		<u>12</u>	<u>8</u>	<u>2</u>	<u>22</u>	
White female	L	7	1	0	8	0.5105
	R	3	2	0	5	
TOTAL		<u>10</u>	<u>3</u>	<u>0</u>	<u>13</u>	
SAMPLE TOTAL		46	44	4	94	

Key: L = left, R = right, AT = acromion type

Morphometric variables

Similar means were seen between left and right sides in both the male and female groups for all measured variables except the AI and ACJ (Tables 4.12 and 4.13). The AI was significantly larger ($p=0.0318$) on the right side (0.87 ± 0.08 mm) compared to the left sides (0.78 ± 0.10 mm) in the black females (Table 4.12). The ACJ was significantly larger ($p=0.0478$) in black males left side (9.94 ± 8.86 mm) versus the right side (5.13 ± 2.92 mm), and significantly larger in the white female left side (7.68 ± 3.92 mm) compared to the right side (3.08 ± 1.93 mm; $p=0.0341$) (Table 4.13).

Table 4.12. Summary statistics with Mann-Whitney test of morphometric skeletal variables (AI, GA, GH and LAA) measured in the X-ray sample

Variable	Sex	Side	N	Mean	SE	SD	95% CI	p-value
AI	BM	L	14	0.78	0.03	0.10	0.72-0.84	0.4237
		R	28	0.81	0.02	0.12	0.76-0.85	
	BF	L	12	0.78	0.03	0.10	0.72-0.85	0.0318*
		R	10	0.87	0.03	0.08	0.81-0.93	
	WM	L	5	0.69	0.02	0.04	0.65-0.74	0.3609
		R	12	0.75	0.04	0.13	0.67-0.83	
	WF	L	8	0.76	0.04	0.11	0.67-0.85	0.9611
		R	5	0.76	0.06	0.02	0.60-0.92	
GA	BM	L	14	40.50	1.08	4.05	38.16-42.83	0.4148
		R	28	41.7	0.88	4.67	39.90-43.51	
	BF	L	12	40.33	1.64	5.68	36.72-43.95	0.9392
		R	10	40.48	0.65	2.05	39.01-41.95	
	WM	L	5	39.94	1.93	4.31	34.59-45.30	0.5788
		R	12	38.46	1.47	5.10	35.22-41.70	
	WF	L	8	38.23	2.11	5.96	33.24-43.21	0.9631
		R	5	38.38	2.39	5.34	31.75-45.02	
GH	BM	L	14	52.23	1.37	5.12	49.27-55.18	0.8728*
		R	28	51.80	1.17	6.16	49.41-54.19	
	BF	L	12	51.38	1.83	6.34	47.35-55.42	0.0669
		R	10	46.71	1.46	4.61	43.41-50.01	
	WM	L	5	57.64	2.61	5.83	50.40-64.88	0.0588
		R	12	51.76	1.51	5.24	48.43-55.09	
	WF	L	8	50.15	1.41	3.98	46.83-53.48	0.8835*
		R	5	50.74	3.11	6.96	42.10-59.38	
LAA (°)	BM	L	14	72.4	5.18	19.37	61.22-83.58	0.9362*
		R	28	74.1	2.01	10.66	69.97-78.24	
	BF	L	12	71.30	3.29	11.41	64.05-78.55	0.7089
		R	10	69.63	2.77	8.76	63.36-75.90	
	WM	L	5	81.42	2.16	4.82	75.44-87.40	0.9862
		R	12	81.53	4.00	13.85	72.73-90.34	
	WF	L	8	72.26	4.52	12.78	61.58-82.95	0.8525
		R	5	70.90	5.44	12.16	55.80-86.00	

Key: N = number of individuals, AI = acromial index, GA = glenoacromial distance, GH = glenohumeral distance, LAA = lateral acromial angle, (°)- degrees, BM = black male, BF = black female, WM = white male, WF = white female, L = left, R = right, *Mann-Whitney p-value due to non-normal distribution

Table 4.13. Summary statistics with Mann-Whitney test of morphometric skeletal variables (ACJ, AHD, GFL, HHMax_dia and HHI) measured in the X-ray sample

Variable	Sex	Side	N	Mean	SE	SD	95% CI	p-value
AHD	BM	L	14	10.39	0.87	3.27	8.50-12.28	0.3963
		R	28	11.43	0.73	3.86	9.93-12.92	
	BF	L	12	10.29	1.26	4.37	7.52-13.07	0.7091
		R	10	10.86	0.63	2.00	9.43-12.29	
	WM	L	5	10.56	0.47	1.05	9.26-11.86	0.3703*
		R	12	11.03	0.89	9.43	9.07-12.98	
	WF	L	8	12.36	0.94	2.66	10.14-14.58	0.0922
		R	5	8.98	1.80	4.02	3.99-13.97	
ACJ	BM	L	14	9.94	2.37	8.86	4.83-15.06	0.0478*
		R	27	5.13	0.56	2.92	3.98-6.28	
	BF	L	12	4.86	0.88	3.04	2.93-6.79	0.5269
		R	10	5.54	0.47	1.49	4.48-6.60	
	WM	L	5	3.58	0.73	1.62	1.56-5.60	0.1134*
		R	12	6.07	0.96	3.33	3.95-8.18	
	WF	L	8	7.68	1.38	3.92	4.40-10.95	0.0341
		R	5	3.08	0.86	1.93	0.68-5.48	
GFL	BM	L	14	36.79	1.18	4.26	34.22-39.37	0.7765
		R	28	37.23	0.88	4.67	35.42-39.04	
	BF	L	12	32.27	0.79	2.74	30.53-34.01	0.0769
		R	10	34.76	1.12	3.54	32.23-37.29	
	WM	L	5	40.76	2.01	4.48	35.19-46.33	0.6720
		R	12	41.83	1.37	4.73	38.83-44.84	
	WF	L	8	36.64	1.35	3.81	33.45-39.82	0.4293
		R	5	34.80	1.85	4.13	29.68-39.92	
HHMax_dia	BM	L	14	49.74	0.96	3.61	47.66-51.83	0.7378
		R	28	49.26	0.89	4.69	47.44-51.08	
	BF	L	12	43.83	1.05	3.62	41.52-46.13	0.7796
		R	10	44.29	1.29	4.07	41.38-47.20	
	WM	L	5	55.06	2.15	4.80	49.11-61.02	0.2375
		R	12	51.81	1.45	5.03	48.62-55.00	
	WF	L	8	44.86	1.26	3.58	41.87-47.85	0.4468
		R	5	46.28	0.99	2.22	43.52-49.04	
HHI (°)	BM	L	14	139.96	1.59	5.94	136.53-143.39	0.5565
		R	28	138.87	1.03	5.45	136.76-140.98	
	BF	L	12	138.94	3.85	13.34	130.46-147.42	0.9737
		R	10	137.18	1.75	5.54	133.22-141.14	
	WM	L	5	142.2	2.96	6.62	133.99-150.41	0.5482
		R	12	140.49	1.33	4.61	137.56-143.42	
	WF	L	8	141.93	1.73	4.90	137.83-146.02	0.8409
		R	5	142.48	1.98	4.43	136.98-147.98	

Key: N = number of individuals, AHD = acromial-humeral distance, ACJ = acromioclavicular joint width, GFL = glenoid fossa length, HHMax_dia = maximum humeral head diameter, HHI = humeral head angle of inclination, (°)- degrees, BM = black male, BF = black female, WM = white male, WF = white female, L = left, R = right, *Mann-Whitney p-value due to non-normal distribution

4.2.3. Comparative statistics

Contingency tables were constructed to look at possible differences between, 1) AT in the male and female population groups with regard to side and 2) AT versus shoulders with pathologies and shoulders without non-pathologies.

Normal data was run through a two-sample t-test while a Mann-Whitney U test was conducted on the non-parametric data to determine if differences existed in the variable measurements (AI, GA, GH, LAA, ACJ, GFL, AHD, HHMax_dia, and HHI) between males and females and then also if differences existed between variable measurement and the two types of acromial shapes.

Acromial type: Contingency tables

Table 4.14. Contingency table for AT between sex and side in the X-ray sample using the Fisher's exact test

Sex	Side	AT I	AT II	AT III	Total	Fisher's exact p-value	Fisher's exact p-value
Black male	L	7	6	1	14	0.5350	0.1056
	R	12	15	1	28		
TOTAL		<u>19</u>	<u>21</u>	<u>2</u>	<u>42</u>		
Black female	L	7	4	1	12	0.2595	
	R	5	4	1	10		
TOTAL		<u>12</u>	<u>8</u>	<u>2</u>	<u>22</u>		
White male	L	2	3	0	9	0.2595	
	R	7	5	0	8		
TOTAL		<u>9</u>	<u>8</u>	<u>0</u>	<u>17</u>		
White female	L	7	1	0	8		
	R	3	2	0	5		
TOTAL		<u>10</u>	<u>3</u>	<u>0</u>	<u>13</u>		
SAMPLE TOTAL		46	44	4	94		
<i>Key: L = left, R = right, AT = acromion type</i>							

Table 4.14 shows that no differences between the distribution of acromial types between the black males and black females, between the white males and white females or between the black population group and the white population group exist ($p > 0.05$). In general, all groups showed a higher distribution of AT I than AT II, with only the black males and black females presenting with four AT III (Table 4.14).

Morphometric variables

The only variables that showed no significant differences ($p>0.05$) between the male and female groups across both populations was the GA, GH and AHD. All other variables (AI, LAA, GFL, ACJ, HHMax_dia and HHI) showed significant differences between some of the comparison groups (Tables 4.15 and 4.16).

The AI was significantly larger ($p=0.0390$) in black males (0.80 ± 0.11 mm) compared to white males (0.73 ± 0.11 mm) and larger ($p=0.0098$) in the black female right sides (0.87 ± 0.08 mm) compared to the white females (0.76 ± 0.11 mm) (Table 4.15). The LAA was significantly larger in white males (81.50 ± 11.7) when compared to black males (73.54 ± 13.94) and white females (71.74 ± 12.05) ($p=0.01823$ and $p=0.0338$) (Table 4.15). The GFL showed significant differences for all comparison groups; BM vs WM ($p=0.0120$), BF vs WF ($p=0.0479$), BM vs BF ($p=0.0012$) and WM vs WF (0.0014) (Table 4.16). In general, the GFL was larger in the white (41.52 ± 4.55 mm) and black (37.09 ± 4.50 mm) male groups compared to the white (35.93 ± 3.87 mm) and black (33.40 ± 3.30 mm) females (Table 4.16).

The ACJ was significantly larger in the white female left side (7.68 ± 3.92 mm) and in the black male left side (9.94 ± 8.86 mm) when both were compared to black females (5.17 ± 2.43 mm) (Table 4.16). The only comparison group that showed no significant difference with regard to the HHMax_dia was the black females and white females ($p=0.2740$). Significant differences were observed between the black males and white males ($p=0.0130$), between the black males and black females ($p=0.0000$) and between the white males and white females ($p=0.0000$). White males displayed the largest HHMax_dia (52.76 ± 5.04 mm) compared to the black males (49.42 ± 4.32 mm), black females (44.04 ± 3.74 mm) and white females (45.41 ± 3.10 mm) (Table 4.16).

The HHI was significantly larger ($p=0.0153$) in the white female group (142.14 ± 4.54) compared to the black females (138.14 ± 10.35) (Table 4.16). No other differences were noted for the HHI between the other comparison groups ($p>0.05$).

Table 4.15. Comparative tests (t-test & Mann-Whitney) comparing variable measurements between population groups and side for AI, GA, GH and LAA in the X-ray sample

Variable	Group	Side	N	Mean	SE	SD	95% CI	p-value
AI	BM	*	42	0.80	0.02	0.11	0.76-0.83	0.0390
	WM	*	17	0.73	0.03	0.11	0.67-0.79	
	BF	L	12	0.78	0.03	0.10	0.72-0.85	0.5741
	WF	*	13	0.76	0.03	0.11	0.69-0.83	
	BF	R	10	0.87	0.03	0.08	0.81-0.93	0.0098**
	WF	*	13	0.76	0.03	0.11	0.69-0.83	
	BM	*	42	0.80	0.02	0.11	0.76-0.83	0.7194
	BF	L	12	0.78	0.03	0.10	0.72-0.85	
	BM	*	42	0.80	0.02	0.11	0.76-0.83	0.0668
BF	R	10	0.87	0.03	0.08	0.81-0.93		
WM	*	17	0.73	0.03	0.11	0.67-0.79	0.4454	
WF	*	13	0.76	0.03	0.11	0.69-0.83		
GA	BM	*	42	41.30	0.69	4.46	39.91-42.69	0.0717
	WM	*	17	38.90	1.16	4.80	36.43-41.36	
	BF	*	22	40.40	0.92	4.33	38.48-42.32	0.2155
	WF	*	13	38.29	1.53	5.50	34.96-41.61	
	BM	*	42	41.30	0.69	4.46	39.91-42.69	0.4427
	BF	*	22	40.40	0.92	4.33	38.48-42.32	
WM	*	17	38.90	1.16	4.80	36.43-41.36	0.7487	
WF	*	13	38.29	1.53	5.50	34.96-41.61		
GH	BM	*	42	51.95	0.89	5.78	50.15-53.75	0.5579**
	WM	*	17	53.49	1.44	5.92	50.45-56.53	
	BF	*	22	49.26	1.28	5.99	46.60-51.92	0.5766**
	WF	*	13	50.38	1.40	5.05	47.33-53.43	
	BM	*	42	51.95	0.89	5.78	50.15-53.75	0.0860**
	BF	*	22	49.26	1.28	5.99	46.60-51.92	
WM	*	17	53.49	1.44	5.92	50.45-56.53	0.1401**	
WF	*	13	50.38	1.40	5.05	47.33-53.43		
LAA (°)	BM	*	42	73.54	2.15	13.94	69.19-77.88	0.0183**
	WM	*	17	81.50	2.85	11.74	75.47-87.54	
	BF	*	22	70.54	2.15	10.09	66.07-75.01	0.7542
	WF	*	13	71.74	3.34	12.05	64.46-79.02	
	BM	*	42	73.54	2.15	13.94	69.19-77.88	0.3762**
	BF	*	22	70.54	2.15	10.09	66.07-75.01	
WM	*	17	81.50	2.85	11.74	75.47-87.54	0.0338	
WF	*	13	71.74	3.34	12.05	64.46-79.02		

Key: N = number of individuals, AI = acromial index, GA = glenoacromial distance, GH = glenohumeral distance, LAA = lateral acromial angle, (°)- degrees, BM = black male, BF = black female, WM = white male, WF = white female, L = left, R = right, *left and right combined due to no significant difference, p-value – two sample t-test or **Mann-Whitney p-value

Table 4.16. Comparative tests (t-test & Mann-Whitney) comparing variable measurements between population groups and sides for ACJ, AHD, GFL, HHMax_dia and HHI in the X-ray sample

Variable	Group	Side	N	Mean	SE	SD	95% CI	p-value
ACJ	BM	L	14	9.94	2.37	8.86	4.83-15.06	0.0739**
	WM	*	17	5.34	0.75	3.10	3.74-6.93	
	BM	R	27	5.13	0.56	2.92	3.98-6.28	0.9232**
	WM	*	17	5.34	0.75	3.10	3.74-6.93	
	BF	*	22	5.17	0.52	2.43	4.09-6.25	0.0438
	WF	L	8	7.68	1.38	3.92	4.40-10.95	
	BF	*	22	5.17	0.52	2.43	4.09-6.25	0.0860
	WF	R	5	3.08	0.86	1.93	0.68-5.48	
	BM	L	14	9.94	2.37	8.86	4.83-15.06	0.0514**
	BF	*	22	5.17	0.52	2.43	4.09-6.25	
	BM	R	27	5.13	0.56	2.92	3.98-6.28	0.8016**
	BF	*	22	5.17	0.52	2.43	4.09-6.25	
WM	*	17	5.34	0.75	3.10	3.74-6.93	0.1225**	
WF	L	8	7.68	1.38	3.92	4.40-10.95		
WM	*	17	5.34	0.75	3.10	3.74-6.93	0.0997**	
WF	R	5	3.08	0.86	1.93	0.68-5.48		
AHD	BM	*	42	11.08	0.57	3.67	9.94-12.22	0.9933**
	WM	*	17	10.89	0.63	2.61	9.55-12.23	
	BF	*	22	10.55	0.73	3.43	9.03-12.07	0.6760
	WF	*	13	11.06	0.98	3.53	8.93-13.19	
	BM	*	42	11.08	0.57	3.67	9.94-12.22	0.5761
	BF	*	22	10.55	0.73	3.43	9.03-12.07	
WM	*	17	10.89	0.63	2.61	9.55-12.23	0.7856**	
WF	*	13	11.06	0.98	3.53	8.93-13.19		
GFL	BM	*	41	37.09	0.70	4.50	35.67-38.51	0.0012
	WM	*	17	41.52	1.10	4.55	39.18-43.86	
	BF	*	22	33.40	0.70	3.30	31.94-34.86	0.0479
	WF	*	13	35.93	1.07	3.87	33.59-38.27	
	BM	*	41	37.09	0.70	4.50	35.67-38.51	0.0012
	BF	*	22	33.40	0.70	3.30	31.94-34.86	
WM	*	17	41.52	1.10	4.55	39.18-43.86	0.0014	
WF	*	13	35.93	1.07	3.87	33.59-38.27		
HHMax_dia	BM	*	42	49.42	0.67	4.32	48.07-50.77	0.0130
	WM	*	17	52.76	1.22	5.04	50.17-55.36	
	BF	*	22	44.04	0.80	3.74	42.38-45.70	0.2740
	WF	*	13	45.41	0.86	3.10	45.53-47.28	
	BM	*	42	49.42	0.67	4.32	48.07-50.77	0.0000
	BF	*	22	44.04	0.80	3.74	42.38-45.70	
WM	*	17	52.76	1.22	5.04	50.17-55.36	0.0000	
WF	*	13	45.41	0.86	3.10	45.53-47.28		
HHI (°)	BM	*	42	139.23	0.86	5.57	137.50-140.97	0.2648
	WM	*	17	140.99	1.24	5.12	138.36-143.63	
	BF	*	22	138.14	2.21	10.35	133.55-142.73	0.0153**

Variable	Group	Side	N	Mean	SE	SD	95% CI	p-value
	WF	*	13	142.14	1.26	4.54	139.39-144.88	
	BM	*	42	139.23	0.86	5.57	137.50-140.97	0.2160**
	BF	*	22	138.14	2.21	10.35	133.55-142.73	
	WM	*	17	140.99	1.24	5.12	138.36-143.63	0.5298
	WF	*	13	142.14	1.26	4.54	139.39-144.88	

*Key: N = number of individuals, ACJ = acromioclavicular joint, AHD = acromial-humeral distance, GFL = glenoid fossa length, HHMax_dia = maximum humeral head diameter, HHI = humeral head angle of inclination, (°)- degrees, BM = black male, BF = black female, WM = white male, WF = white female, L = left, R = right, *left and right combined due to no significant difference, **Mann-Whitney p-value*

4.3. MRI imaging component

4.3.1. Normality tests

In Table 4.17 it is clear that the AI for the white females right side ($p=0.0233$), GA for the white males right side ($p=0.0249$) and white females right side ($p=0.0224$), ACJ for the white males left side ($p=0.0263$), AHD for the white females left side ($p=0.0121$) and HHMax_dia for white females left side ($p=0.0445$) did not have a normal distribution. Normal distributions are observed for all other variables measured ($p>0.05$) (Table 4.17).

Table 4.17. Normality tests for data distribution for the measured variables (AI, GA, GH and LAA) in the MRI sample

Variable	Sex	Side	N	p-value
AI	WM	L	9	0.9769
		R	11	0.1068
	WF	L	14	0.4758
		R	12	0.0233
GA	WM	L	9	0.9451
		R	11	0.0249
	WF	L	14	0.6932
		R	12	0.0224
GH	WM	L	9	0.8993
		R	11	0.5974
	WF	L	14	0.4511
		R	12	0.0516
LAA (°)	WM	L	9	0.9513
		R	11	0.5709
	WF	L	14	0.1446
		R	12	0.1112
ACJ	WM	L	9	0.0263
		R	11	0.1077
	WF	L	14	0.1811
		R	12	0.2896
GFL	WM	L	8	0.0766
		R	11	0.1721
	WF	L	14	0.9638
		R	12	0.6076
AHD	WM	L	9	0.1748
		R	11	0.4661
	WF	L	14	0.0121
		R	12	0.0683
HHMax_dia	WM	L	9	0.2345
		R	11	0.8548
	WF	L	14	0.0445
		R	12	0.7767
HHI (°)	WM	L	9	0.2429
		R	11	0.5586
	WF	L	14	0.0620
		R	12	0.5442

Key: N = number of individuals, AI = acromial index, GA = glenoacromial distance, GH = glenohumeral distance, LAA = lateral acromial angle, (°)- degrees, ACJ = acromioclavicular joint width, GFL = glenoid fossa length, AHD = acromial-humeral distance, HHMax_dia = maximum humeral head diameter, HHI = humeral head angle of inclination, WM = white male, WF = white female, L = left, R = right

4.3.2. Descriptive statistics

Acromial type

Table 4.18 shows that both the male and female samples had a higher ratio for the occurrence of AT I than AT II. Only the female sample presented with two AT III. In general, AT I was the most common type to present in this MRI sample with no difference observed between left and right distributions in the males and in the females or between the AT distributions between the sexes ($p=0.3357$) (Table 4.18).

Table 4.18. Contingency table for AT between males and the females left and right side in the MRI sample using Fisher's exact test

Sex	Side	AT I	AT II	AT III	Total	Fisher's exact p-value	Fisher's exact p-value
Male	L	7	6	0	13	0.4439	0.3357
	R	5	2	0	7		
TOTAL		<u>12</u>	<u>8</u>	<u>0</u>	<u>20</u>		
Female	L	9	4	1	14	0.9762	
	R	8	3	1	12		
TOTAL		<u>17</u>	<u>7</u>	<u>2</u>	<u>26</u>		
SAMPLE TOTAL		29	15	2	46		

Key: L = left, R = right, AT = acromion type

Morphometric variables

Similar means were seen between the left and right sides in both the male and female groups for all measured variables except the GH, LAA and ACJ (Tables 4.19 and 4.20). The GH on the right side in the white females was significantly larger (47.09 ± 3.04 mm) compared to the left side (44.21 ± 3.77 mm) ($p=0.0445$). The LAA and ACJ was observed to be significantly larger (LAA; $p=0.0165$ and ACJ; $p=0.0432$) on the left side (LAA; 83.14 ± 5.02 mm and ACJ; 5.86 ± 1.99 mm) in the white females when compared to the right side (LAA; 78.17 ± 4.76 mm and ACJ; 4.42 ± 1.31 mm) (Tables 4.19 and 4.20).

Table 4.19. Summary statistics with Mann-Whitney test of morphometric skeletal variables (AI, GA, GH and LAA) measured in the MRI sample

Variable	Sex	Side	N	Mean	SE	SD	95% CI	p-value
AI	WM	L	9	0.60	0.03	0.10	0.53-0.68	0.5308
		R	11	0.63	0.01	0.05	0.59-0.66	
	WF	L	14	0.68	0.02	0.08	0.63-0.72	0.9589**
		R	12	0.66	0.03	0.09	0.60-0.72	
GA	WM	L	9	31.90	1.48	4.45	28.48-35.32	0.5918**
		R	11	33.64	1.17	3.88	31.03-36.24	
	WF	L	14	30.07	1.07	4.01	27.76-32.39	0.3368**
		R	12	31.17	1.17	4.06	28-59-33.75	
GH	WM	L	9	52.89	1.16	3.48	50.21-55.56	0.7179
		R	11	53.46	1.02	3.39	51.18-55.73	
	WF	L	14	44.21	1.01	3.77	42.04-46.39	0.0445
		R	12	47.09	0.88	3.04	45.16-49.02	
LAA (°)	WM	L	9	83.33	1.91	5.72	78.93-87.73	0.8726
		R	11	83.82	2.19	7.28	78.93-88.71	
	WF	L	14	83.14	1.34	5.02	80.24-86.04	0.0165
		R	12	78.17	1.38	4.76	75.14-81.19	

*Key: N = number of individuals, SE = standard error, SD = standard deviation, CI = confidence interval, AI = acromial index, GA = glenoacromial distance, GH = glenohumeral distance, LAA = lateral acromial angle, (°)- degrees, WM = white male, WF = white female, L = left, R = right, **Mann-Whitney p-value due to non-normal distribution*

Table 4.20. Summary statistics with Mann-Whitney test of morphometric skeletal variables (ACJ, AHD, GFL, HHMax_dia and HHI) measured in the MRI sample

Variable	Sex	Side	N	Mean	SE	SD	95% CI	p-value
ACJ	WM	L	9	5.11	0.42	1.27	4.14-6.09	0.4323**
		R	11	5.64	0.45	1.50	4.63-6.65	
	WF	L	14	5.86	0.53	1.99	4.71-7.01	0.0432
		R	12	4.42	0.38	1.31	3.58-5.25	
AHD	WM	L	9	9.00	0.91	2.74	6.90-11.11	0.7133
		R	11	8.64	0.47	1.57	7.58-9.69	
	WF	L	14	8.00	0.39	1.47	7.15-8.85	0.2657**
		R	12	7.67	0.33	1.16	6.93-8.40	
GFL	WM	L	9	36.50	1.89	5.35	32.03-40.97	0.3704
		R	11	34.36	1.43	4.74	31.18-37.55	
	WF	L	14	29.50	1.20	4.50	26.90-32.10	0.0857
		R	12	32.67	1.29	4.48	29.82-35.51	
HHMax_dia	WM	L	9	48.22	1.32	3.96	45.17-51.27	0.7626
		R	11	48.73	1.03	3.41	46.44-51.02	
	WF	L	14	41.50	0.63	2.35	40.15-42.85	0.4336**
		R	12	42.50	0.54	1.88	41.30-43.70	
HHI (°)	WM	L	9	136.44	1.68	5.03	132.58-140.31	0.5931
		R	11	135.45	0.95	3.13	133.34-137.55	
	WF	L	14	135.36	1.27	4.77	132.61-138.11	0.5902
		R	12	136.42	1.48	5.13	133.16-139.67	

Key: N = number of individuals, SE = standard error, SD = standard deviation, CI = confidence interval, ACJ = acromioclavicular joint width, AHD = acromial-humeral distance, GFL = glenoid fossa length, HHMax_dia = maximum humeral head diameter, HHI = humeral head angle of inclination, (°)- degrees, WM = white male, WF = white female, L = left, R = right, **Mann-Whitney p-value due to non-normal distribution

4.3.3. Comparative statistics

Normal data was run through a two-sample t-test while a Mann-Whitney U test was conducted on the non-parametric data to determine if differences existed in the variable measurements (AI, GA, GH, LAA, ACJ, GFL, AHD, HHMax_dia and HHI) between males and females and then also if differences existed between left and right sides. A Kruskal-wallis test was conducted on the non-parametric data to determine if differences existed in the variable's measurements (AI, GA, GH, LAA, ACJ, GFL, AHD, HHMax_dia and HHI) between: 1) 1,2,3 and 4 pathology groups and 2) the intact and fray/tear glenoid labrum.

Morphometric variables

In Tables 4.21 and 4.22 it can be seen that no significant differences were noted between the male and female groups for the GA, ACJ, AHD and HHI ($p>0.05$). Variables that showed significant differences between males and females included the AI, GH, LAA, GFL and the HHMax_dia (Tables 4.21 and 4.22).

The AI was observed to be larger in white females (0.67 ± 0.09 mm) compared to the white males (0.62 ± 0.07 mm, $p=0.0094$). The GH was larger in white males (53.20 ± 3.35 mm) compared to the white females left side (44.21 ± 3.77 mm, $p=0.0000$) as well as the right side (47.09 ± 3.04 , $p=0.0000$). The LAA was also significantly larger ($p=0.0171$) in the white males' right side (83.60 ± 6.46) compared to white females' right side (78.17 ± 4.76); no difference was noted between the white males left side and white females left side ($p=0.8260$) (Table 4.21).

The GFL and HHMax_dia were significantly larger (GFL; $p=0.0037$ and HHMax_dia; $p=0.0000$) in white males (GFL; 35.30 ± 4.85 mm and HHMax_dia; 48.50 ± 3.58 mm) compared to the white females (GFL; 30.96 ± 4.69 mm and HHMax_dia; 41.96 ± 2.16 mm) (Table 4.22).

Table 4.21. Comparative tests (t-test & Mann-Whitney) comparing variable measurements between males and females and side for AI, GA, GH and LAA in the MRI sample

Variable	Sex	Side	N	Mean	SE	SD	95% CI	p-value
AI	WM	*	20	0.62	0.02	0.07	0.58-0.65	0.0094**
	WF	*	26	0.67	0.02	0.09	0.64-0.70	
GA	WM	*	20	32.86	0.92	4.13	30.92-34.79	0.0707**
	WF	*	26	30.58	0.78	3.99	28.97-32.19	
GH	WM	*	20	53.20	0.75	3.35	51.63-54.77	0.0000
	WF	L	14	44.21	1.01	3.77	42.04-46.39	
	WM	*	20	53.20	0.75	3.35	51.63-54.77	0.0000
	WF	R	12	47.09	0.88	3.04	45.16-49.02	
LAA (°)	WM	*	20	83.60	1.44	6.46	80.58-86.62	0.8260
	WF	L	14	83.14	1.34	5.02	80.24-86.04	
	WM	*	20	83.60	1.44	6.46	80.58-86.62	0.0171
	WF	R	12	78.17	1.38	4.76	75.14-81.19	

Key: N = number of individuals, SE = standard error, SD = standard deviation, CI = confidence interval, AI = acromial index, GA = glenoacromial distance, GH = glenohumeral distance, LAA = lateral acromial angle, (°) - degrees, WM = white male, WF = white female, L = left, R = right, *left and right combined, **Mann-Whitney p-value

Table 4.22. Comparative tests (t-test & Mann-Whitney) comparing variable measurements between males and females and side for ACJ, AHD, GFL, HHMax_dia and HHI in the MRI sample

Variable	Sex	Side	N	Mean	SE	SD	95% CI	p-value
ACJ	WM	*	20	5.40	0.31	1.39	4.75-6.05	0.6027**
	WF	L	14	5.86	0.53	1.99	4.71-7.01	
	WM	*	20	5.40	0.31	1.39	4.75-6.05	0.1096**
	WF	R	12	4.42	0.38	1.31	3.58-5.25	
AHD	WM	*	20	8.80	0.47	2.12	7.81-9.79	0.1704**
	WF	*	26	7.85	0.26	1.32	7.31-8.38	
GFL	WM	*	20	35.30	1.10	4.85	33.03-37.57	0.0037
	WF	*	26	30.96	0.92	4.69	29.07-32.85	
HHMax_dia	WM	*	20	48.50	0.80	3.58	46.83-50.17	0.0000**
	WF	*	26	41.96	0.42	2.16	41.09-42.84	
HHI (°)	WM	*	20	135.90	0.90	4.01	134.02-137.77	0.9712
	WF	*	26	135.85	0.95	4.86	133.88-137.81	

Key: N = number of individuals, SE = standard error, SD = standard deviation, CI = confidence interval, ACJ = acromioclavicular joint width, AHD = acromial-humeral distance, GFL = glenoid fossa length, HHMax_dia = maximum humeral head diameter, HHI = humeral head angle of inclination, (°)- degrees, WM = white male, WF = white female, L = left, R = right, *left and right combined, **Mann-Whitney p-value

Table 4.23 shows the pathology groups 1,2,3 and 4 compared to morphometric variables. No significant differences ($p>0.05$) are observed for all measured morphometric variables (Tables 4.23). Table 4.24 shows that the means for the GH, LAA, AHD and GFL did not differ significantly between the intact glenoid labrum compared to the fray/tear glenoid labrum ($p>0.05$) and therefore they were grouped together for a single mean (Table 4.25). Only the AI, GA and ACJ showed significant differences between their mean values. The AI shows a significant difference in the means between the intact glenoid labrum (0.69 ± 0.06 mm) when compared to the fray/tear glenoid labrum (0.62 ± 0.09 mm; $p=0.0169$). The GA distance is larger in the intact glenoid labrum (33.54 ± 4.16 mm) when compared to the fray/tear glenoid labrum (30.61 ± 4.14 mm; $p=0.0363$), whereas the ACJ distance tends to be smaller with the intact glenoid labrum (4.38 ± 1.04 mm) when compared to the fray/tear glenoid labrum (5.64 ± 1.71 mm; $p=0.0181$) (Table 4.24).

Table 4.23. Kruskal-wallis test comparing pathology groups 1,2,3 and 4 and variable measurements in the MRI sample

Variable	Path group	N	Median	r ²	d	iqr	p-value
AI	1,2,3,4	46	0.637	3.281	3	0.60-0.69	0.3502
GA	1,2,3,4	46	31	0.637	3	30-34	0.8879
GH	1,2,3,4	46	49	2.314	3	45-53	0.5098
LAA (°)	1,2,3,4	46	82	2.127	3	78-86	0.5465
ACJ	1,2,3,4	46	5	1.398	3	4-6	0.7061
AHD	1,2,3,4	46	8	3.540	3	7-9	0.3156
GFL	1,2,3,4	46	33	2.267	3	29-36	0.5189
HHMax_dia	1,2,3,4	46	43.5	0.915	3	42-48	0.8218
HHI (°)	1,2,3,4	46	135.5	4.935	3	132-138	0.1766

Key: N = sample size, pathology groups = 1,2,3,4, r² = chi squared, df = degree of freedom, iqr = interquartile range, AI = acromial index, GA = glenoacromial distance, GH = glenohumeral distance, LAA = lateral acromion angle, (°)- degrees, ACJ = acromioclavicular joint, AHD = acromial-humeral distance, GFL = glenoid fossa length, HHMax_dia = maximum humeral head diameter, HHI = humeral head angle of inclination, (°)- degrees

Table 4.24. Two-sample t-tests comparing the glenoid labrum (intact, fray/tear) and AI, GA, GH, LAA, ACJ, AHD and GFL in the MRI sample

Variable	GL	N	Mean	SE	SD	95 % CI	p-value
AI	Intact	13	0.69	0.02	0.06	0.65-0.73	0.0169
	Fray/tear	33	0.62	0.02	0.09	0.59-0.66	
GA	Intact	13	33.54	1.15	4.16	31.03-36.05	0.0363
	Fray/tear	33	30.61	0.72	4.14	29.14-32.08	
GH	Intact	46	48.87	0.77	5.20	47.33-50.41	0.6492
	Fray/tear	46	48.87	0.77	5.20	47.33-50.41	
LAA (°)	Intact	46	82.04	0.88	5.99	80.26-83.82	0.2658
	Fray/tear	46	82.04	0.88	5.99	80.26-83.82	
ACJ	Intact	13	4.38	0.29	1.04	3.75-5.02	0.0181
	Fray/tear	33	5.64	0.30	1.71	5.03-6.24	
AHD	Intact	46	8.28	0.26	1.76	7.76-8.80	0.9019
	Fray/tear	46	8.28	0.26	1.76	7.76-8.80	
GFL	Intact	46	32.78	0.76	5.16	31.25-34.31	0.2039
	Fray/tear	46	32.78	0.76	5.16	31.25-34.31	

Key: N = number of individuals, GL = glenoid labrum, SE = standard error, SD = standard deviation, CI = confidence interval, AI = acromial index, GA = glenoacromial distance, GH = glenohumeral distance, LAA = lateral acromion angle, (°)- degrees, ACJ = acromioclavicular joint width, AHD = acromial-humeral distance, GFL = glenoid fossa length

Table 4.25 shows the intact glenoid labrum compared to the fray/tear glenoid labrum with no significant differences (p=0.3113) for the HHI variable. The HHMax_dia in the sample with an intact glenoid labrum was smaller (43 mm) when compared to the fray/tear glenoid labrum (45 mm; p=0.0383) in the same sample (Table 4.25).

Table 4.25. Kruskal-wallis test comparing the glenoid labrum (intact, fray/tear) and HHMax_dia and HHI in the MRI sample

Variable	GL	N	Median	r ²	df	iqr	p-value
HHMax_dia*	Intact	13	43	4.293	1	41.44	0.0383
	Fray/tear	33	45			42-49	
HHI (°)*	Intact	46	135.5	1.033	1	132-138	0.3113
	Fray/tear						

*Key: N = number of individuals, GL = glenoid labrum, r² = chi squared, df = degree of freedom, iqr = interquartile range, HHMax_dia = maximum humeral head diameter, HHI = humeral head angle of inclination, (°)- degrees, *non-parametric data*

4.4. Intra- and Interobserver error (repeatability tests)

Intraclass Correlation Coefficient measurements are presented in Tables 4.26 to 4.29 as intra- and interobserver results for X-ray and MRI samples. Intraclass Correlation Coefficient is one test that is capable of assessing the repeatability of a method. The ideal result for these tests is to obtain a value of 1.00, which would indicate a 100% repeatability of the method.

Table 4.26 shows the intraobserver results for the X-ray sample. The highest correlation with regard to the intraobserver error was noted for the AI, GH, ACJ, AHD and GFL (r=1) and the lowest for the GA (r=0.9969). In general, the most reliable variables to measure would be the AI, GH, ACJ, AHD and GFL; the most unreliable would be the average glenoacromial distance. The intra observer's results were compared to the original results and tabulated. (Table 4.26). (See Appendix C)

Table 4.26. Intraclass Correlation Coefficient and confidence interval test for the intraobserver results of the X-ray sample

Variable	ICC (r)	95 % CI
AI	1	
GA	0.9969	0.9906-0.9989
GH	1	
LAA (°)	0.9998	0.9995-0.9999
ACJ	1	
AHD	1	
GFL	1	
HHMax_dia	0.9999	0.9999-0.9999
HHI (°)	0.9995	0.9986-0.9998

Key: ICC = intraclass correlation coefficient, CI = confidence interval, AI = acromial index, GA = glenoacromial distance, GH = glenohumeral distance, LAA = lateral acromion angle, ACJ = acromioclavicular joint width, AHD = acromial-humeral distance, GFL = glenoid fossa length, HHMax_dia = maximum humeral head diameter, HHI = humeral head angle of inclination, (°)- degrees,

Table 4.27 shows the analysis of the intraobserver results for the MRI sample. The highest correlation in the sex-pooled sample shows the percentage of AI, GH, LAA, AHD, GFL and HHMax_dia (r=1) and the lowest for the ACJ (r=0.9705). In general, all the measurements seem to be reliable of which AI, GH, LAA, AHD, GFL and HHMax_dia (r=1) would be the most reliable variable to measure given the small sample number used to check intraobserver reliability (Table 4.27). (See Appendix D).

Table 4.27. Intraclass Correlation Coefficient and confidence interval test for the intraobserver results of the MRI sample

Variable	ICC (r)	95 % CI
AI	1	
GA	0.9999	0.9997-0.9999
GH	1	
LAA (°)	1	
ACJ	0.9705	0.8929-0.9925
AHD	1	
GFL	1	
HHMax_dia	1	
HHI (°)	1	

Key: ICC = intraclass correlation coefficient, CI = confidence interval, AI = acromial index, GA = glenoacromial distance, GH = glenohumeral distance, LAA = lateral acromion angle, ACJ-acromioclavicular joint width, AHD = acromial-humeral distance, GFL = glenoid fossa length, HHMax_dia = maximum humeral head diameter, HHI = humeral head angle of inclination, (°)- degrees,

Table 4.28 shows the interobserver results for the X-ray sample. The highest correlation with regard to the interobserver error was noted for the GH ($r=0.9980$) and the lowest for the LAA ($r=0.9113$). In general, the most reliable variables to measure would be the GH, ACJ and HHI; the most unreliable would be the average lateral acromion angle. The interobserver's results were compared to the original results, with the highest correlation coefficient derived for ($r=0.9980$) GH and the lowest ($r=0.9113$) for LAA (Table 4.28). (See Appendix C).

Table 4.28. Intraclass Correlation Coefficient and confidence interval test for the interobserver results of the X-ray sample

Variable	ICC (r)	95 % CI
AI	0.9169	0.7617-0.9725
GA	0.9858	0.9579-0.9953
GH	0.9980	0.9940-0.9993
LAA (°)	0.9113	0.7546-0.9703
ACJ	0.9974	0.9982-0.9992
AHD	0.9830	0.9494-0.9944
GFL	0.9951	0.9704-0.9987
HHMax_dia	0.9920	0.9732-0.9975
HHI (°)	0.9969	0.9987-0.9990

Key: ICC = intraclass correlation coefficient, CI = confidence interval, AI = acromial index, GA = glenoacromial distance, GH = glenohumeral distance, LAA = lateral acromion angle, ACJ = acromioclavicular joint width, AHD = acromial-humeral distance, GFL = glenoid fossa length, HHMax_dia = maximum humeral head diameter, HHI = humeral head angle of inclination, (°)- degrees,

Table 4.29 shows the analysis of the interobserver results for the MRI sample. The highest correlation in the sex-pooled sample shows ($r=0.9999$) for GA and the lowest ($r=0.9336$) for GFL. Given the small sample size used to check interobserver reliability the most reliable variable to measure will be the GA (Table 4.29). (See Appendix D)

Table 4.29. Intraclass Correlation Coefficient and confidence interval test for the interobserver results of the MRI sample

Variable	ICC (r)	95 % CI
AI	0.9932	0.9748-0.9983
GA	0.9999	0.9997-0.9999
GH	0.9974	0.9905-0.9993
LAA (°)	0.9989	0.9961-0.9997
ACJ	0.9485	0.8104-0.9869
AHD	0.9688	0.8871-0.9920
GFL	0.9336	0.7648-0.9829
HHMax_dia	0.9798	0.9210-0.9949
HHI (°)	0.9934	0.9740-0.9983

Key: ICC = intraclass correlation coefficient, CI = confidence interval, AI = acromial index, GA = glenoacromial distance, GH = glenohumeral distance, LAA = lateral acromion angle, ACJ-acromioclavicular joint width, AHD = acromial-humeral distance, GFL = glenoid fossa length, HHMax_dia = maximum humeral head diameter, HHI = humeral head angle of inclination, (°)- degrees

Chapter 5: Discussion

Research has defined numerous musculoskeletal disorders involving the GHJ, with some of these disorders having correlations to the osseous anatomy of the scapula and proximal humerus (Boileau and Walch, 1997, Wilk *et al.*, 1997, McClure and Michener, 2015; Pandey and Willems, 2015). Previous studies have shown that certain skeletal morphology such as the acromion type (AT) and the dimensions of the glenoid fossa, are often correlated with common shoulder pathologies (Reilly *et al.*, 2006; Rajput *et al.*, 2012; Sarwar *et al.*, 2015). In this discussion this study's aim of investigating the association of certain morphological traits of the humerus and scapula, as well as some soft tissue components commonly associated with shoulder pathologies in a South African sample, are presented. The researcher's aim was met with regard to the above by dividing the study into three parts in an attempt to establish a trend, and to inter-relate the results that were obtained within the three parts; 1) cadaver part; 2) X-ray images part and 3) MRI images.

Measurements and observations of the morphometric skeletal and soft tissue components of the shoulder joint have often been used to analyse associations with commonly diagnosed shoulder pathologies (Wafae *et al.*, 2010; Singh *et al.*, 2013; Nyffeler and Meyer, 2017). These measurements and observations have included, acromial type (AT–type I (flat), II (round) or III (hooked)), intertubercular groove width (ITGW), glenoid fossa depth (GFD), acromial index (AI), lateral acromial angle (LAA), acromioclavicular joint distance (ACJ), acromiohumeral distance (AHD), glenoid fossa length (GFL), maximum humeral head diameter (HHMax_dia), humeral angle of inclination (HHI), rotator cuff (RC) - intact/pathology; capsule-pathology/non-pathology, ligaments tears/intact/fray and GL-intact, tears/fray (Carmichael and Hart, 1985; Bigliani *et al.*, 1986; Zanca, 1971; Perry, 1978; Howell and Galinat, 1989; Flatow *et al.*, 1994; Banas *et al.*, 1995; Nishida *et al.*, 1996; Boileau and Walch, 1997; Nyffeler *et al.*, 2006; Martínez *et al.*, 2006; Murlimanju *et al.*, 2012; Balke *et al.*, 2013; Hanciau *et al.*, 2013; Gupta *et al.*, 2014; Sarwar *et al.*, 2015). All these measurements/observations were used in this study with some being specific to the cadaver part versus the imaging (X-ray & MRI) parts, and were all measured/observed according to definitions provided and extrapolated from multiple supportive studies methods (Carmichael and Hart, 1985; Bigliani *et al.*, 1986; Howell and Galinat, 1989; Chan *et al.*, 1991; Flatow *et al.*, 1994; Banas *et al.*, 1995; Nishida *et al.*, 1996; van der Helm, 1996; Boileau and Walch,

1997; Nyffeler *et al.*, 2006; Reilly *et al.*, 2006; Lugo *et al.*, 2008; Lewis and Armstrong, 2011; Hanciau *et al.*, 2012; Rajput *et al.*, 2012; Balke *et al.*, 2013; Huegel *et al.*, 2015).

All of the above listed variables were used in this study to examine the relationship of commonly diagnosed shoulder pathologies with general skeletal measurements and observations.

5.1. Acromial type (AT)

Cadaveric component: incidence of AT

In the cadaver specimens only, AT I (flat) and AT II (round) variations were observed in accordance with the definitions provided in the Bigliani-Morrison-April classification (Bigliani *et al.*, 1986); no AT III were observed. The morphology of the acromial process is considered to be an extrinsic factor in the development of RC pathology. Individuals with AT I have been shown to be at lower risk of RC impingement, while individuals with AT II or III have been shown to have higher incidences of subacromial impingement linked to partial and full RC tears (Bigliani *et al.*, 1986; Dave *et al.*, 2006; Seitz *et al.*, 2011). Therefore, when considering the study sample split into shoulders without pathologies and shoulders with pathologies the incidence of AT I was found to be significantly higher ($p < 0.0001$) in the group without pathologies, in both males and females (Table 4.5), while AT II was more commonly associated with shoulders with pathologies (degenerative osteoarthritic changes, acromial thickness). This is to be expected and further strengthens the evidence of the extrinsic influence that the acromial process may have on pathology of the shoulder.

When pathology was not considered as an exclusion factor, the distribution of AT I and AT II between left and right sides was found to be fairly equal among the male and female sample (Table 4.2). A significant difference ($p = 0.046$) was noted between males and females with regard to the distribution of AT I versus AT II (Table 4.4). Of the total AT I present in the sample, males had higher counts, while females had higher incidences of AT II in all the AT II observed in the sample (Table 4.4). Although vast amounts of cadaveric studies were noted in the literature, only a few met the criteria to form a comparison with this study. Of the comparable literature, most studies showed contradictory results to those found in this study. Previous authors instead found higher incidences of AT II in males and higher incidences of AT I in females (Getz *et al.*, 1996; Green *et al.*, 2004; Natsis *et al.*, 2007; Paraskevas *et al.*, 2008; and Collipal *et al.*, 2010). Another study found that AT II had higher incidences in both

males and females compared to AT I (Sangiampong *et al.*, 2007). Of the many studies showing opposite results, one study that also used a South African sample, was found to show similar results to this current study, in that higher incidences of AT I was observed in males when compared to females (Naidoo *et al.*, 2015). It is unclear as to why there are different results reported in the literature, but it could be suggestive of the possible population specificity, which is known to exist between various population groups in the European, Asian and South Africans context (Natsis *et al.*, 2007; Miyazaki *et al.*, 2011; Naidoo *et al.*, 2018). Previous studies have suggested that in addition to population specificity with regard to just acromial morphology, other factors such as age, occupation, diet and disease prevalence on the different continents could also be causative to the occurrence of different shoulder diseases amongst different population groups and the link to acromion type (Schippinger *et al.*, 1997; Natsis *et al.*, 2007; Sangiampong *et al.*, 2007).

Cadaveric component: measurements relating to different AT

The only measurements that showed any difference between the pathology versus without pathology group as well as between the two acromial type groups (AT I and AT II) was the maximum humeral head diameter (HHMax_dia) in males, and the depth of the glenoid fossa (GFD). The only measurements that showed any difference between the pathological versus non-pathological group as well as between the two acromial type groups (AT I and AT II) was the maximum humeral head diameter (HHMax_dia) in males, and the depth of the glenoid fossa (GFD).

When considering the shape of the acromion, the AT I male specimens displayed a significantly larger HHMax_dia (50.21 ± 4.53 mm) when compared to the HHMax_dia (44.94 ± 5.88 mm) in AT II male specimens ($p=0.0500$) (Table 4.7). Although these results show significance, they should be interpreted with caution due to the small sample of AT II ($n=4$) compared to AT I ($n=22$). This difference was also observed when the pathology versus without pathology groups were compared (Table 4.8); once again a much larger humeral head diameter was noted in the without pathology group compared to the pathology group; however, the same can be said with regard to the sample size. It should be noted the 4 male samples that were classified as AT II were also the sample that comprised the pathological group and therefore the measurements are the same. It is unclear as to the possible reason why the humeral head diameter would be larger in healthy shoulders compared to shoulders with pathologies, but it

may be considered, like the acromial morphology, to be an extrinsic influence for the incidence of shoulder pathology, especially if it is found in conjunction with another skeletal abnormality.

The GFD appears to be significantly deeper in individuals with AT I (5.80 ± 2.31 mm) when compared to those with AT II (3.06 ± 1.24 mm) (Table 4.7). For the GFD group, male and female measurements were combined due to the non-significant difference between the two samples (Table 4.6; $p>0.05$). In the group without pathologies, the GFD was also significantly deeper (5.76 ± 2.25 mm) compared to the group with pathologies (2.68 ± 0.83 mm) (Table 4.8). To the authors knowledge, no studies comparing the GFD and AT in shoulders with pathologies and shoulders without pathologies could be found. However, what was noted in the literature was rather comparisons of the AT to soft tissue components associated with common diagnosed shoulder pathologies; i.e. RC tears and impingement syndrome in cadaveric studies (Aragão *et al.*, 2014; Naidoo *et al.*, 2015; Yadav and Zhu, 2017; Sinha *et al.*, 2018).

The results of this study provide a unique insight into the possible relationship between humeral head size and glenoid fossa depth with the occurrence of shoulder pathology. If an interpretation had to be made from the results presented here, it is possible that with a smaller humeral head, and shallower glenoid fossa, there could be a higher chance for the occurrence of a shoulder pathology. This would make sense due to the fact that a large portion of the mechanical stability of the GHJ relies on the shape of the humeral head (Torrens *et al.*, 2007) and the concavity of the glenoid fossa (Ovesen and Nielsen, 1985). Should there be an imbalance in this structural alignment, the normal functionality of the joint will be affected and could therefore potentially place strain on the soft tissues surrounding the joint, eventually leading to pathology. Another interesting observation in this study is that more females ($n=7$) were recorded with pathology than males ($n=4$) and, in general, females tend to have smaller humeral head diameters than males (evident in Table 4.6). It was not evident from the results that there was any significant difference between the size of the humeral heads in females between the group with pathology and the group without pathology or even between acromial types, however what is interesting is that the average size of the female humeral head (44.56 ± 4.10 mm) is very similar to the humeral head size of the male sample shoulder with pathologies (44.94 ± 5.88 mm) (Tables 4.6 and 4.8). Ultimately, what the results show is that those with an AT II are linked to the shallower glenoid fossa depth as well as the smaller humeral head in males; this being said, it is likely that a combination of irregular morphological traits (AT II, shallow glenoid fossa and small humeral head), are strong extrinsic factors leading to the incidence of pathology of the shoulder; e.g. humeral head dislocation. This finding

corresponds to what von Eisenhart-Rothe et al. (2010) and Peltz et al. (2010) suggest in their studies in that chronic humeral head dislocation is associated with a flattened glenoid fossa in the anterior to posterior and superior to inferior directions (decreased depth). The flattened fossa anatomically compromises the glenoid and is also associated with multidirectional GHJ instability as seen in the results of this study and, corresponds with what von Eisenhart-Rothe et al. (2010) and Peltz et al. (2015) suggests in their studies.

Imaging component: AT incidence in the X-ray and MRI sample

In the X-ray sample, the white male (n=17), white female (n=13) and the black female (n=22) samples showed a higher ratio of the occurrence of AT I compared to AT II, whereas the black male sample (n=42) showed a higher incidence of AT II, compared to AT I and AT III (Table 4.11). The MRI sample, which was just from a white population group, also showed a higher incidence of AT I in both males and females (Table 4.18). Comparison to other studies with regard to the incidence of AT I, showed similar and dissimilar results in that AT II had a higher incidence in male individuals with common diagnosed shoulder pathologies than females (Jacobson *et al.*, 1995; Akram *et al.*, 2014; Jacinth *et al.*, 2018), which concurs with the black male sample but disagrees with what was observed in the white male sample in both the X-ray and MRI groups. However, when just considering the white sample, these are similar AT incidences seen with the cadaveric part of this study.

The presence of AT III was only observed in the black sample (black male=2; black female=2) in the X-ray group and in the white females (n=2) in the MRI group, but this could probably be attributed to the fact that the white X-ray sample size was considerably smaller than the black sample (n=64 vs n=30) and could be misrepresentative of the truth; although Bigliani et al. (1986) do state that AT III is a rare acromial morphology. What is interesting about this sample however, is the fact that all of the X-ray and MRI individuals had some or other form of diagnosed shoulder pathology and even so, the incidence of AT I in the sample is generally higher than AT II, which was seen to be of higher prevalence in the shoulders without pathologies in the cadaveric component.

Based on the previous literature, which states that individuals with AT I are less inclined to have shoulder pathology (Bigliani *et al.*, 1986; Dave *et al.*, 2006; Seitz *et al.*, 2011) and that it is more likely in those with AT II and AT III, the results of this study contradict those findings when only the imaging sample is considered. Could it therefore be possible that AT, when considered on its own, may not necessarily be a strong extrinsic factor contributing to the

development of shoulder pathology, especially since these results provide evidence that there was almost an even chance of seeing AT I (n=46) and AT II (n=44) in a sample of 94 shoulders with pathologies? Few previous studies have shown that AT I demonstrates a relationship with rotator cuff tears (Aoki *et al.*, 1986) and that in some pathology instances, a higher ratio of AT I (45.8%) and a lower occurrence of AT II (37.5%) was found in black male individuals (Naidoo *et al.*, 2015). Few previous studies have shown that AT I demonstrates a relationship with rotator cuff tears (Aoki *et al.*, 1986) and that in some pathology instances, a higher ratio of AT I (45.8%) and a lower occurrence of AT II (37.5%) was found in black male individuals (Naidoo *et al.*, 2015). Other studies however, have reports that demonstrate an association between shoulder pathology, such as impingement syndrome, in males with AT II and in females with AT I (Dwivedi and Varshney, 2015). Acromion type II in an MRI study conducted by Mayerhoefer *et al.* (2005) and in an X-ray study conducted by Peh and Totty (1995), were most commonly associated with shoulder pathologies such as, RC tears and subacromial impingement. It is likely, that the AT alone, does not play a strong enough role to influence the mechanics of the shoulder, but it is possible that there may have to be another accompanying morphological factor such as perhaps a modified GFD, in order for a prominent pathology to develop.

Left and right side distribution of AT I and AT II showed no significant difference within, and between the white and black population groups ($p>0.05$) in the X-ray sample however, then AT I showed a higher incidence on the left in the female sample, while males had a higher incidence of AT I on the right side (Table 4.11). In three of the groups, the incidence of AT II was higher on the right side whilst black females showed a 50/50 distribution between AT II on the left and right side. The MRI group showed a higher incidence of AT I on the left side in both males and females as well as a higher incidence of AT II on the left. Previous studies indicated a higher incidence of AT I and AT II on the right side within their sample groups (Peh and Totty, 1995; Mayerhoefer *et al.*, 2005; Naidoo *et al.*, 2015; Ravindranath, *et al.* 2018) and this may be indicative of possible population differences such as handedness which is a genetic component that could present strong control over this kind of incidence.

It is clear based on the contradicting literature, and the results presented in this study across all three components (cadaver, X-ray and MRI) that the actual extrinsic role of the acromial morphology in the development of shoulder pathology is not clearly understood. It is possible that the incidence of different AT ratios could be ascribed to the differences in occupation, age and prevalence to disease within these population groups as suggested by

previous literature studies with other population demographics (Jacobson *et al.*, 1995; Akram *et al.*, 2014; Jacinth *et al.*, 2018) and not necessarily a standalone contributor to shoulder pathology development.

5.2. Morphometric variables

The morphometric variables measured in this study varied slightly between the cadaver, X-ray and MRI components. In the cadaver part, 5 measurements were taken which included; the AHD, ITGW, HHI, HHMax_dia and GFD. In the X-ray and MRI components, 9 measurements were taken which included; the AI, GA, GH, LAA, ACJ, AHD, GFL, HHMax_dia and HHI. Of all the measurements taken, HHMax_dia was the only measurement that showed a significant difference in all three sample groups; the AI, LAA, GFL showed significant differences in both the X-ray and MRI groups, the HHI and ACJ only showed significant differences in the X-ray group, while the GH only showed differences in the MRI group. Therefore, only the measurements that showed significance will be discussed.

Humeral head diameter (HHMax_dia)

The diameter of the humeral head is a well-studied morphological trait especially in an anthropological setting (Steyn and İşcan, 1997). It has been used to successfully differentiate between males and females (İşcan, 1998; Milner and Boldsen, 2012), as well as between population groups (Steyn and İşcan, 1997). Humeral head diameter differences between males and females may also be influenced by oestrogen and androgen hormones, which allow for a thicker cortical humeral bone in males because of a larger cortical distribution, a considerable periosteal bone layering and a larger endosteal width because of a longer bone maturation period than females during puberty (Bonjour *et al.*, 1999; Laurent *et al.*, 2014).

Few studies have looked at the relationship of the humeral head with various shoulder pathologies (Tackett and Ablove, 2011; Iyem *et al.*, 2017; Syed *et al.*, 2017). Studies that did look at dimensions of the humeral head such as the diameter, neck angle, medial offset and posterior offset in a clinical setting, included fresh cadaveric shoulders and dried cadaveric humeri but excluded comparative parameters used in this study such as common shoulder pathologies. In other cases, MRI methods were used to measure cadavers and often sex was unreported (Boileau and Walch, 1997; Hertel *et al.*, 2002; Roche *et al.*, 2005; DeLude *et al.*, 2007). Minimal cadaveric studies were found that were comparable with the methodology

employed in this study. Most studies focussed on comparing AT to soft tissue components such as RC, and impingement syndrome (Aragão *et al.*, 2014; Yadav and Zhu, 2017).

Looking at group comparisons in this study, the male specimens' HHMax_dia was significantly larger when compared to the female specimens in all three test groups; cadaver, X-ray and MRI (Tables 4.6, 4.16 and 4.22). In the cadaver sample, which included a control group without shoulder pathologies, the humeral head diameters were significantly ($p=0.0153$) larger in the male, group without pathologies (50.21 ± 4.53 mm) compared to the male group with pathologies (44.94 ± 5.88 mm); interestingly the females showed no difference between the pathology and without pathology groups (Table 4.8). According to Steyn and İşcan (1999) the average humeral head diameter for white South African males is around 49 ± 3.2 mm, for white South African females, 43.2 ± 3.5 mm, for black South African males, 43.7 ± 2.1 , and for black South African females around 37.7 ± 2.0 (Steyn and İşcan, 1999). Comparing the researcher's results with what the normal averages are, the cadaver sample in this study showed a much smaller humeral head diameter for the white male pathology group (44.94 ± 5.88 mm) compared to the average range (49 ± 3.2 mm) (Steyn and İşcan, 1999), and both the pathology X-ray (52.76 ± 5.04 mm) and MRI (48.50 ± 3.58 mm) groups. This is an odd finding especially since the X-ray sample humeral head diameter was larger than the normal range and the MRI was smaller. All three the groups (cadaver, X-ray and MRI) were shoulder samples with pathologies, and yet displayed varying means compared to the normal range as well as to each other. Perhaps it could be attributed to the method of measurements for each sample as measuring the diameter on an X-ray is dependent on the angle of GHJ while the X-ray was taken, and the MRI could also be misaligned during the imaging procedure. The only comparable method to that of Steyn and İşcan (1999) is probably the cadaver sample, since these were physically measured from the dry bone and may present more accurate results if comparison with the normal range is considered.

For the white female cadaver group, the average humeral head diameter (45.57 ± 4.44 mm) was larger than the normal average (43.2 ± 2.5 – Steyn and İşcan, 1999) as well as both the X-ray (45.41 ± 3.10 mm) and MRI group (41.96 ± 2.16 mm). The MRI group showed a considerably smaller humeral head diameter for white females than any of the other groups. The only sample that included black South Africans was the X-ray sample and the results indicated that the average humeral head diameters for both the male (49.42 ± 4.32 mm) and female (44.04 ± 3.74 mm) pathology groups was considerably larger than what the reported normal averages (Steyn and İşcan, 1999) are for black males (43.7 ± 2.1 mm) and females

(37.7 ± 2.0 mm), which is similar to what was observed with the white female group mentioned above. Male and female humeral head pathology could be attributed to different osteoporotic changes in the humeral head as suggested by Kanatli et al. (2013) and places shear strain on the surrounding rotator cuff tendons during humeral head articulation. This articulative stress causes morphological and morphometric changes of the humeral head and this, in turn causes an interaction between soft tissues and the humeral head as suggested by Huegel et al. (2015).

Humeral head angle of inclination (HHI)

The humeral head angle of inclination is a known morphological measurement that has previously been well associated with various shoulder pathologies, i.e. rotator cuff tears and impingement syndrome (Takase *et al.*, 2004; Iyem *et al.*, 2017). Studies that did look at dimensions of the humerus such as the neck angle, posterior and medial offset in clinical settings, included different population groups and dried cadaveric humeri and excluded comparative parameters used in this study such as common shoulder pathologies. In other studies, computed tomography (CT) methods were used to measure individuals and often sex was unreported (Boileau and Walch, 1997; Hertel *et al.*, 2002; Roche *et al.*, 2005; DeLude *et al.*, 2007; Matsumura *et al.*, 2015). Minimal X-ray studies were found that were comparable with the methodology employed in this study. Most studies focussed on anthropometric analysis with arthroplasty in mind (Hertel *et al.*, 2002; Matsumura *et al.*, 2015; Matsuki *et al.*, 2017).

Looking at group comparisons in this study, the three test groups; cadaver, X-ray and MRI (Tables 4.6, 4.16 and 4.22) only the white females could be compared since the black females were not represented in the cadaver and MRI sample. The white female angle of inclination was 142.14 ± 4.54 compared to the black females' HHI of 138.14 ± 10.35 in the X-ray sample (Table 4.16). This shows a significant difference between the two population groups; $p=0.0153$ (Table 4.16). This is an odd finding for the white female group especially since the X-ray sample humeral head angle of inclination was so much larger than the average range of the cadaver (131.85 ± 3.23) and the MRI (Table 4.6, 4.16 and 4.22). All three the groups (cadaver, X-ray and MRI) were pathological samples and yet displayed varying means compared to the average range as well as to each other. Perhaps it could be attributed to the method of measurements for each sample as measuring the diameter on an X-ray is dependent on the angle of GHJ while the X-ray was taken, and the MRI could also be misaligned during the imaging procedure. Comparing the researcher's results with what the suggested averages are, both female pathology X-ray groups in this study showed a larger and smaller humeral

angle of inclination compared to the average range (139.5 ± 4.4) (Takase *et al.*, 2004). When the researcher compared this study's results to an Indian study, which suggests that the average humeral head angle of inclination of females was 136.2 ± 3.53 on anteroposterior X-rays (Iyem *et al.*, 2017) a large difference was noted between their results and the researcher's results which may be indicative of possible population differences.

Acromial index (AI)

The acromial index is a well-known morphological measurement that has previously been well associated with various shoulder pathologies, i.e. rotator cuff tears and tendinopathy within the shoulder joint (Nyffeler *et al.*, 2006; Sukthankar *et al.*, 2009). The acromial index is a measurement ratio where the distance from the glenoid plane to the lateral border of the acromion (GA) is divided by the distance from the glenoid plane to the lateral aspect of the humeral head (GH) (Nyffeler *et al.*, 2006). It has been used to differentiate between males and females (Nyffeler *et al.*, 2006) as well as between population groups (Kum *et al.*, 2016).

Previous studies have shown AI's of between 0.60 and 0.73 in shoulders displaying various degrees and, types of shoulder pathology (Miyazaki *et al.*, 2010; Ames *et al.*, 2012; Kim *et al.*, 2012; Kircher *et al.*, 2012; Kum *et al.*, 2016) and an acromial index of 0.64 ± 0.06 and 0.6677 have been reported for individuals with undamaged RC units (Nyffeler *et al.*, 2006; Miyazaki *et al.*, 2010). The first noticeable difference between this study and the literature with regard to the AI taken in the X-ray group, is that all groups (BM, BF, WM and WF) showed significantly larger AI's than the range given above. The black males and females displayed the largest AI's (0.80 ± 0.11 mm and $0.78-0.87\pm 0.08-0.10$ mm, respectively) compared to the white males and females (0.73 ± 0.11 mm and 0.76 ± 0.11 mm). In both instances, the females showed a significantly larger AI than the males (Table 4.15). These large differences could be attributed to either population specificity or the measurement methodology. The black and white South African population groups present with differing body size and may be a reason for acromial index differences (Robinette *et al.*, 1979; Miyazaki *et al.*, 2010; Naidoo *et al.*, 2018). In order to measure GA and GH for the AI, the X-ray needs to be a true AP orientation; it may be possible that some of the X-rays used in this study may have been slightly misaligned which may lead to measurement errors.

The reason that the authors have taken this into account is based largely on the results obtained in the MRI portion of this study. In the MRI group (which has a true AP orientation), the white male group showed an AI of 0.62 ± 0.07 mm and the white females an AI of 0.67 ± 0.09

mm; the AI in the female group was significantly larger than the males ($p=0.0094$) (Table 4.21). Similar ratios were found in male and female individuals (0.62 ± 0.09 mm) with fray/torn glenoid labrum and in male and female individuals with an intact glenoid labrum in common diagnosed shoulder pathology (0.69 ± 0.06 mm) ($p=0.0169$) (Table 4.24). These results all fall within the ranges found in previous studies (Miyazaki *et al.*, 2011; Ames *et al.*, 2012; Kim *et al.*, 2012; Kircher *et al.*, 2012; Kum *et al.*, 2016). An average AI ratio in shoulders with pathology was 0.73 ± 0.06 and 0.72 ± 0.07 in RC tears and 0.60 ± 0.08 in those with osteoarthritic degeneration (Nyffeler *et al.*, 2006; Miyazaki *et al.*, 2011). Shoulders without pathologies' AI was 0.64 ± 0.06 (Nyffeler *et al.*, 2006).

The question arises, does the presence of pathology change the strain and stress on the shoulder to a degree that there is morphological adaptation occurring in the skeleton resulting in slightly altered measurements leading to differing AI's, or is it the different morphological features that, over time, lead to increased stress and strain on the shoulder, leading to pathology development.

Lateral acromial angle (LAA)

The LAA is a well-known morphometric measurement and differences in the LAA is often associated with common diagnosed shoulder pathologies (Banas *et al.*, 1995). A LAA of less than 75 degrees has been previously associated with diagnosed shoulder pathologies, due to the smaller space present to house the soft tissue components of the shoulder joint (Hanciau *et al.*, 2012). This being said, studies have however found LAA's of $\pm 76.8-87$ degrees in individuals (male and female) with different diagnosed stages of impingement syndrome pathology (Kanatli *et al.*, 2013; Yu *et al.*, 2013) as well as between 77 ± 8 and 83 ± 6 degrees in other commonly diagnosed shoulder pathologies (Balke *et al.*, 2013); showing an angle of greater than 75 degrees. In another study looking at a Korean population, the LAA was 72.6 ± 6.5 degrees in individuals with diagnosed shoulder pathologies (Lee *et al.*, 2008); which falls within the range of less than 75 degrees.

In this study, the LAA for the black males in the X-ray group was 73.54 ± 13.94 and the black females, 70.54 ± 10.09 . The white males in the X-ray and MRI group showed a LAA of 81.50 ± 11.74 and 83.6 ± 6.46 and the white females, 71.74 ± 12.05 and $78.17-83.14\pm 4.76-12.05$ in the X-ray and MRI sample, respectively. What is clear from the results is that the black population both had LAA's of less than 75 degrees which corresponds with what Banas *et al.* (1995) suggested for shoulders with pathology conditions.

However, the white population group in both X-ray and MRI samples had most LAA's over 75 degrees (except the white female X-ray group). All of these individuals had a diagnosed shoulder pathology and therefore these results align more with what was found by Balke et al. (2013), Kanatli et al. (2013) and Yu et al. (2013).

This could be another indicator of population specificity and is a worthwhile trait to further explore, especially obtaining a control sample to see what the general normal LAA would be in a South African sample. Lateral acromial angle differences between population groups and, between males and females could be influenced by the thickness of the acromion process in its anterior third (Hanciau *et al.*, 2012; Miyazaki *et al.*, 2010). The thick acromion process entraps the soft tissue components, i.e. the capsule and Supraspinatus tendon predisposing the components to pathological changes (Nyffeler *et al.*, 2006). This could also tie in with the acromial type classification; perhaps the different morphology of the acromion in AT I, AT II and AT III could lead to changes in the LAA since the measurement is dependent on the slope of the acromion process.

Glenoid fossa length (GFL)

The glenoid fossa length is a morphometric measurement that is measured in conjunction with other glenoid cavity measurements such as the glenoid height, glenoid width and glenoid depth (Hassanein, 2015). The actual shape of the glenoid cavity is highly variable and few studies have investigated the actual classification of the various shapes and sizes (De Wilde *et al.*, 2004). The dimensions of the glenoid cavity have been used in previous studies to classify sex (Di Vella *et al.*, 1994; Prescher and Klümpen, 1995; Frutos, 2002; Macaluso, 2010) and estimate stature (Campobasso *et al.*, 1998). The GFL in the X-ray group showed significant differences ($p < 0.05$) between the black males (37.09 ± 4.5 mm) and white males (41.52 ± 4.55 mm) and between the black females (33.40 ± 3.30 mm) and white females (35.93 ± 3.87 mm); these measurements were also significantly different between males and females in each population group. In the MRI group, there was also a significant difference between the white males (35.30 ± 4.85 mm) and females (30.96 ± 4.69 mm). Strangely, the white males between the X-ray and MRI group show a ± 6.0 mm difference in the GFL and the white females between the 2 groups show a ± 5.0 mm difference; in both cases the GFL is smaller in the MRI group. This could be attributed to the different imaging modalities and clearly could have a role in the correct and accurate measurement of the GFL. In X-rays the GFL is measured from a sagittal

view point whereas in the MRI's, the GFL is measured from a coronal view point; this could account for the large discrepancy between the two groups.

Coskun et al. (2006) suggests that the GFL in shoulders with pathologies measured 36.3 ± 3 mm, which differed from both the black and white male groups in this study sample. While the females in this study sample (black - 33.40 ± 3.30 mm and white - 35.93 ± 3.87 mm) fell below the suggested 36.3 ± 3 mm, by Coskun et al. (2006) for females with shoulder pathology. These varying measurements could be another indicator of population specificity and is a worthwhile trait to further explore, especially to research the GFL of a healthy shoulder in a South African population group, with the interest to obtain thus values of shoulders without pathologies. GFL differences between population groups and males and females could also be influenced by the different body types between males and females as mentioned in Goud et al. (2008). This could also be linked to changes in AI ratio and LAA angle since these morphometric measurements depend on the angle of the glenoid cavity. These changes in morphometric measurements could also tie in with glenoid cavity bone loss, osteoarthritic degeneration, shoulder instability and shoulder dislocations (Moineau *et al.*, 2012; Lee *et al.*, 2014; Skupiński *et al.*, 2017).

Acromioclavicular joint distance (ACJ)

The soft tissue components, which surround the ACJ, such as the acromioclavicular ligaments, provide protection and some laxity to the ACJ and forms an integral part of the biomechanical support of the GHJ (Väättäinen *et al.*, 1991). The ACJ is stabilised anterior-to-posterior by the acromioclavicular ligaments, and superior stability is provided by the coracoclavicular ligaments (Li *et al.*, 2014). Osteoarthritic degeneration in the ACJ is often accidentally noticed on an X-ray image taken of a symptomatic shoulder/GHJ, and this degeneration has previously been said not to be linked to the aging process (Zanca, 1971). However, contradictory studies have said that the presence of ACJ osteoarthritic degeneration is indeed age-related degeneration of the ACJ and can be associated with the normal ageing process (Worcester and Green, 1968; Stein, 2001).

The ACJ space is either measured on a true anteroposterior (AP) X-ray image or on an MRI scan (Lehtinen, 1999; Stein, 2001). In the presence of suspected ACJ pathology, Zanca (1971) suggests that an X-ray focussing on the ACJ, should also be taken simultaneously with the true AP shoulder X-ray. With the ACJ space being a well-known measurement, it has been suggested that a distance between 1 mm and 3 mm between the clavicle and acromion can be considered normal (Oppenheimer, 1943; Zanca, 1971), however some authors have suggested

that to be considered normal and not a pathology, a leeway of not wider than 6mm in females and 7 mm in male shoulders can be considered (Petersson and Redlund-Johnell, 1983).

All individuals in this study's X-ray and MRI sample had some form of diagnosed shoulder pathology, with known ACJ pathology, i.e. joint degeneration. In the X-ray sample, it was interesting to note that there was a significant difference between the left and right sides in the black male (L = 9.94 ± 8.86 mm; R = 5.13 ± 2.92 mm) and white female (L = 7.68 ± 3.92 mm; R = 3.08 ± 1.93 mm) groups, with the left side being significantly larger in both; no side difference was noted in the black females and white males. The white females in the MRI sample once again showed a side difference with the left side (5.86 ± 1.99 mm) being significantly larger than the right (4.42 ± 1.31 mm); white males again showed no side difference in ACJ measurement.

All the ACJ measurements taken from the sample exceeded the 1 mm to-3 mm range as suggested by (Oppenheimer, 1943; Zanca, 1971) and clearly fell in line with what Lehtinen et al. (1999) suggest with regard to the presence of a wider ACJ space in diagnosed shoulder pathology. However, Petersson and Redlund-Johnell (1983) also suggest that in general, shoulders without pathologies should have an ACJ space smaller than 7 mm in males and 6 mm in females, only some of the measurements in this study do exceed this range as well, especially the left sides of the black males and white females. Comparing to an average ACJ space of 6.9 ± 5.1 mm in males and 4.5 ± 3.0 mm in females which Lehtinen et al. (1991) suggest, it measures smaller than this study's black male population but compares well with the white female population's right shoulders. Authors such as Yu et al. (2000) concur with Petersson and Redlund-Johnell (1983) in that an ACJ space of 6 mm is considered the cut off for a joint without pathology in anteroposterior X-rays, with measurement above 6 mm coinciding with pathologies such as osteoarthritic degeneration and calcifications. With an ultrasound method used to measure the ACJ space with osteoarthritic degeneration, Alasaarela et al. (1997) suggest that the average joint space be 4.1 mm. With this in mind, Lehtinen et al. (1999) used X-rays to measure the ACJ space with osteoarthritic degeneration and found their results to be only 0.8 mm less than what Alasaarela et al. (1997) suggested. This shows that regardless of which preferred method is used to measure the ACJ space, the results compared well with each other in the presence of osteoarthritic changes (Lehtinen *et al.*, 1999). Although the ACJ is comparable between different studies and different population groups, it appears that differences between different degrees/types of pathology is rather seen than between non-pathology and pathology.

X-rays are the preferred method to classify ACJ pathologies (Rockwood and Green, 1984) and to examine the ACJ (Zanca, 1971; Li *et al.*, 2014; Gastaud *et al.*, 2015). This method of research is not supported by Ernberg and Potter (2003) and Väättäinen *et al.* (1991) who disagree and suggest that with X-rays the structures often overlap each other, soft tissues cannot be outlined and joints are often tilted at the incorrect angle. With that being said, their preferred method as well as other studies are computed tomography, ultrasound, MRIs and comparing various treatment modalities (Alasaarela *et al.*, 1997; Buttaci *et al.*, 2004; Gordon and Chew, 2004; Sanders and Miller, 2005) to assess the ACJ for pathology because of the advantage to directly see any ligamentous disruptions (Alyas *et al.*, 2008; Li *et al.*, 2014).

Glenohumeral distance (GH)

The glenohumeral distance is a well-studied morphometric measurement and is always used in conjunction with the GA to define the AI, which is a morphometric ratio that is obtained when the GA is divided by the GH (Nyffeler *et al.*, 2006). The GH is linked to the AI and existing studies usually only focus on the AI ratio and not the GH in isolation (Mohamed and Abo-Sheisha, 2014; Engelhardt *et al.*, 2017). Vast amounts of X-ray and MRI studies looking at the AI were noted in the literature and only a few met the criteria to form a comparison with this study. Although the AI is comparable between different studies and different population groups, the GH has not been compared in isolation from the AI. The GH forms part of the differences that appear to be between different degrees/types of pathology rather than between no-pathology and pathology. An average AI ratio in shoulders with pathologies were 0.73 ± 0.06 and 0.72 ± 0.07 in RC tears and 0.60 ± 0.08 in those with osteoarthritic degeneration (Nyffeler *et al.*, 2006; Miyazaki *et al.*, 2011). Shoulders without pathologies' AI was 0.64 ± 0.06 (Nyffeler *et al.*, 2006).

Interesting results were noted by the researcher with regard to the GH taken in the X-ray group, versus the GH taken in the MRI group. Only significant differences between males and females were noted in the MRI group; no significant differences were noted in the X-ray group between both sexes and between population groups. This once again brings about the question as to the measurement methodology employed in the X-rays versus the MRI's. It may be that the two different imaging modalities would have to have two defined sets of measurements to accurately measure the GH distance. It is strange that there is this difference seen in the MRI group but not in the X-ray group. The GH of the MRI group was measured as suggested by Nyffeler *et al.* (2006) and Hanciau *et al.* (2012). The white male group showed no

difference between the left and right sides, while the white females showed significantly larger right-side GH measurements (47.09 ± 3.04 mm) compared to the left side (44.21 ± 3.77 mm) (Table 4.19). The white males in general showed a significantly larger GH distance (53.20 ± 3.35 mm) than both sides of the white female group (Table 4.21). In the X-ray group, the males (black and white) had GH measurements between 51.95-53.49 mm and the females (black and white) between 49.26-50.38 mm. It is clear from the results that the males between the two imaging modalities are similar whereas the MRI female sample showed much smaller GH distances than the females in the X-ray group. This is difficult to explain and could possibly be linked to the measuring technique more than anything else.

It is clear based on the literature, and the results presented in this study's X-ray component that the actual extrinsic role of the glenohumeral distance in the development of shoulder pathology is not clearly understood. It is possible that the incidence of different GH ratios could be ascribed to the differences in sport preferences, occupation, age and prevalence to disease within population groups as suggested by previous literature studies with other population demographics (Kumar *et al.*, 2013; Engelhardt *et al.*, 2016; Kum *et al.*, 2016) and not necessarily a standalone contributor to shoulder pathology development.

5.3. Limitations of study

Several limitations were encountered in this study. The first being the limited sample size for X-ray and MRI imaging components. Having a small sample size reduces the accuracy of comparative testing and therefore results obtained from such samples should be interpreted with caution and serve as more of a guide as to the identification of possible trends and associations. Another limitation was the lack of actual diagnoses for the X-ray group; the only information provided was that the patients had some or other shoulder pathology but these were not specified and we did not have access to the patient files for a retrospective investigation.

Limitations with regard to the measurement methodology were also encountered during this study. At times it was found difficult to measure some of the variables on the X-rays due to malalignment as well as the MRI's due to a poorly positioned patient and blurring of the MRI itself led to difficulties in defining measurement landmarks. This may account for some of the differences noted between the same measurements taken in the X-ray and MRI samples; some showed significant differences between measurements of the same variable.

Chapter 6: Conclusion and Recommendations

This morphometric study illustrated that variations in certain skeletal-and soft tissue components could possibly be associated with common shoulder pathologies and anticipated that some of the morphometric components would show a statistically significant trend across all three samples; i.e. cadaver-, X-ray images and MRI images.

Acromial type

The association of the acromial type (AT) and shoulder pathology was found to be contradicting in this study when compared to various other published works. In the cadaver component of this study it was clear that AT I was linked to non-pathological shoulders, while AT II was more likely found in pathological shoulders. This, together with the glenoid fossa depth and humeral head diameter, provided an interesting insight into the association of these morphological traits and shoulder pathology. Based on the results for this component, it appears as though the AT may not alone lead to the development of shoulder pathology, but rather the combined morphological deviations from the norm in respect of the glenoid fossa depth and humeral head diameter, may be the link that can be associated with the development of shoulder dysfunction and pathology. A shallower glenoid fossa depth and smaller humeral head appear to be linked to the incidence of shoulder pathology, together with an AT II.

In the imaging component (X-ray and MRI) it was clear that AT I displayed a higher incidence in most groups compared to AT II or AT III; except in black males who had a higher incidence of AT II. This was found contradictory to the cadaver component and what has been published in the literature. Since all individuals in the X-ray and MRI sample presented with shoulders with pathologies, it would have been expected to note higher incidences of AT II and AT III, and this was not the case. This brings to question does the AT really have such an extrinsic role on the development of shoulder pathology, especially the development of rotator cuff (RC) pathology as previously thought – or is it dependant on the accompanying morphology of the glenoid and the humeral head.

Morphometric variables

The maximum humeral head diameter (HHMax_dia) was the only variable to show a significant difference between males and females in all three (cadaver, X-ray and MRI) sample components. This interesting trend was followed throughout the three study samples and the

humeral head diameter difference corresponded marginally in all three study samples in individuals diagnosed with shoulder pathologies. The association of the maximum humeral head diameter, glenoid fossa length, lateral acromion angle and the acromion index and shoulder pathology was found to be contradicting in this study when compared to various other published works. In the cadaver and MRI component of this study it was clear that a smaller humeral head diameter was linked to shoulders with pathology, while a larger humeral head diameter in the X-ray sample was also linked to shoulders with pathologies.

This, together with the glenoid fossa length, provided an interesting insight into the association of these morphological traits and shoulder pathology. Based on the results for these components, it appears as though these variables are the lead in the development of shoulder pathology, especially the combined morphological deviations from the norm in respect of the glenoid fossa length and humeral head diameter, may be the link that can be associated with the development of shoulder debilitation and pathology. A smaller glenoid fossa length could also be linked to changes in acromion index ratio and lateral acromion angle since these morphometric measurements depend on the angle of the glenoid cavity. Interesting results were noted in the study with regard to the GH taken in the X-ray group, versus the GH taken in the MRI group. Only significant differences between males and females were noted in the MRI group; no significant differences were noted in the X-ray group between both sexes and between population groups. This once again brings about the question as to the measurement methodology employed in the X-rays versus the MRI's.

In the imaging component (X-ray and MRI) it was clear that the acromion index was significantly larger in South African black population groups compared to South African white population groups. Since all individuals in the X-ray and MRI sample presented with shoulders with pathologies, it would have been expected to see some morphometric deviations. This brings to question the extrinsic impact and role these skeletal components have and play in the development of shoulder pathology, especially the development of rotator cuff (RC) pathology as previously thought – or is it dependant on the concomitant morphology of the glenoid and the humeral head.

In South African population groups where there is a clinically difficult diagnosis, the X-ray and MRI measurements could be helpful to clinicians in diagnosis and treatment planning.

Future recommendations:

- Investigate the role - function and position of the acromial type (AT) in a larger sample of shoulders with pathologies and shoulders without pathologies across sexes and population groups.
- Investigate the role - function and position of the glenohumeral distance (GH) in isolation from the acromial index in a larger sample of shoulders with pathologies and shoulders without pathologies across sexes and population groups.
- Investigate the role - function and position of the glenoid labrum (GL) in a larger sample of shoulders with pathologies and shoulders without pathologies across sexes and population groups.
- Investigate the role - function and position of the lateral acromion angle (LAA) in a larger sample of shoulders with pathologies and shoulders without pathologies across sexes and population groups.
- Investigate the role - function and position of the glenoid fossa length (GFL) in a larger sample of shoulders with pathologies and shoulders without pathologies across sexes and population groups.

References

- Ackland, D.C., Pak, P., Richardson, M. & Pandy, M.G. 2008. Moment arms of the muscles crossing the anatomical shoulder. *Journal of Anatomy*, 213(4):383-390.
- Akram, M., Pasha, I.F., Shah, S.F.U.H., Farooqi, F.M. & Awais, S.M. 2014. Types of acromion and its association with shoulder impingement syndrome. *Annals of King Edward Medical University*, 20(2):144-144.
- Alasaarela, E., Tervonen, O., Takalo, R., Lahde, S. & Suramo, I. 1997. Ultrasound evaluation of the acromioclavicular joint. *Journal of Rheumatology*, 24:1959-1963.
- Alilet, M., Behr, J., Nueffer, J.P., Barbier-Brion, B. & Aubry, S. 2016. Multi-modal imaging of the subscapularis muscle. *Insights into imaging*, 7(6):779-791.
- Alyas, F., Curtis, M., Speed, C., Saifuddin, A. & Connell, D. 2008. MR imaging appearances of acromioclavicular joint dislocation. *Radiographics*, 28(2):463-479.
- Amabile, C., Bull, A.M. & Kedgley, A.E. 2016. The centre of rotation of the shoulder complex and the effect of normalisation. *Journal of Biomechanics*, 49(9):1938-1943.
- Ames, J.B., Horan, M.P., Van der Meijden, O.A., Leake, M.J. & Millett, P.J. 2012. Association between acromial index and outcomes following arthroscopic repair of full-thickness rotator cuff tears. *Journal of Bone and Joint Surgery*, 94(20):1862-1869.
- Aoki, M., Ishii, S. & Usui, M. 1986. The slope of the acromion and rotator cuff impingement. *Orthopaedic Transaction*, 10:228.
- Aragão, J.A., Silva, L.P., Reis, F.P. & Menezes, C.S.de S. 2014. Analysis on the acromial curvature and its relationships with the subacromial space and types of acromion. *Revista Brasileira de Ortopedia, (English Edition)*, 49(6):636-641.

Balke, M., Liem, D., Greshake, O., Hoehner, J., Bouillon, B. & Banerjee, M. 2016. Differences in acromial morphology of shoulders in patients with degenerative and traumatic supraspinatus tendon tears. *Knee Surgery, Sports Traumatology, Arthroscopy*, 24(7):2200-2205.

Balke, M., Schmidt, C., Dedy, N., Banerjee, M., Bouillon, B. & Liem, D. 2013. Correlation of acromial morphology with impingement syndrome and rotator cuff tears. *Acta Orthopaedica*, 84(2):178-183.

Banas, M.P., Miller, R.J. & Totterman, S. 1995. Relationship between the lateral acromion angle and rotator cuff disease. *Journal of Shoulder and Elbow Surgery*, 4(6):454-461.

Basmajian, J.V. & Bazant, F.J. 1959. Factors preventing downward dislocation of the adducted shoulder joint: an electromyographic and morphological study. *Journal of Bone and Joint Surgery*, 41(7):1182-1186.

Bdaiwi, A.H. 2014. Acromio-humeral distance; its measurement reliability, sensitivity and the influence of scapular position (Doctoral dissertation, University of Salford).

Bencardino, J.T., Gyftopoulos, S. & Palmer, W.E. 2013. Imaging in anterior glenohumeral instability. *Radiology*, 269(2):323-337.

Bigliani, L. U. & Levine, W. N. 1997. Subacromial impingement syndrome. *Journal of Bone and Joint. Surgery, American edition*, 79(12):1854-1868.

Bigliani, L.U., Morrison, D.S. & April, E.W. 1986. Morphology of the acromion and its relationship to rotator cuff tears. *Orthopaedic Transactions*, 10:459-460.

Boileau, P., Ahrens, P.M. & Hatzidakis, A.M. 2004. Entrapment of the long head of the biceps tendon: The hourglass biceps—A cause of pain and locking of the shoulder. *Journal of Shoulder and Elbow Surgery*, 13:249-257.

Boileau, P. & Walch, G. 1997. The three-dimensional geometry of the proximal humerus: Implications for surgical technique and prosthetic design. *Journal of Bone and Joint Surgery British*, 79(5): 857-865.

Bonjour, J.P., Ammann, P. & Rizzoli, R. 1999. Importance of preclinical studies in the development of drugs for treatment of osteoporosis: a review related to the 1998 WHO guidelines. *Osteoporosis International*, 9(5):379-393.

Bosworth, B.M. 1941. Examination of the shoulder for calcium deposits: technique of fluoroscopy and spot-film roentgenography. *Journal of Bone and Joint Surgery*, 23(3):567-577.

Briggs, A.M., Cross, M.J., Hoy, D.G., Sánchez-Riera, L., Blyth, F.M., Woolf, A.D. & March, L., 2016. Musculoskeletal health conditions represent a global threat to healthy aging: a report for the 2015 World Health Organization world report on ageing and health. *The Gerontologist*, 56(Suppl_2):S243-S255.

Brodie, C.G. 1890. Note on the transverse-humeral, coraco-acromial, and coraco-humeral ligaments. *Journal of Anatomy and Physiology*, 24(Pt 2):247.

Brown, D.P., Freeman, E.D., Cuccurullo, S.J., Ng, U., Maitin, I.B., Brown, M.L.E.D.P. & Freeman, M.S.T.L. 2004. Musculoskeletal medicine. In: *Physical Medicine and Rehabilitation Board Review*, pp.131-293. Demos, New York.

Bunker, T.D. & Anthony, P.P. 1995. The pathology of frozen shoulder. A Dupuytren-like disease. *Bone and Joint Journal*, 77(5):677-683.

Burbank, K.M., Stevenson, J.H., Czarnecki, G.R. & Dorfman, J. 2008. Chronic shoulder pain: part I. Evaluation and diagnosis. *American Family Physician*, 77(4).

Buttaci, C.J., Stitik, T.P., Yonclas, P.P. & Foye, P.M. 2004. Osteoarthritis of the acromioclavicular joint: A review of anatomy, biomechanics, diagnosis, and treatment. *American Journal of Physical Medicine and Rehabilitation*, 83(10):791-797.

Cadet, E.R., Hsu, J.W., Levine, W.N., Bigliani, L.U. & Ahmad, C.S. 2008. The relationship between greater tuberosity osteopenia and the chronicity of rotator cuff tears. *Journal of Shoulder and Elbow Surgery*, 17(1):73-77.

Campobasso, C.P., Di Vella, G. & Introna, F. 1998. Using scapular measurements in regression formulae for the estimation of stature. *Bollettino-Societa Italiana Di Biologia Sperimentale*, 74(7/8):75-82.

Carmichael, S.W. & Hart, D.L. 1985. Anatomy of the shoulder joint. *Journal of Orthopaedic and Sports Physical Therapy*, 6(4):225-228.

Carrazzone, O.L., Tamaoki, M.J.S., Ambra, L.F.M., Neto, N.A., Matsumoto, M.H. & Belloti, J.C. 2011. Prevalence of lesions associated with traumatic recurrent shoulder dislocation. *Revista Brasileira de Ortopedia (English Edition)*, 46(3):281-287.

Chan, T.W., Dalinka, M.K., Kneeland, J.B. & Chervrot, A. 1991. Biceps tendon dislocation: evaluation with MR imaging. *Radiology*, 179(3):649-652.

Choi, C.H., Kim, S.S., Kim, S.J. & Lee, J.H. 2015. Arthroscopic changes of the biceps pulley in rotator cuff tear and its clinical significance in relation to treatment. *Clinics in Orthopaedic Surgery*, 7(3):365-371.

Christodoulou, C. & Cooper, C. 2003. What is osteoporosis? *Postgraduate Medical Journal*, 79(929):133-138.

Chung, C.B. & Steinbach, L.S. 2009. *MRI of the upper extremity: shoulder, elbow, wrist and hand*. Lippincott Williams & Wilkins.

Churchill, R.S., Brems, J.J., & Kotschi, H. 2001. Glenoid size, inclination, and version: an anatomic study. *Journal of Shoulder and Elbow Surgery*, 10:327-332.

Codman, E.A. & Akerson, I.B. 1931. The pathology associated with rupture of the supraspinatus tendon. *Annual Surgery*, 93:348-359.

Collin, P., Matsumura, N., Lädermann, A., Denard, P.J. & Walch, G. 2014. Relationship between massive chronic rotator cuff tear pattern and loss of active shoulder range of motion. *Journal of Shoulder and Elbow Surgery*, 23(8):1195-1202.

Collipal, E., Silva, H., Ortega, L., Espinoza, E. & Martinez, C. 2010. The acromion and its different forms. *International Journal of Morphology*, 28(4):1189-1192.

Conroy, R.M. 2012. What hypotheses do "nonparametric" two-group tests actually test? *Stata Journal*, 12(2):182.

Cooper, D.E., Arnoczky, S.P., O'Brien, S.J., Warren, R.F., DiCarlo, E. & Allen, A.A. 1992. Anatomy, histology, and vascularity of the glenoid labrum. An anatomical study. *Journal of Bone and Joint Surgery, American volume*, 74:46-52.

Coskun, N., Karaali, K., Cevikol, C., Demirel, B.M. & Sindel, M. 2006. Anatomical basics and variations of the scapula in Turkish adults. *Saudi Medical Journal*, 27(9):1320-1325.

Culham, E. & Peat, M. 1993. Functional anatomy of the shoulder complex. *Journal of Orthopaedic & Sports Physical Therapy*, 18(1):342-350.

Dahiru, T. 2008. P-value, a true test of statistical significance? A cautionary note. *Annals of Ibadan postgraduate medicine*, 6(1):21-26.

Dave, A., Kane, S.M., Haque, A. & Langston, K. 2006. The incidence of rotator cuff disease in smoking and non-smoking patients: a cadaveric study. *Orthopaedics*, 29(4).

De Duca, C.J. & Forrest, W.J. 1973. Force analysis of individual muscles acting simultaneously on the shoulder joint during isometric abduction. *Journal of Biomechanics*, 6:38S-93S.

De Groot, J.H. 1997. The variability of shoulder motions recorded by means of palpation. *Clinical Biomechanics*, 12(7-8):461-472.

DeLude, J.A., Bicknell, R.T., MacKenzie, G.A., Ferreira, L.M., Dunning, C.E., King, G.J., Johnson, J.A. & Drosdowech, D.S. 2007. An anthropometric study of the bilateral anatomy of the humerus. *Journal of Shoulder and Elbow Surgery*, 16(4):477-483.

Denard, P.J., Ladermann, A., Jiwani, A.Z. & Burkhart, S.S. 2012. Functional outcome after arthroscopic repair of massive rotator cuff tears in individuals with pseudo paralysis. *Arthroscopy*, 28:1214-1219.

Depalma, A.F. & Kruper, J.S. 1961. Long-term study of shoulder joints afflicted with and treated for calcific tendinitis. *Clinical Orthopaedics and Related Research*, 20:61-72.

De Wilde, L.F., Berghs, B.M., Audenaert, E., Sys, G., Van Maele, G.O. & Barbaix, E. 2004. About the variability of the shape of the glenoid cavity. *Surgical and Radiologic Anatomy*, 26(1):54-59.

Dias, R., Cutts, S., & Massoud, S. 2005. Frozen Shoulder. *British Medical Journal (Clinical Research Edition)*, 331(7530):1453-1456.

Di Vella, G., Campobasso, C.P., Dragone, M. & Introna, F. 1994. Skeletal sex determination by scapular measurements. *Bollettino-Societa Italiana Di Biologia Sperimentale*, 70:299-299.

Dugas, J.R., Campbell, D.A., Warren, R.F., Robie, B.H. & Millett, P.J. 2002. Anatomy and dimensions of rotator cuff insertions. *Journal of Shoulder and Elbow Surgery*, 11(5):498-503.

Dunham, K.S., Bencardino, J.T. & Rokito, A.S. 2012. Anatomic variants and pitfalls of the labrum, glenoid cartilage, and glenohumeral ligaments. *Magnetic Resonance Imaging Clinics*, 20(2):213-228.

Dwivedi, M. & Varshney, A. 2015. Study of correlation between Bigliani's acromion types and shoulder problems. *Indian Journal of Orthopaedics*, 2(2):111-115.

Edelson, J.G., Taitz, C. & Grishkan, A. 1991. The coracohumeral ligament. Anatomy of a substantial but neglected structure. The Journal of Bone and Joint Surgery. British volume, 73(1):150-153.

EIshewy, M.T. 2016. Calcific tendinitis of the rotator cuff. World Journal of Orthopaedics, 7(1):55.

Engelhardt, C., Farron, A., Becce, F., Place, N., Pioletti, D.P. & Terrier, A. 2016. Effects of glenoid inclination and acromion index on humeral head translation and glenoid articular cartilage strain. Journal of Shoulder and Elbow Surgery, 26(1):157-164.

Ernberg, L.A. & Potter, H.G. 2003. Radiographic evaluation of the acromioclavicular and sternoclavicular joints. Clinics in Sports Medicine, 22:255–275.

Evolve, H.D.T. 2017. Tendonitis and Tendinopathy. Treatment of Acute and Chronic Tendon Rupture and Tendinopathy, An Issue of Foot and Ankle Clinics of North America, E-Book, 22(4):665.

Flatow, E.L., Soslowsky, L.J., Ticker, J.B., Pawluk, R.J., Hepler, M., Ark, J., Mow, V.C. & Bigliani, L.U. 1994. Excursion of the rotator cuff under the acromion: patterns of subacromial contact. The American Journal of Sports Medicine, 22(6):779-788.

França, F.D.O., Godinho, A.C., Ribeiro, E.J.S., Falster, L., Búrigo, L.E.G. & Nunes, R.B. 2016. Evaluation of the acromiohumeral distance by means of magnetic resonance imaging umerus. Revista Brasileira de Ortopedia, 51(2):169-174.

Fremont, P., Desmeules, F., & Guimont C. 2000. Ultrasonographic measurement of the acromio-humeral distance at the inlet of the subacromial space: A reliability study. CASAM Annual Symposium. Clinical Journal of Sports Medicine, (10):221.

Frutos, L.R. 2002. Determination of sex from the clavicle and scapula in a Guatemalan contemporary rural indigenous population. The American Journal of Forensic Medicine and Pathology, 23(3):284-288.

Fukuda, H. 2003. The management of partial-thickness tears of the rotator cuff. *The Journal of Bone and Joint Surgery, British volume*, 85(1):3-11.

Gastaud, O., Raynier, J.L., Duparc, F., Baverel, L., Andrieu, K., Tarissi, N. & Barth, J. 2015. Reliability of radiographic measurements for acromioclavicular joint separations. *Orthopaedics and Traumatology: Surgery & Research*, 101(8):S291-S295.

Gemne, G., Saraste, H., Christ, E. & Dupuis, H.G. 1987. Bone and joint pathology in workers using hand-held vibrating tools: An overview [with Discussion]. *Scandinavian Journal of Work, Environment and Health*, pp.290-300.

Gerber, C. & Nyffeler, R.W. 2002. Classification of glenohumeral joint instability. *Clinical Orthopaedics and Related Research (1976-2007)*, 400:65-76.

Gerber, C., Terrier, F.R.A.N.C.O.I.S. & Ganz, R., 1985. The role of the coracoid process in the chronic impingement syndrome. *The Journal of Bone and Joint Surgery, British volume*, 67(5):703-708.

Getz, J.D., Recht, M.P., Piraino, D.W., Schils, J.P., Latimer, B.M., Jellema, L.M. & Obuchowski, N.A. 1996. Acromial morphology: relation to sex, age, symmetry, and subacromial enthesophytes. *Radiology*, 199(3):737-742.

Goga, I.E. 2003. Chronic shoulder dislocations. *Journal of Shoulder and Elbow Surgery*, 12(5):446-450.

Gordon, B.H. & Chew, F.S. 2004. Isolated acromioclavicular joint pathology in the symptomatic shoulder on magnetic resonance imaging: a pictorial essay. *Journal of Computer Assisted Tomography*, 28(2):215-222.

Goutallier, D. Le Guilloux, P., Postel, J.M., Radier, C., Bernageau, J. & Zilber, S. 2011. Acromio humeral distance less than six millimetre: its meaning in full-thickness rotator cuff tear. *Orthopaedics and Traumatology: Surgery and Research*, 97(3):246-251.

Green, A., Griggs, S. & Labrador, D. 2004. Anterior acromial anatomy: Relevance to arthroscopic acromioplasty. *Arthroscopy*, 20(10):1050-1054.

Green, S.B. & Salkind, N.J. 2008. *Using SPSS for Window and Macintosh: Analyzing and understanding data*. 5th ed. Upper Saddle River, NJ: Pearson Prentice Hall.

Grewal, T.J. 2011. *Quantifying the shoulder rhythm and comparing non-invasive methods of scapular tracking for overhead and axially rotated humeral postures* (Master's thesis, University of Waterloo).

Gu, G. & Yu, M. 2013. Imaging features and clinical significance of the acromion morphological variations. *Journal of Novel Physiotherapies S*, 2(2).

Gupta, C., Priya, A., Kalthur, S.G. & D'Souza, A.S. 2014. A morphometric study of acromion process of scapula and its clinical significance. *CHRISMED Journal of Health and Research*, 1(3):164.

Gursel, Y.K., Ulus, Y., Bilgic, A., Dincer, G. & van der Heijden, G.J. 2004. Adding ultrasound in the management of soft tissue disorders of the shoulder: a randomized placebo-controlled trial. *Physical Therapy*, 84(4):336-343.

Habermeyer, P., Magosch, P., Pritsch, M., Scheibel, M.T. & Lichtenberg, S. 2004. Anterosuperior impingement of the shoulder as a result of pulley lesions: a prospective arthroscopic study. *Journal of Shoulder and Elbow Surgery*, 13(1):5-12.

Halder, A.M., Itoi, E. & An, K.N. 2000. Anatomy and biomechanics of the shoulder. *Orthopedic Clinics*, 31(2):159-176.

Hamada, J., Tamai, K., Ono, W. & Saotome, K. 2006. Does the nature of deposited basic calcium phosphate crystals determine clinical course in calcific periarthritis of the shoulder? *Journal of Rheumatology*, 33:326e-332e.

Hanciau, F.A., da Silva., Marcos André Mendes., Martins, F.S. & Ogliari, A. 2012. Association clinical-radiographic of the acromion index and the lateral acromion angle. *Revista Brasileira de Ortopedia*, 47(6):730-735.

Hand, G.C.R., Athanasou, N.A., Matthews, T. & Carr, A.J. 2007. The pathology of frozen shoulder. *Bone & Joint Journal*, 89(7):928-932.

Harryman 2nd, D.T., Sidles, J.A., Clark, J.M., McQuade, K.J., Gibb, T.D. & Matsen 3rd, F.A. 1990. Translation of the humeral head on the glenoid with passive glenohumeral motion. *Journal of Bone and Joint Surgery*, 72(9):1334-1343.

Hassanein, G.H.E.S. 2015. Morphometry of Glenoid fossa in Adult Egyptian Scapulae. *International Journal of Anatomy and Research [Internet]*, 3(2):1138-42.

Hata, Y., Nakatsuchi, Y., Saitoh, S., Hosaka, M. & Uchiyama, S. 1992. Anatomic study of the glenoid labrum. *Journal of Shoulder and Elbow Surgery*, 1(4):207-214.

Hayes, K., Callanan, M., Walton, J., Paxinos, A. & Murrell, G.A. 2002. Shoulder instability: management and rehabilitation. *Journal of Orthopaedic and Sports Physical Therapy*, 32(10):497-509.

Hecker, A.T., Shea, M., Hayhurst, J.O., Myers, E.R., Meeks, L.W. & Hayes, W.C. 1993. Pull-out strength of suture anchors for rotator cuff and Bankart lesion repairs. *The American Journal of Sports Medicine*, 21(6):874-879.

Henderson, R.E., Walker, B.F. & Young, K.J. 2015. The accuracy of diagnostic ultrasound imaging for musculoskeletal soft tissue pathology of the extremities: a comprehensive review of the literature. *Chiropractic & Manual Therapies*, 23(1):31.

Heron, S.R., Woby, S.R. & Thompson, D.P. 2017. Comparison of three types of exercise in the treatment of rotator cuff tendinopathy/shoulder impingement syndrome: A randomized controlled trial. *Physiotherapy*, 103(2):167-173.

Hertel, R., Knothe, U. & Ballmer, F.T. 2002. Geometry of the proximal humerus and implications for prosthetic design. *Journal of Shoulder and Elbow Surgery*, 11(4):331-338.

Hess, S.A. 2000. Functional stability of the glenohumeral joint. *Manual therapy*, 5(2):63-71.

Huegel, J., Williams, A.A. & Soslowsky, L.J. 2015. Rotator cuff biology and biomechanics: a review of normal and pathological conditions. *Current rheumatology reports*, 17(1):476.

Howell, S.M. & Galinat, B.J. 1989. The glenoid–labral socket: A constrained articular surface. *Clinical Orthopaedics and Related Research*, 243:122-125.

Hsu, J. & Keener, J.D. 2015. Natural history of rotator cuff disease and implications on management. *Operative techniques in orthopaedics*, 25(1):2-9.

Huber, W.P. & Putz, R.V. 1997. Periarticular fibre system of the shoulder joint. *Arthroscopy: The Journal of Arthroscopic and Related Surgery*, 13(6):680-691.

Imhoff, A.B., Ansah, P., Tischler, T., Reiter, C., Bartl, C., Hench, M., Spang, J.T. & Vogt, S. 2010. Arthroscopic repair of anterior-inferior glenohumeral instability using a portal at the 5:30-o'clock position: analysis of the effects of age, fixation method, and concomitant shoulder injury on surgical outcomes. *The American Journal of Sports Medicine*, 38(9):1795-1803.

Inman, V.T., Saunders, M. & Abbott, L.C. 1944. Observations on the function of the shoulder joint. *Journal of Bone and Joint Surgery, American volume*, 26A:1–30.

Iannotti, J., Gabriel, J., Schneck, S., Evans, B. & Misra, S. 1992. The normal glenohumeral relationships. An anatomical study of one hundred and forty shoulders. *Journal of Bone and Joint Surgery*, 74(4): 491-500.

İşcan, Y.M. 1998. Progress in forensic anthropology: The 20th century. *Forensic Science International*, 98(1-2):1-8.

Itoi, F., Grabowski, J.J., Morrey, B.F. & An, K.N. 1993. Capsular properties of the shoulder. *The Tohoku Journal of Experimental Medicine*, 171(3):203-210.

Iyem, C., Serbest, S., Inal, M., Burulday, V., Kaya, A., Kultur, T. & Tiftikci, U, 2017. A morphometric evaluation of the humeral component in shoulder arthroplasty. *Biomedical Research*, 28(4):0970-938X.

Jacinth, J.S., Pushpam, E.S., Slater, S. & Muniyappan, V. 2018. Morphometry of the acromion process of human scapulae and its clinical implications. *Journal of Evolution of Medical and Dental Sciences-JEMDS*, 7(18):2205-2209.

Jacobson, S.R., Speer, K.P., Moor, J.T., Janda, D.H., Saddemi, S.R., MacDonald, P.B. & Mallon, W.J. 1995. Reliability of radiographic assessment of acromial morphology. *Journal of Shoulder and Elbow Surgery*, 4(6):449-453.

Jacxsens, M., Van Tongel, A., Henninger, H.B., De Coninck, B., Mueller, A.M. & De Wilde, L., 2016. A three-dimensional comparative study on the scapulohumeral relationship in normal and osteoarthritic shoulders. *Journal of Shoulder and Elbow Surgery*, 25(10):1607-1615.

Jia, X., Chen, Y., Qiang, M., Zhang, K., Li, H., Jiang, Y. & Zhang, Y., 2016. Compared to X-ray, Three-dimensional computed tomography measurement is a reproducible radiographic method for normal proximal humerus. *Journal of Orthopaedic Surgery and Research*, 11(1):82.

Jost, B. & Gerber C. 2004. What the shoulder surgeon would like to know from MR imaging. *Magnetic Resonance Imaging Clinics of North America*, 12(1):161-168.

Kanatli, U., Gemalmaz, H.C., Ozturk, B.Y., Voyvoda, N.K., Tokgoz, N. & Bolukbasi, S. 2013. The role of radiological subacromial distance measurements in the subacromial impingement syndrome. *European Journal of Orthopaedic Surgery and Traumatology*, 23(3):317-322.

Kanatli, U., Ozturk, B.Y. & Bolukbasi, S. 2010. Anatomical variations of the anterosuperior labrum: prevalence and association with type II superior labrum anterior-posterior (SLAP) lesions. *Journal of Shoulder and Elbow surgery*, 19(8):1199-1203.

Kim, J.R., Ryu, K.J., Hong, I.T., Kim, B.K. and Kim, J.H. 2012. Can a high acromion index predict rotator cuff tears? *International Orthopaedics*, 36(5):1019-1024.

Kircher, J., Morhard, M., Patzer, T., Magosch, P., Lichtenberg, S. & Habermeyer, P. 2012. Do anatomic variants of the acromion shape in the frontal plane influence pain and function in calcifying tendinitis of the shoulder? *Knee Surgery, Sports Traumatology, Arthroscopy*, 20(2):368-372.

Knowles, N.K., Carroll, M.J., Keener, J.D., Ferreira, L.M. & Athwal, G.S. 2016. A comparison of normal and osteoarthritic humeral head size and morphology. *Journal of Shoulder and Elbow Surgery*, 25(3):502-509.

Ko, J.Y. & Wang, F.S. 2011. Rotator cuff lesions with shoulder stiffness: updated pathomechanisms and management. *Chang Gung Medical Journal*, 34(4):331-340.

Koester, M.C., George, M.S. & Kuhn, J.E. 2005. Shoulder impingement syndrome. *The American Journal of Medicine*, 118(5):452-455.

Kruskal, W.H. & Wallis, W.A. 1952. Use of ranks in one-criterion variance analysis. *Journal of the American Statistical Association*, 47(260):583-621.

Kum, D.H., Kim, J.H., Park, K.M., Lee, E.S., Park, Y.B. & Yoo, J.C. 2017. Acromion Index in Korean Population and Its Relationship with Rotator Cuff Tears. *Clinics in Orthopedic Surgery*, 9(2):218-222.

Laubscher, P. & Rösch, T. 2009. Frozen shoulder: A review. *South African Orthopaedic Journal*, 8(3):24-29.

Laurent, M., Antonio, L., Sinnesael, M., Dubois, V., Gielen, E., Classens, F. & Vanderschueren, D. 2014. Androgens and oestrogens in skeletal sexual dimorphism. *Asian Journal of Andrology*, 16(2):213-222.

Lee, C.S., Davis, S.M., McGroder, C., Kouk, S., Sung, R.M., Stetson, W.B. & Powell, S.E. 2014. Analysis of low-field MRI scanners for evaluation of shoulder pathology based on arthroscopy. *Orthopaedic Journal of Sports Medicine*, 2(7), 2325967114540407.

Lee, R.K., Griffith, J.F., Tong, M.M., Sharma, N. & Yung, P. 2013. Glenoid bone loss: assessment with MR imaging. *Radiology*, 267(2):496-502.

Lee, K.W., Lee, S.H., Jung, S.H., Kim, H.Y., Ahn, J.H., Kim, K.J. & Choy, W.S. 2008. The effect of the acromion shape on rotator cuff tears. *Journal of the Korean Orthopaedic Association*, April, 43(2):181-186.

Lehtinen, J.T., Kaarela, K., Belt, E.A., Kautiainen, H.J., Kauppi, M.J. & Lehto, M.U. 1999. Incidence of acromioclavicular joint involvement in rheumatoid arthritis: a 15 year endpoint study. *The Journal of Rheumatology*, 26(6):1239-1241.

Lewis, G.S. & Armstrong, A.D. 2011. Glenoid spherical orientation and version. *Journal of Shoulder and Elbow Surgery*, 20(1):3-11.

Lewis, J.S. 2009. Rotator cuff tendinopathy: A review. *British Journal of Sports Medicine*, 43:236-241.

Li, X., Ma, R., Bedi, A., Dines, D.M., Altchek, D.W. & Dines, J.S. 2014. Management of acromioclavicular joint injuries. *Journal of Bone and Joint Surgery*, 96(1):73-84.

Lippitt, S.B., Matsen, F.A. & Rockwood, C.A. 2003. *Shoulder surgery: principles and procedures*. Springer.

Lugo, R., Kung, P. & Ma, C.B. 2008. Shoulder Biomechanics. *European Journal of Radiology*, 68(1):16-24.

Lundberg, B.J. 1969. The frozen shoulder: clinical and radiographical observations the effect of manipulation under general anaesthesia structure and glycosaminoglycan content of the joint capsule local bone metabolism. *Acta Orthopaedica Scandinavica*, 40(suppl119):1-59.

Macaluso, P.J. 2011. Sex discrimination from the glenoid cavity in black South Africans: morphometric analysis of digital photographs. *International Journal of Legal Medicine*, 125(6):773-778.

Marieb, E.N., Wilhelm, P.B. & Mallatt, J. 2014. Human anatomy. Pearson.

Marieb, E.N. & Zao, P.Z. 1992. The skeletal system. Benjamin/Cummings.

Martínez, J.J., Ríos, J., Martínez, F. & Martínez-Almagro, A. 2006. Dependency of the long head of the brachial biceps and its relation to the bicipital groove. Morphological and morphometric ultrasonography study. In Orthopaedic Proceedings (Vol. 88, SUPP_II:327-327). The British Editorial Society of Bone and Joint Surgery.

Martinoli, C., Bianchi, S., Prato, N., Pugliese, F., Zamorani, M.P., Valle, M. & Derchi, L.E. 2003. US of the shoulder: Non-rotator cuff disorders. Radiographics, 23(2):381-401.

Massengill, A.D., Seeger, L.L., Yao, L., Gentili, A., Shnier, R.C., Shapiro, M.S. & Gold, R.H. 1994. Labrocapsular ligamentous complex of the shoulder: normal anatomy, anatomic variation, and pitfalls of MR imaging and MR arthrography. Radiographics, 14(6):1211-1223.

Matsuki, K., Sugaya, H., Hoshika, S., Ueda, Y., Takahashi, N., Tokai, M., Onishi, K. & Banks, S.A. 2017. Geometric Analysis of the Proximal Humerus in Elderly Japanese Patients: Implications for Implant Selection in Reverse Shoulder Arthroplasty. Orthopedics, 40(3):e485-e490.

Matsumura, N., Oki, S., Ogawa, K., Iwamoto, T., Ochi, K., Sato, K. & Nagura, T. 2016. Three-dimensional anthropometric analysis of the glenohumeral joint in a normal Japanese population. Journal of Shoulder and Elbow Surgery, 25(3):493-501.

Mayerhoefer, M.E., Breitenseher, M.J., Roposch, A., Treitl, C. & Wurnig, C. 2005. Comparison of MRI and conventional radiography for assessment of acromial shape. American Journal of Roentgenology, 184(2):671-675.

McClure, P.W. & Michener, L.A. 2015. Staged approach for rehabilitation classification: shoulder disorders (STAR-shoulder). Physical Therapy, 95(5):791-800.

McClure, P.W., Michener, L.A. & Karduna, A.R. 2006. Shoulder function and 3-dimensional scapular kinematics in people with and without shoulder impingement syndrome. *Physical Therapy*, 86(8):1075-1090.

McMahon, P.J., Debski, R.E., Thompson, W.O., Warner, J.J., Fu, F.H. & Woo, S.L. 1995. Shoulder muscle forces and tendon excursions during glenohumeral abduction in the scapular plane. *Journal of Shoulder and Elbow Surgery*, 4(3):199-208.

McQuade, K.J., Wei, S.H. & Smidt, G.L. 1995. Effects of local muscle fatigue on three-dimensional scapulohumeral rhythm. *Clinical Biomechanics*, 10(3):144-148.

Mehta, S., Gimbel, J.A. & Soslowsky, L.J. 2003. Etiologic and pathogenetic factors for rotator cuff tendinopathy. *Clinics in Sports Medicine*, 22(4):791-812.

Michener, L.A., McClure, P.W. & Karduna, A.R. 2003. Anatomical and biomechanical mechanisms of subacromial impingement syndrome. *Clinical Biomechanics*, 18(5):369-379.

Millett, P.J., Gobeze, R. & Boykin, R.E. 2008. Shoulder Osteoarthritis: Diagnosis and Management. *American Family Physician*, 78(5):605-611.

Milgrom, C., Schaffler, M., Gilbert, S. & van Holsbeeck, M. 1995. Rotator-cuff changes in asymptomatic adults. The effect of age, hand dominance and gender. *Journal of Bone and Joint Surgery, British volume*, 77(2):296–298.

Milner, G.R. & Boldsen, J.L. 2012. Humeral and femoral head diameters in recent white American skeletons. *Journal of Forensic Sciences*, 57(1):35-40.

Miyazaki, A.N., Fregoneze, M., Santos, P.D., da Silva, L.A., do Val Sella, G., Neto, D.L.L., Junior, M.M. & Checchia, S.L. 2014. Osteoid osteoma of the acromion simulating acromioclavicular pain. *Revista Brasileira de Ortopedia (English Edition)*, 49(1):82-85.

Miyazaki, A.N., Fregoneze, M., Santos, P.D., Silva, L.A.D., Martel, É.M., Debom, L.G., Andrade, M.L. and Checchia, S.L. 2010. Radiographic analysis of the acromion index and its association with rotator cuff tears. *Revista Brasileira de Ortopedia*, 45(2):151-154.

Miyazaki, A.N., Itoi, E., Sano, H., Fregoneze, M., Santos, P.D., da Silva, L.A., Guiherme, do V.S., Eder, M.M., Leandro, G.D., Manoel, L.A. & Sérgio, L.C. 2011. Comparison between the acromion index and rotator cuff tears in the Brazilian and Japanese populations. *Journal of Shoulder and Elbow Surgery*, 20:1082-1086.

Mohamed, R.E. & Abo-Sheisha, D.M. 2014. Assessment of acromial morphology in association with rotator cuff tear using magnetic resonance imaging. *The Egyptian Journal of Radiology and Nuclear Medicine*, 45(1):169-180.

Moineau, G., Levigne, C., Boileau, P., Young, A., Walch, G. & French Society for Shoulder & Elbow (SOFEC). 2012. Three-dimensional measurement method of arthritic glenoid cavity morphology: feasibility and reproducibility. *Orthopaedics and Traumatology: Surgery and Research*, 98(6):S139-S145.

Moore, S.M., Ellis, B., Weiss, J.A., McMahon, P.J. & Debski, R.E. 2010. The glenohumeral capsule should be evaluated as a sheet of fibrous tissue: a validated finite element model. *Annals of Biomedical Engineering*, 38(1):66-76.

Moseley, H.F. & Overgaard, B. 1962. The anterior capsular mechanism in recurrent anterior dislocation of the shoulder. *Journal of Bone and Joint Surgery, British volume*, 44-B:913-927.

Mullaji, A.B., Beddow, F.H. & Lamb, G.H. 1994. CT measurement of glenoid erosion in arthritis. *The Journal of Bone and Joint Surgery, British volume*, 76(3):384-388.

Murlimanju, B.V., Prabhu, L.V., Pai, M.M., Shreya, M., Prashanth, K.U., Kumar, C.G. & Rao, C.P. 2012. Anthropometric study of the bicipital groove in Indians and its clinical implications. *Chang Gung Medical Journal*, 35(2):155-159.

Naidoo, N., Lazarus, L., Osman, S.A. & Satyapal, K.S. 2015. Acromial Morphology and Subacromial Architecture in a South African Population. *International Journal of Morphology*, 33(3).

Naidoo, N., Lazarus, L., Van Tongel, A., Osman, S.A. & Satyapal, K.S. 2018. Predictors of Shoulder Degeneration in the KwaZulu-Natal Population of South Africa. *International Journal of Morphology*, 36(1).

Nakata, W., Katou, S., Fujita, A., Nakata, M., Lefor, A.T. & Sugimoto, H. 2011. Biceps pulley: normal anatomy and associated lesions at MR arthrography. *Radiographics*, 31(3):791-810.

Nakazawa, M., Nimura, A., Mochizuki, T., Koizumi, M., Sato, T. & Akita, K. 2016. The orientation and variation of the acromioclavicular ligament: An anatomic study. *The American Journal of Sports Medicine*, 44(10):2690-2695.

Natsis, K., Tsikaras, P., Totlis, T., Gigis, I., Skandalakis, P., Appel, H.J. & Koeke J. 2007. Correlation between the four types of acromion and the existence of enthesophytes: A study on 423 dried scapulas and review of the literature. *Clinical Anatomy (Review)*, (20):267–272.

Neer, C.S. 1972. 2nd Anterior acromioplasty for the chronic impingement syndrome in the shoulder: A preliminary report. *The Journal of Bone and Joint Surgery, American volume*, 54(1):41-50.

Neer 2nd C.S., Satterlee, C.C., Dalsey, R.M. & Flatow, E.L. 1992. The anatomy and potential effects of contracture of the coracohumeral ligament. *Clinical Orthopaedics and Related Research*, (280):182.

Neviaser, J.S. 1945. Adhesive capsulitis of the shoulder: a study of the pathological findings in peri-arthritis of the shoulder. *The Journal of Bone and Joint Surgery*, 27(2):211-222.

Nicholson, G.P., Goodman, D.A., Flatow, E.L. & Bigliani, L.U. 1996. The acromion: morphologic condition and age-related changes. A study of 420 scapulas. *Journal of Shoulder and Elbow Surgery*, 5(1):1-11.

Nishida, K., Hashizume, H., Toda, K. & Inoue, H. 1996. Histologic and scanning electron microscopic study of the glenoid labrum. *Journal of Shoulder and Elbow Surgery*, 5(2):132-138.

Nyffeler, R.W. & Meyer, D.C. 2017. Acromion and glenoid shape: Why are they important predictive factors for the future of our shoulders? *EFORT open reviews*, 2(5):141-150.

Nyffeler, R.W., Werner, C.M., Sukthankar, A., Schmid, M.R. & Gerber, C. 2006. Association of a large lateral extension of the acromion with rotator cuff tears. *The Journal of Bone and Joint Surgery, American volume*, 88(4):800-805.

O' Brien, S.I., Neves, M.C., Arnoczky, S.P., Rozbruch, S.R., Di Carlo, E.F., Warren, R.F., Schwartz, R. & Wickiewicz, T.L. 1990. The anatomy and histology of the inferior glenohumeral ligament complex of the shoulder. *American Institute of Sports Medicine*, 18(5):449-456.

O' Connell, P.W., Nuber, G.W., Mileski, R.A. & Lautenschlager, E. 1990. The contribution of the glenohumeral ligaments to anterior stability of the shoulder joint. *The American Journal of Sports Medicine*, 18(6):579-584.

Omoumi, P., Teixeira, P., Lecouvet, F. & Chung, C.B. 2011. Glenohumeral joint instability. *Journal of Magnetic Resonance Imaging*, 33(1):2-16.

Otis, J.C., Jiang, C.C., Wickiewicz, T.L., Peterson, M.G., Warren, R.F. & Santner, T.J. 1994. Changes in the moment arms of the rotator cuff and deltoid muscles with abduction and rotation. *Journal of Bone and Joint Surgery*, 76(5):667-676.

Ovesen, J. & Nielsen, S., 1985. Stability of the shoulder joint: cadaver study of stabilizing structures. *Acta Orthopaedica Scandinavica*, 56(2):149-151.

Paine, R. & Voight, M.L. 2013. The role of the scapula. *International Journal of Sports Physical Therapy*, 8(5):617.

Pandey, V. & Willems, W.J. 2015. Rotator cuff tear: A detailed update. *Asia-Pacific Journal of Sports Medicine, Arthroscopy, Rehabilitation and Technology*, 2(1):1-14.

Paraskevas, G., Tzaveas, A., Papaziogas, B., Kitsoulis, P., Natsis, K. & Spanidou, S. 2008. Morphological parameters of the acromion. *Folia Morphologica*, 67(4):255-260.

Park, H.M. 2002. *Univariate Analysis and Normality Test Using SAS, STATA, and SPSS*.

Park, H.M. 2009. *Comparing Group Means: T-tests and One-way ANOVA using Stata, SAS, R, and SPSS*.

Peat, M. 1986. Functional anatomy of the shoulder complex. *Physical Therapy*, 66(12):1855-1865.

Peh, W.C., Farmer, T.H. & Totty, W.G. 1995. Acromial arch shape: assessment with MR imaging. *Radiology*, 195:501–505.

Peltz, C.D., Zauel, R., Ramo, N., Mehran, N., Moutzouros, V. & Bey, M.J. 2015. Differences in glenohumeral joint morphology between patients with anterior shoulder instability and healthy, uninjured volunteers. *Journal of Shoulder and Elbow Surgery*, 24(7):1014-1020.

Perry, J. 1978. Normal upper extremity kinesiology. *Physical Therapy*, 58(3):265-278.

Petersson, C.J. & Redlund-Johnell, I. 1983. Radiographic joint space in normal acromioclavicular joints. *Acta Orthopaedica Scandinavica*, 54(3):431-433.

Pettitt, A.N. 1979. A non-parametric approach to the change-point problem. *Applied statistics*, 126-135.

Phadke, V., Camargo, P.R. & Ludewig, P.M. 2009. Scapular and rotator cuff muscle activity during arm elevation: a review of normal function and alterations with shoulder impingement. *Brazilian Journal of Physical Therapy*, 13(1):1-9.

Pinzon, E. 2016. Thirty Years with Stata: A Retrospective.

Polit, D.F. & Beck, C.T. 2012. Nursing Research: Generating and assessing evidence for nursing practice. 9th ed. Lippincott Williams & Wilkins.

Poppen, N.K. & Walker, P.S. 1978. Forces at the glenohumeral joint in abduction. *Clinical Orthopaedics and Related Research*, (135):165-170.

Prescher, A. 2000. Anatomical basics, variations, and degenerative changes of the shoulder joint and shoulder girdle. *European Journal of Radiology*, 35(2):88-102.

Prescher, A. & Klümpen, T. 1997. The glenoid notch and its relation to the shape of the glenoid cavity of the scapula. *The Journal of Anatomy*, 190(3):457-460.

Rajani, S. & Man, S. 2013. Review of bicipital groove morphology and its analysis in North Indian Population. *International Scholarly Research Notices: Anatomy*, 2013.

Rajendra, G.K., Ubbaida, S.A. & Kumar, V.V. 2016. The Glenoid Cavity: its morphology and clinical significance. *International Journal of Biological & Medical Research*, (7):5552-5555.

Rajput, H.B., Vyas, K.K. & Shroff, B.D. 2012. A study of morphological patterns of glenoid cavity of scapula. *National Journal of Medical Research*, 2(4):504-507.

Ranjan, D.V. & Antao, N.A. 2002. Anterior inferior shoulder instability-Part I: The pathogenesis of anterior inferior shoulder instability. *Indian Journal of Orthopaedics*, 36(4):214.

Ravindranath, Y., Abraham, A., Thelekatt, D.J., Oomen, A.T. & Johnsia, S., Acromion–Anatomic Study of South Indian Dry Scapulae.

Reed, D., Cathers, I., Halaki, M. & Ginn, K. 2013. Does supraspinatus initiate shoulder abduction? *Journal of Electromyography and Kinesiology*, 23(2):425-429.

Reilly, P., Macleod, I., Macfarlane, R., Windley, J. & Emery, R.J.H. 2006. Dead men and radiologists don't lie: a review of cadaveric and radiological studies of rotator cuff tear prevalence. *The Annals of The Royal College of Surgeons of England*, 88(2):116-121.

Robinette, K., Churchill, T. & McConville, J. T. 1979. A Comparison of Male and Female Body Sizes and Proportions. Yellow Springs, Anthropology Research Project.

Roche, C., Angibaud, L., Flurin, P.H., Wright, T., Fulkerson, E. & Zuckerman, J. 2005. Anatomic validation of an " anatomic" shoulder system. *BULLETIN-HOSPITAL FOR JOINT DISEASES NEW YORK*, 63(3/4):93.

Rockwood Jr, C.A. & Green, D.P. 1984. Injuries to the acromioclavicular joint. In: *Fractures in adults*, vol 1, 2nd ed. Philadelphia: JB Lippincott; pp 860-910.

Rolf, O., von Weyhern, A.H., Ewers, A., Boehm, T.D. & Gohlke, F. 2008. Acromioclavicular dislocation Rockwood III–V: results of early versus delayed surgical treatment. *Archives of Orthopaedic and Trauma Surgery*, 128(10):1153-1157.

Romeo, A.A., Hang, D.W., Bach, B.R. & Shott, S. 1999. Repair of full thickness rotator cuff tears. *Clinical Orthopaedics*, 367:243-255.

Ruckstuhl-Knüssel, H. 2008. Mechanics of the shoulder complex and clinical investigation in spinal cord injured individuals (Doctoral dissertation, ETH Zurich).

Saha, A. 1971. Dynamic stability of the glenohumeral joint. *Acta Orthopaedica Scandinavica*, 42(6):491-505.

Saha, S. & Vasudeva, N. 2017. Morphometric Evaluation of Adult Acromion Process in North Indian Population. *Journal of Clinical and Diagnostic Research*, 11(1):AC08.

Sanders, T.G. & Miller, M.D. 2005. A systematic approach to magnetic resonance imaging interpretation of sports medicine injuries of the shoulder. *The American Journal of Sports Medicine*, 33(7):1088-1105.

Sangiampong, A., Chompoonong, S., Sangvichien, S., Thongtong, P. & Wongjittraporn, S. 2007. The acromial morphology of Thais in relation to gender and age: study in scapular dried bone. *Journal of the Medical Association of Thailand*, 90(3):502-507.

Sansone, V., Consonni, O., Maiorano, E., Meroni, R. & Goddi, A. 2016. Calcific tendinopathy of the rotator cuff: the correlation between pain and imaging features in symptomatic and asymptomatic female shoulders. *Skeletal Radiology*, 45(1):49-55.

Sarrafian, S.K. 1983. Gross and functional anatomy of the shoulder. *Clinical Orthopaedics and Related Research*, 173:11-19.

Sarwar, M.S., Diwan, C.V., Rahamn, H., Raheman, H. & Moosa, S.M. 2015. A Morphometric study of glenoid cavity of adult human scapula. *International Journal of Recent Trends in Science and Technology*, 2015:15(3):486-490.

Schippinger, G., Bailey, D., McNally, E. G., Kiss, J. & Carr, A. J. 1997. Anatomy of the normal acromion investigated using MRI. *Langenbecks Archiv Für. Chirurgie*, 382(3):141-144.

Schenkman, M. & Rugo de Cartaya, V. 1987. Kinesiology of the shoulder complex. *Journal of Orthopaedic & Sports Physical Therapy*, 8(9):438-450.

Schulz, T.J., Jacobs, B. & Patterson, R.L. 1969. Unrecognized dislocations of the shoulder. *Journal of Trauma and Acute Care Surgery*, 9(12):1009-1023.

Seitz, A.L., McClure, P.W., Finucane, S., Boardman III, N.D. & Michener, L.A. 2011. Mechanisms of rotator cuff tendinopathy: intrinsic, extrinsic, or both? *Clinical Biomechanics*, 26(1):1-12.

Shahabpour, M., Pouliart, N. & De Maeseneer, M. 2017. Glenohumeral Ligaments and Unstable Shoulder: CT and MR Arthrography. *Journal of the Belgian Society of Radiology*, 101(S2).

Shapiro, S.S. & Wilk, M.B. 1965. An analysis of variance test for normality (complete samples). *Biometrika*, 52(3/4):591-611.

Sher, J.S., Uribe, J.W., Posada, A., Murphy, B.J. & Zlatkin, M.B. 1995. Abnormal findings on Magnetic Resonance Images of asymptomatic shoulders. *Journal of Bone and Joint Surgery, American volume*, 77:10-15.

Shuman, W.P., Kilcoyne, R.F., Matsen, F.A., Rogers, J.V. & Mack, L.A. 1983. Double-contrast computed tomography of the glenoid labrum. *American Journal of Roentgenology*, 141(3):581-584.

Sinha, M.B., Sinha, H.P. & Joy, P. 2018. The acromial morphology and its implication in impingement syndrome: An anatomical study. *Journal of the Anatomical Society of India*, 67(1):30-34.

Singh, J., Pahuja, K. & Aggarwal, R. 2013. Morphometric parameters of the acromion process in adult human scapulae. *Indian Journal of Basic Applied Medical Research*, 8(2):1165-1170.

Skupiński, J., Piechota, M.Z., Wawrzynek, W., Maczuch, J. & Babińska, A. 2017. The bony Bankart lesion: how to measure the glenoid bone loss. *Polish Journal of Radiology*, 82:58.

Smith, R.L. & Brunolli, J. 1989. Shoulder kinesthesia after anterior glenohumeral joint dislocation. *Physical Therapy*, 69(2):106-112.

Souchon, E. 1891. Operative treatment of irreducible dislocations of the shoulder joint. Recent or old, simple or complicated. *Transaction of the Meeting of the American Surgical Association*, 15:311-442.

Spiegl, U.J., Warth, R.J. & Millett, P.J. 2014. Symptomatic internal impingement of the shoulder in overhead athletes. *Sports Medicine and Arthroscopy Review*, 22(2):120-129.

Stein, B.E., Wiater, J.M., Pfaff, H.C., Bigliani, L.U. & Levine, W.N. 2001. Detection of acromioclavicular joint pathology in asymptomatic shoulders with Magnetic Resonance Imaging. *Journal of Shoulder and Elbow Surgery*, 10(3):204.

Steyn, M. & İşcan, M.Y. 1999. Osteometric variation in the humerus: sexual dimorphism in South Africans. *Forensic Science International*, 106(2):77-85.

Sukthankar, A., Werner, C.M., Brucker, P., Nyffeler, R.W. & Gerber, C. 2009, March. Lateral extension of the acromion and rotator cuff tears—a prospective study. In *Orthopaedic Proceedings*, Vol. 91:(No. SUPP_I:123-123). The British Editorial Society of Bone and Joint Surgery.

Syed, U.A.M., Davis, D.E., Wei Ko, J., Lee, B.K., Huttman, D., Seidl, A., Deirmengian, C. & Abboud, J.A. 2017. Quantitative anatomical differences in the shoulder. *Orthopedics*, 40(3):155-160.

Tackett, J.J. & Ablove, R.H. 2011. Magnetic Resonance Imaging study of glenohumeral relationships between genders. *Journal of Shoulder and Elbow Surgery*, 20(8):1335-1339.

Tate, A.R., McClure, P., Kareha, S., Irwin, D. & Barbe, M.F. 2009. A clinical method for identifying scapular dyskinesis, Part 2: Validity. *Journal of Athletic Training*, 44(2):165-173.

Tea, M. 1981. Fisher's exact test.

Terry, G.C. & Chopp, T.M. 2000. Functional anatomy of the shoulder. *Journal of athletic training*, 35(3):248.

Thomazeau, H., Rolland, Y., Lucas, C., Duval, J.M. & Langlais, F. 1996. Atrophy of the supraspinatus belly assessment by MRI in 55 patients with rotator cuff pathology. *Acta Orthopaedica Scandinavica*, 67(3):264-268.

Tischer, T., Vogt, S., Kreuz, P.C. & Imhoff, A.B. 2011. Arthroscopic anatomy, variants, and pathologic findings in shoulder instability. *Arthroscopy: The Journal of Arthroscopic and Related Surgery*, 27(10):1434-1443.

Torrens, C., López, J.M., Puente, I. & Cáceres, E. 2007. The influence of the acromial coverage index in rotator cuff tears. *Journal of Shoulder and Elbow Surgery*, 16(3):347-351.

Urita, A., Funakoshi, T., Amano, T., Matsui, Y., Kawamura, D., Kameda, Y. & Iwasaki, N., 2016. Predictive factors of long head of the biceps tendon disorders—the bicipital groove morphology and subscapularis tendon tear. *Journal of shoulder and elbow surgery*, 25(3):384-389.

Väättäinen, U., Pirinen, A. & Mäkelä, A. 1991. Radiological evaluation of the acromioclavicular joint. *Skeletal Radiology*, 20(2):115-116.

Van der Helm, F.C.T. 1996. A standardized protocol for motions recordings of the shoulder. In: Veeger, H.E.J., Van der Helm, F.C.T., Rozing, P.M. (Editors), pp1-7. *Proceedings of the First Conference of the International Shoulder Group*, Shaker Publishing, Maastricht.

Vangsness Jr, C.T., Jorgenson, S.S., Watson, T.R.O.Y. & Johnson, D.L. 1994. The origin of the long head of the biceps from the scapula and glenoid labrum. An anatomical study of 100 shoulders. *The Journal of Bone and Joint Surgery. British volume*, 76(6):951-954.

Von Eisenhart-Rothe, R., Mayr, H.O., Hinterwimmer, S. & Graichen, H. 2010. Simultaneous 3D assessment of glenohumeral shape, humeral head centering, and scapular positioning in atraumatic shoulder instability: A Magnetic Resonance-based in vivo analysis. *American Journal of Sports Medicine*, 38:375-382.

Von Schroeder, H.P., Kuiper, S.D. & Botte M.J. 2001. Osseous anatomy of the scapula. *Clinical Orthopaedics*, 303:131–139.

Wafae, N., Atencio Santamaría, L.E., Vitor, L., Pereira, L.A., Ruiz, C.R. & Wafae, G.C. 2010. “Morphometry of the human bicipital groove (sulcus intertubercularis),” *Journal of Shoulder and Elbow Surgery*, vol. 19:(1):65–68.

Warth, R.J., Martetschläger, F., Gaskill, T.R. & Millett, P.J. 2013. Acromioclavicular joint separations. *Current reviews in musculoskeletal medicine*, 6(1):71-78.

Wei-Xun, F. & Chun-Tu, Q. 1993. Load distribution of multi-fastener laminated composite joints. *International Journal of Solids and Structures*, 30(21):3013-3023.

Wiley, W.B., Goradia, V.K. & Pearson, S.E. 2005. Arthroscopic capsular plication-shift. *Arthroscopy: The Journal of Arthroscopic and Related Surgery*, 21(1):119-121.

Wilk, K.E., Arrigo, C.A. & Andrews, J.R. 1997. Current concepts: the stabilizing structures of the glenohumeral joint. *Journal of Orthopaedic and Sports Physical Therapy*, 25(6):364-379.

Wilk, K.E., Macrina, L.C., Cain, E.L., Dugas, J.R. & Andrews, J.R. 2013. The recognition and treatment of superior labral (slap) lesions in the overhead athlete. *International Journal of Sports Physical Therapy*, 8(5):579.

Worcester Jnr, J.N. & Green, D.P. 1968. Osteoarthritis of the acromioclavicular joint. *Clinical Orthopaedics*, 58:69-73.

Wu, G., Van der Helm, F.C., Veeger, H.D., Makhsous, M., Van Roy, P., Anglin, C., Nagels, J., Karduna, A.R., McQuade, K., Wang, X. & Werner, F.W. 2005. ISB recommendation on definitions of joint coordinate systems of various joints for the reporting of human joint motion—Part II: shoulder, elbow, wrist and hand. *Journal of Biomechanics*, 38(5):981-992.

Yadav, S.K. & Zhu, W.H. 2017. A systematic review: Of acromion types and its effect on degenerative rotator cuff tear. *International Journal of Orthopaedics*, 3(1):453-458.

Yamaguchi, K., Tetro, A.M., Blam, O., Evanoff, B.A., Teefey, S.A. & Middleton, W.D. 2001. Natural history of asymptomatic rotator cuff tears: A longitudinal analysis of asymptomatic tears detected sonographically. *Journal of Shoulder and Elbow Surgery*, 10(3):199.

Yang, H.F., Tang, K.L., Chen, W., Dong, S.W., Jin, T., Gong, J.C., Li, J., Wang, H., Wang J. & Xu, J. 2009. An anatomic and histologic study of the coracohumeral ligament. *Journal of Shoulder and Elbow Surgery*, 18(2):305-310.

Yiannakopoulos, C.K., Mataragas, E. & Antonogiannakis, E. 2007. A comparison of the spectrum of intra-articular lesions in acute and chronic anterior shoulder instability. *Arthroscopy: The Journal of Arthroscopic and Related Surgery*, 23(9):985-990.

Yu, J.S., Dardani, M. & Fischer, R.A. 2000. MR observations of posttraumatic osteolysis of the distal clavicle after traumatic separation of the AC joint. *Journal of Computed Assisted Tomography*;24(1):159–164.

Zanca, P. 1971. Shoulder pain: involvement of the acromioclavicular joint: (analysis of 1,000 cases). *American Journal of Roentgenology*, 112(3):493-506.

Appendix A

Ethics Documentation: Certificate of Approval and progress reports

The Research Ethics Committee, Faculty Health Sciences, University of Pretoria complies with ICH-GCP guidelines and has US Federal wide Assurance.

- FWA 00002567, Approved dd 22 May 2002 and Expires 03/20/2022.
- IRB 0000 2235 IORG0001762 Approved dd 22/04/2014 and Expires 03/14/2020.



UNIVERSITEIT VAN PRETORIA
UNIVERSITY OF PRETORIA
YUNIBESITHI YA PRETORIA

Faculty of Health Sciences Research Ethics Committee

27/07/2017

Approval Certificate New Application

Ethics Reference No: 304/2017

Title: A morphometric study of skeletal and soft tissue components of the glenohumeral joint associated with shoulder pathologies

Dear Milinda Kruger

The **New Application** as supported by documents specified in your cover letter dated 18/07/2017 for your research received on the 19/07/2017, was approved by the Faculty of Health Sciences Research Ethics Committee on its quorate meeting of 26/07/2017.

Please note the following about your ethics approval:

- Ethics Approval is valid for 1 year
- Please remember to use your protocol number (**304/2017**) on any documents or correspondence with the Research Ethics Committee regarding your research.
- Please note that the Research Ethics Committee may ask further questions, seek additional information, require further modification, or monitor the conduct of your research.

Ethics approval is subject to the following:

- The ethics approval is conditional on the receipt of **6 monthly written Progress Reports**, and
- The ethics approval is conditional on the research being conducted as stipulated by the details of all documents submitted to the Committee. In the event that a further need arises to change who the investigators are, the methods or any other aspect, such changes must be submitted as an Amendment for approval by the Committee.

We wish you the best with your research.

Yours sincerely

Dr R Sommers; MBChB; MMed (Int); MPharMed, PhD
Deputy Chairperson of the Faculty of Health Sciences Research Ethics Committee, University of Pretoria

The Faculty of Health Sciences Research Ethics Committee complies with the SA National Act 61 of 2003 as it pertains to health research and the United States Code of Federal Regulations Title 45 and 46. This committee abides by the ethical norms and principles for research, established by the Declaration of Helsinki, the South African Medical Research Council Guidelines as well as the Guidelines for Ethical Research: Principles Structures and Processes, Second Edition 2015 (Department of Health).

☎ 012 356 3084 ✉ deepeka.behari@up.ac.za / fnsethics@up.ac.za 🌐 <http://www.up.ac.za/healthethics>
✉ Private Bag X323, Arcadia, 0007 - Tswelopele Building, Level 4, Room 60, Gezina, Pretoria



UNIVERSITEIT VAN PRETORIA
UNIVERSITY OF PRETORIA
YUNIBESITHI YA PRETORIA

Faculty of Health Sciences Research Ethics Committee

28/06/2018

Milinda Kruger
Clinical Anatomy
BMW Gebou
University of Pretoria

Dear Milinda Kruger

RE: Progress Report for Protocol Number 304/2017

304/2017 A morphometric study of skeletal and soft tissue components of the glenohumeral joint associated with shoulder pathologies

Principal Investigator Milinda Kruger

The above mentioned document has been tabled at the meeting of 27/06/2018 and noted.

The document will be filed.

With regards

DR R SOMMERS; MBChB; M.Med (Int); MPhar Med; PhD
Deputy Chair: Main Research Ethics Committee
Faculty of Health Sciences
University of Pretoria

☎ 012 356 3085 📧 fhsethics@up.ac.za 📦 Private Bag X323, Arcadia, 0007
🌐 <http://www.up.ac.za/healthethics>, Tswelopele Building, Level 4-59



30/08/2018

Milinda Kruger
Department of Anatomy
University of Pretoria

Dear Milinda Kruger

RE: Final Progress Report for Protocol Number 304/2017

304/2017 A morphometric study of skeletal and soft tissue components of the glenohumeral joint associated with shoulder pathologies.

Principal Investigator Milinda Kruger

The above mentioned document has been tabled at the meeting of 29/08/2018 and noted.

The document will be filed.

With regards

DR R SOMMERS; MBChB; M.Med (Int); MPhar.Med; PhD
Deputy Chair: Main Research Ethics Committee
Faculty of Health Sciences
University of Pretoria

☎ 012 356 3085 ✉ fhsethics@up.ac.za ✉ Private Bag X323, Arcadia, 0007
☐ <http://www.up.ac.za/healthethics> Tswelopele Building, Level 4-59

Appendix B

Cadaveric measurements

Specimen	Age	Sex	Pop	Side	AT	AHD	HHMax_dia	HHI	ITGW	GFD
1	36	male	white	l	I	4,19	51,77	130	3,2	7,18
2	36	male	white	r	I	3,55	52,61	130	3,5	7,14
3	55	male	white	l	I	4,68	51,05	131	5,05	8
4	55	male	white	r	I	4,82	55,24	131	5,91	5,1
5	57	male	white	l	II	3,3	40,36	134	7,02	2,3
6	57	male	white	r	II	4,73	40,4	134	1,03	2,35
7	58	male	white	l	I	3,41	55	129	5	2,81
8	58	male	white	r	I	4,8	57,8	129	5,69	3,41
9	60	male	white	l	I	5,02	47,7	130	5,02	3,88
10	60	male	white	r	I	6,02	50,7	130	5,7	4,98
11	61	male	white	l	II	6,31	52,7	130	6,63	4,17
12	61	male	white	r	II	4,7	46,31	134	5,51	3,11
13	62	male	white	l	I	4,8	52,77	132	6,25	6,1
14	62	male	white	r	I	3,78	52,38	129	5,2	6
15	62	male	white	l	I	4,53	54,71	130	4,32	2,01
16	62	male	white	r	I	4,69	54,7	131	4,8	5,11
17	64	male	white	l	I	3,14	51,9	132	5,3	4,32
18	64	male	white	r	I	4,59	37,71	134	6,59	5,95
19	64	male	white	l	I	3,19	46,44	131	4,5	2,94
20	64	male	white	r	I	1,13	44,28	130	5,98	2,01
21	66	male	white	l	I	4,28	48,88	131	6,52	6,01
22	66	male	white	r	I	5,41	50,3	129	4	6,42
23	68	male	white	l	I	6,19	45,03	130	7,51	7,9
24	78	male	white	r	I	5,49	49,5	128	6,08	8,11
25	80	male	white	l	I	3,69	47,02	130	6,99	6,7
26	80	male	white	r	I	3,69	47,02	130	6,99	9,52
27	45	female	white	l	II	4,08	45,98	130	6,73	2,38
28	45	female	white	r	II	4,51	48,39	130	6,4	2,31
29	49	female	white	l	II	4,81	44,34	130	7,84	2,91
30	49	female	white	r	II	4,75	44,39	130	7,2	3,41
31	58	female	white	l	II	4,18	49,02	130	7,02	1,88
32	58	female	white	r	II	4,92	50,02	131	8,54	1,18
33	59	female	white	l	I	3,89	42,51	139	7,61	5,39
34	59	female	white	r	I	3,41	42,06	139	7,59	11,62
35	64	female	white	r	I	2	52,9	132	3,5	8,81
36	67	female	white	l	II	6,07	40,72	130	3,62	4,32
37	67	female	white	r	II	4,1	43	130	5,03	5,95
38	80	female	white	l	II	5,13	36,88	131	4,44	3,44
39	82	female	white	l	I	5,4	50,52	139	8,51	6,13
40	82	female	white	r	I	4	45,49	130	3,81	6,06
41	82	female	white	l	I	3,81	45,21	130	5,69	5,21
42	82	female	white	r	I	2,47	40,12	130	4,43	5,45
43	84	female	white	l	I	3,33	40,74	133	7,02	2,43

Specimen	Age	Sex	Pop	Side	AT	AHD	HHMax_dia	HHI	ITGW	GFD
44	84	female	white	r	I	3	42,05	133	6,7	2,42
45	91	female	white	l	I	4,18	40,5	130	5,4	7,53
46	91	female	white	r	I	5,39	46,29	130	5,44	8,62
47	46	male	black	l	II	5,31	45,52	129	4,46	4,91
48	46	male	black	r	II	5,22	48,12	129	5,22	3,2
49	62	male	black	l	II	3,59	47,38	132	8,19	5,52
50	62	male	black	r	II	4,84	46,18	132	4,03	7,1

Appendix C

X-ray measurements with intra-and inter observer

Number	sex	race	Age	side	AT	NK	MCK	MCK	AI	NK	MCK	MCK	GA	NK	MCK	MCK	GH	NK	MCK	MCK	ACJ	NK	MCK	MCK	LAA	NK	MCK	MCK	AHD	NK	MCK	MCK	GFL	NK	MCK	MCK	HHMax Diam	NK	MCK	MCK	HHI	NK	MCK	MCK
1	male	black	26	r	III				0,7				38,3				50,6				3,6				95,7				12,3				32,6				47,3				135,6			
2	male	black	27	r	II				0,92				45,5				49,6				4,9				55,8				14,1				48				45,6				137,8			
3	male	black	28	r	II				0,69				32,7				47				2,4				74,6				10,9				33,4				41,3				133,3			
4	male	black	28	l	II				0,84				39,4				46,7				9,4				64,8				12,1				36,6				52,6				142,5			
5	male	black	29	r	I				0,72				40,5				56,2				3,2				72,3				9,8				39,4				51,6				144			
6	male	black	30	l	I				0,81				38,1				46,7				7,8				93,4				12,4				31,8				45,1				141,2			
7	male	black	30	r	II				0,72				40,4				56				3,1				72,1				8,7				34,9				38,6				142,4			
8	male	black	31	r	I				0,86				38,5				44,4				7,4				77,3				18,4				37,1				45				144,9			
9	male	black	33	r	I				0,84				39,4				46,7				5,9				78,9				11,5				39,2				50,5				143,9			
10	male	black	33	l	II				0,93				39,7				42,4				4,8				69				12,3				30,4				48,8				130,7			
11	male	black	34	l	I				0,59				30,2				51				24,5				90				10,9				35				51				138,2			
12	male	black	34	r	I				0,63				36				57				9,6				91,1				8,6				32,8				46,9				141,2			
13	male	black	34	r	I				0,79				44,2				55,9				2,3				80,5				4				33,1				49,3				130			
14	male	black	36	r	I				0,81				42,5				52,4				3,3				77,1				11,8				38,5				52,9				136			
15	male	black	36	r	I				0,8				41,6				52				5,2				76				10,6				33,5				46,4				143,5			
16	male	black	37	r	II				0,74				42,7				57,6				7,1				74,5				11,4				35,1				54				137,9			
17	male	black	37	l	II				0,74				41,4				55,4				3,3				76,3				12,7				33,2				49,3				141			
18	male	black	37	r	II				0,83				46,9				55,9				3				79,3				13,7				42				42				141			
19	male	black	38	r	II	II	II	II	0,63	0,6	0,63	0,63	37,1	35,5	35,6	37,1	56,5	56,2	56,5	56,5	1,8	1,6	1,8	1,8	82,6	82,5	81,9	82,6	5,9	3,5	5,9	5,9	39,1	39,3	39,1	39,1	55,3	55,5	55,3	55,3	127,3	127,5	127,3	127,3
20	male	black	38	r	I				0,67				41				60,5				6,3				71,1				15				35,8				45,7				133,1			
21	male	black	38	l	II	II	II	II	0,79	0,8	0,79	0,79	45,4	46,3	45,4	45,4	57,5	57,7	57,5	57,5	2,2	2,5	2,2	2,2	68,3	49,2	68,3	68,3	10,9	11	10,9	10,9	38,2	38,3	38,2	38,2	50,2	51,6	50,2	50,2	132,1	131,7	132,1	132,1
22	male	black	39	r	II				0,96				53,9				55,9				9,2				90,2				14,5				31,3				48				134			
23	male	black	39	l	I				0,92				44,7				48,2				11				63,3				11							45,6				134,5				
24	male	black	39	r	I				0,8				44,8				56				11,8				72,4				9,2				32,1				46,4				139,3			
25	male	black	42	l	I				0,88				42				47,6				9				78,7				5,6				36,4				42				146,5			
26	male	black	43	r	II	II	II	II	0,75	0,73	0,75	0,75	43,4	43,3	43,4	43,4	57,6	58,8	57,6	57,6	6,5	6,8	6,5	6,5	80,9	81,6	80,9	80,9	13,5	13,5	13,5	13,5	43,5	43,9	43,5	43,5	57,1	57	57	57,1	132,8	132,9	132,8	132,8
27	male	black	44	l	II	II	II	II	0,72	0,7	0,72	0,72	42,2	42,8	42,2	42,2	58	58,1	58	58	6,9	7	6,9	6,9	76,5	76	76,5	76,5	7,7	7,8	7,7	7,7	43	43,7	43	43	53	53,4	53	53	144	144,3	144	144
28	male	black	44	l	II				0,75				39,7				52,6				11,6				77,9				9				32,9				51,6				150			
29	male	black	44	r	II				0,93				39,7				42,4								72,8				14,1				43				54				141			
30	male	black	44	r	II				0,7				31,9				45,5				3				62,8				9,6				30,1				46,2				145,6			
31	male	black	45	r	II				0,8				44,7				55,8				6,6				65,3				15,9				41,8				51,4				139,5			
32	male	black	51	l	III				0,63				36,1				57,2				4,7				96,8				16,8				37,9				54,2				136,6			
33	male	black	54	r	I				0,94				42,1				44,7				3,7				69,7				19,8				35,9				47,4				144,8			
34	male	black	54	r	II				1,17				46,5				39,5				7				74,3				9,6				30,9				53,5				136			
35	male	black	55	l	I				0,7				40,7				57,4				11				75,4				10,7				42				53,2				137			
36	male	black	55	l	I				0,73				41,2				56,4				0				15,6				3,4				36,9				52,5				148,7			
37	male	black	55	r	II				0,68				41				59,9				11,3				82,3				13,2				42,9				52,3				142,6			
38	male	black	57	l	I	II	II	I	0,85	0,9	0,85	0,85	46,1	46,5	46,1	46,1	54,1	54	54,1	54,1	3,3	3,4	3,3	3,3	67,6	67,7	67,6	67,6	10	10,2	10	10	44	44,1	44	44	47,3	47,3	47,3	47,3	136,4	136,7	136,4	136,4
39	male	black	62	r	II				0,88				42				47,2				0,9				41,6				1,9				39				47,3				152			
40	male	black	63	r	I				0,92				45,8				49,7				3,1				68				9,4				34,3				54,2				137			
41	male	black	64	r	II				0,91				36,7				39,9				4,2				67,4				12,2				39,5				53,7				133,7			
42	male	black	65	r	I	I	I	I	0,82	0,8	0,82	0,82	47,8	47,9	47,8	47,8	58,1	58	58,1	58,1	2,1	2,3	2,1	2,1	68,3	68,9	68,3	68,3	10,3	10,5	10,3	10,3	43,6	43,8	43,6	43,6	55,4	55,5	55,4	55,4	138,1	138,2	138,1	138,1
43	female	black	29	r	II				0,91				37				41,4				8,7				81,9				11,2				34,1				42,8				130			
44	female	black	31	r	II				0,84				40,5				47,9				6				78,3				11,9				28,5				39,2				146,7			
45	female	black	33	r	I				1,05				42,2				40,2				4,7				58,9				9,4				34				38				141			
46	female	black	34	r	II				0,83				39,6				47,3				5,7				69				12,8				39,1				45				134,2			
47	female	black	36	l	III	III	III	III	0,87	0,9	0,87	0,87	39,5	39</																														

Number	sex	race	Age	side	AT	NK	MCK	MCK	AI	NK	MCK	MCK	GA	NK	MCK	MCK	GH	NK	MCK	MCK	ACJ	NK	MCK	MCK	LAA	NK	MCK	MCK	AHD	NK	MCK	MCK	GFL	NK	MCK	MCK	HHMax Diam	NK	MCK	MCK	HHI	NK	MCK	MCK
48	female	black	39	r	III				0,85				40,1				46,7				6,6				79,6				13,6				32,4				42,8				137,4			
49	female	black	42	l	I	I	I	I	0,65	0,6	0,65	0,65	31	30	31	31	47,6	47,8	47,6	47,6	8	8	8	8	82,3	82,4	82,3	82,3	18,2	18,3	18,2	18,2	33,5	35,8	33,5	33,5	43	42	43	43	137	137,7	137	137
50	female	black	43	l	I				0,8				41,9				52,1				6,2				81,4				11,9				29,3				41,5				144,5			
51	female	black	47	r	II				0,85				40,1				46,7				5,5				76,1				10,6				37,5				43,3				138,2			
52	female	black	48	l	II				0,97				53,3				54,7				4,6				71,5				9,9				30,7				40,6				176			
53	female	black	52	l	I				0,68				41				60,2				3				85,1				13,4				33,7				53				137,4			
54	female	black	52	l	I				0,63				36,4				57				1,9				48,6				2,3				32,6				47				120			
55	female	black	55	l	I				0,79				44,7				55,9				7,1				69,8				10,4				28,9				44,7				138			
56	female	black	55	l	II				0,73				41				56				3,4				79,8				9,2				32,8				43,2				144			
57	female	black	57	r	I				0,94				40,1				42,5				5,4				60				10,9				35,4				45,5				143,8			
58	female	black	57	l	I				0,91				36,7				39,9				0,8				79,6				9,6				31,9				42,2				133			
59	female	black	60	l	II	II	II	II	0,81	0,8	0,81	0,81	35,2	35	35,2	35,2	43	42,9	43	43	1,42	1,4	1,42	1,42	64,5	64,2	64,5	64,5	9,5	9,7	9,5	9,5	33,3	33,6	33,3	33,3	39	39,2	39	39	139,2	139,2	139,2	139,2
60	female	black	62	r	I				0,79				44,7				55,9				4,7				61				8,3				38,4				51,7				133,5			
61	female	black	63	r	I				0,82				41,6				50,7				5,2				63,4				12,5				37,7				48,5				137			
62	female	black	63	l	I				0,78				38,6				49,1				8,8				71				14,7				28,6				46				130,2			
63	female	black	63	l	II				0,79				44,7				55,9				3,3				68,1				3,3				33,3				42,9				135			
64	female	black	63	r	I				0,81				38,9				47,8				2,9				68,1				7,4				30,5				46,1				130			
65	male	white	26	l	I				0,68				41,4				60,4				2,9				88,7				9,2				35,6				53,1				143,5			
66	male	white	26	r	I				0,69				32,7				47,1				4,3				97,9				13,3				40,7				47,2				140			
67	male	white	32	l	II	II	II	II	0,64	0,7	0,64	0,64	38,9	39,1	38,9	38,9	60	59,2	60	60	3,5	3,7	3,5	3,5	82,1	82	82,1	82,1	11,1	11,1	11,1	11,1	43,4	43	43,4	43,4	58	60,2	58	58	138,3	138,9	138,3	138,9
68	male	white	33	r	I				0,63				34,9				55				9,5				76,5				9,7				44,4				51,5				139			
69	male	white	34	l	I				0,68				38,2				56,1				2,5				82				10,3				39,6				51,1				149,5			
70	male	white	35	r	I				0,53				29,8				55,5				7,1				89,5				12,8				38,9				42				144,1			
71	male	white	35	r	I				0,72				40,7				56				14,3				93,2				10,1				44,2				50,9				144,9			
72	male	white	35	r	I				0,87				46,1				52,9				3,6				80,9				5,1				42,5				56				142			
73	male	white	38	r	II				0,71				33				46				6				86,8				13,5				49,3				55				146,4			
74	male	white	41	r	I				0,81				38,1				46,7				6,8				87,7				11,6				39,1				49				145,3			
75	male	white	44	r	II				0,86				42				48,6				6,2				55,9				11,9				41,9				52,4				139,8			
76	male	white	45	r	II	II	II	II	0,64	0,63	0,64	0,64	40,2	40	40,2	40,2	62,3	62,7	62,3	62,3	2,2	2,1	2,2	2,2	81,9	82	81,9	81,9	14,3	14,3	14,3	14,3	45,4	45,5	45,4	45,4	62,7	63,9	62,7	62,7	141,5	141,3	141,5	141,5
77	male	white	45	r	II				0,66				37				56				6,2				98,7				11,4				39,5				53				134,2			
78	male	white	52	l	II	II	II	II	0,73	0,7	0,73	0,73	46,4	46,6	46,4	46,4	63,4	63,5	63,4	63,4	2,6	2,8	2,6	2,6	78,3	78,3	78,3	78,3	10,2	10,5	10,2	10,2	47	47,9	47	47	62	62,1	62	62	133	133,6	133	133
79	male	white	57	l	II				0,72				34,8				48,3				6,4				76				12				38,2				51,1				146,7			
80	male	white	59	r	I				0,86				42,1				48,6				4				68,8				13,4				45,6				52				131			
81	male	white	62	r	II				0,96				44,9				46,4				2,6				60,6				5,2				30,5				50				137,7			
82	female	white	29	r	II	II	II	II	0,81	0,8	0,81	0,81	45,1	45,5	45,1	45,1	55,2	55,3	55,2	55,2	1,5	1,9	1,5	1,5	51,7	50,7	51,7	51,7	3,4	3,3	3,4	3,4	39,3	39,6	39,3	39,3	50	51,9	50	50	135,2	135,2	135,2	135,2
83	female	white	31	l	I				0,61				32,1				52,1				3,2				56,7				15,2				39,4				51				142			
84	female	white	37	l	I				0,9				49,4				54,4				5,7				74,4				15,1				34,3				41,3				141			
85	female	white	49	l	I	I	I	I	0,81	0,9	0,81	0,81	36	38,8	36	36	44,3	44,2	44,3	44,3	15,2	!!	15,2	15,2	54,3	54,6	54,3	54,3	12,9	12,1	12,9	12,9	37	37,1	37	37	43,5	43,2	43,5	43,5	147,8	147,6	147,8	147,8
86	female	white	51	l	I				0,83				40,1				48,1				9,6				80,5				9,3				35				43				140,5			
87	female	white	54	l	II				0,81				38,1				46,7				9				69,8				10,6				37,7				43				143,2			
88	female	white	55	l	I				0,6				30				50				9,4				90,8				12				31,5				49,3				142			
89	female	white	55	r	I				0,58				32,5				55,9				1				83,6				12,3				39				45,4				145			
90	female	white	58	r	II				0,93				39,7				42,4				3,2				74,3				6,7				33,6				46,6				141,6			
91	female	white	63	r	I				0,73				41,2				56,3				5,8				67,7				13,1				30,5				44,8				146,4			
92	female	white	63	l	I				0,73				41,4				56,3				4,6				83,9				8,7				34,3				41,8				147,1			
93	female	white	63	l	I				0,78				38,7				49,3				4,7				67,7				15,1				43,9				46				131,8			
94	female	white	65	r	I				0,76				33,4				4																											

Appendix D

MRI measurements with intra-and inter observer

Number	Age	Path group	sex	Side	LAA	NK	MCK	MCK	ACJ	NK	MCK	MCK	RC	GHJ_L_C	GL	AT	NK	MCK	MCK	AI	NK	MCK	MCK	GA	NK	MCK	MCK	GH	NK	MCK	MCK	AHD	NK	MCK	MCK	GFL	NK	MCK	MCK	GHJ_space	NK	MCK	MCK	HHMax_Diam	NK	MCK	MCK	HHI	NK	MCK	MCK
1	25	2	male	l	88	88	88	88	4	5	4	4	Pathology	Pathology	tear	I	I	I	I	0,57	0,57	0,57	0,57	33	33	33	33	58	58	58	58	9	9	9	9	45	45	45	45	4	4	4	4	53	54	53	53	142	142	142	142
2	25	1	male	l	82				4				Pathology	Pathology	intact	I				0,7				35			50				10				36				2				43				138				
3	25	1	male	l	88				4				Pathology	Pathology	tear	I				0,53				30			56				15				36				1				49				143				
4	31	2	male	l	81				5				Pathology	Pathology	tear	I				0,43				24			56				7				32				5				52				131				
5	32	3	male	l	84				7				Pathology	Pathology	tear	I				0,61				33			54				8				31				4				53				130				
6	33	2	male	l	73	73	73	73	5	5	5	5	Pathology	Pathology	tear	II	II	II	II	0,76	0,76	0,76	0,76	39	39	39	39	51	51	51	51	7	7	7	7	44	44	44	44	4	4	4	4	48	49	48	48	138	138	138	138
7	35	3	male	r	72				8				Pathology	Pathology	tear	I				0,63				35			55				9				27				4				46				135				
8	36	2	male	l	92				4				Pathology	Pathology	tear	I				0,66				35			53				6				32				3				43				141				
9	36	2	male	r	87				5				Pathology	Pathology	tear	II				0,6				31			51				7				27				2				42				142				
10	37	2	male	r	91				6				Pathology	Pathology	tear	I				0,59				32			54				10				37				4				55				137				
11	41	1	male	r	73				4				Pathology	Pathology	intact	I				0,74				43			58				11				35				2				48				134				
12	42	1	male	r	93	94	93	93	7	8	7	7	Pathology	Pathology	tear	I	I	I	I	0,60	0,60	0,60	0,60	32	32	32	32	53	53	53	53	9	9	9	9	39	44	39	39	5	5	5	5	50	50	50	50	136	136	136	136
13	45	1	male	r	94				6				Pathology	Pathology	tear	II				0,66				33			50				11				34				2				48				134				
14	46	2	male	r	82				5				Pathology	Pathology	tear	II				0,6				32			53				8				35				4				50				137				
15	48	2	male	l	84				7				Pathology	Pathology	tear	II				0,60				28			47				11				36				3				45				132				
16	51	2	male	r	85	85	85	85	4	4	4	4	Pathology	Pathology	tear	II	II	II	II	0,63	0,63	0,63	0,63	30	30	30	30	48	48	48	48	8	8	8	8	41	42	41	41	3	3	3	3	46	44	46	46	137,9	138	137,9	137,9
17	52	4	male	r	82				8				Pathology	Pathology	tear	I				0,63				38			60				8				29				6				52				131				
18	53	1	male	l	78				6				Pathology	Pathology	tear	I				0,58				30			51				8				36				5				48				133				
19	57	2	male	r	80				4				Pathology	Pathology	tear	II				0,64				34			53				6				37				5				50				131				
20	57	1	male	r	83				5				Pathology	Pathology	tear	II				0,56				30			53				8				37				4				49				135				
21	29	3	female	r	74				6				Pathology	Pathology	intact	II				0,67				34			51				10				32				2				41				143				
22	34	2	female	l	82				4				Pathology	Pathology	tear	I				0,57				28			49				9				30				1				43				141				
23	34	1	female	r	80	80	80	80	4	4	4	4	Pathology	Pathology	intact	II	II	II	II	0,67	0,67	0,67	0,67	32	32	32	32	48	48	48	48	9	9	9	9	33	33	33	33	4	4	4	4	44	44	44	44	137	136	137	137
24	37	3	female	l	74				3				Pathology	Pathology	intact	II				0,79				34			43				8				31				1				38				131				
25	39	3	female	r	73	73	73	73	3	4	4	3	Pathology	Pathology	tear	I	I	I	I	0,67	0,69	0,67	0,67	30	30	30	30	43	43	43	43	7	8	7	7	32	31	31	31	4	4	4	4	42	42	42	42	130	130	130	130
26	40	3	female	r	87				6				Pathology	Pathology	intact	III				0,78				39			50				8				31				2				42				147				
27	40	1	female	r	76				3				Pathology	Pathology	intact	I				0,76				33			43				6				29				4				41				133				
28	42	3	female	l	75	75	75	75	4	4	4	4	Pathology	Pathology	intact	II	II	II	II	0,69	0,69	0,69	0,69	34	34	34	34	49	49	49	49	5	5	5	5	39	39	39	39	3	3	3	3	43	43	43	43	142	142	142	142
29	43	1	female	l	82				4				Pathology	Pathology	intact	I				0,59				28			47				8				28				3				44				132				
30	43	1	female	r	79				4				Pathology	Pathology	intact	I				0,61				30			49				9				26				4				42				134				
31	46	3	female	l	91				4				Pathology	Pathology	intact	I				0,64				31			48				9				24				4				41				145				
32	46	2	female	r	86				6				Pathology	Pathology	tear	II				0,7				31			44				8				26				5				39				138				
33	47	3	female	r	80	80	80	80	5	5	5	5	Pathology	Pathology	tear	I	I	I	I	0,69	0,69	0,69	0,69	30	30	30	30	43	43	43	43	7	7	7	7	37	38	37	37	4	4	4	4	42	42	42	42	131	131	131	131
34	48	3	female	l	91				6				Pathology	Pathology	intact	I				0,63				28			44				5				33				4				43				135				
35	49	4	female	l	82				8				Pathology	Pathology	tear	I				0,68				28			41				8				28				4				42				133				
36	51	2	female	r	78				5				Pathology	Pathology	tear	I				0,64				31			48				7				33				2				43				140				
37	51	4	female	r	73				4				Pathology	Pathology	tear	I				0,42				21			50				7				34				2				46				131				
38	53	4	female	l	82				5				Pathology	Pathology	intact	I				0,72				35			48				9				29				4				44				133				
39	53	4	female	l	81				5				Pathology	Pathology	tear	I				0,86				37			43				7				22				1				38				132				
40	54	4	female	l	84				7				Pathology	Pathology	tear	III				0,66				30			45				9				34				3				44				139				
41	54	4	female	l	82				9				Pathology	Pathology	tear	II				0,64				24			37				10				27				4				41				131				
42	55	1	female	r	73	73	73	73	5	5	5	5	Pathology	Pathology	tear	I	I	I	I	0,63	0,63	0,63	0,63	31	31	31	31	49,1	49	49,1	49,1	7	7	7	7	40	40	40	40	3	3	3	3	45	45	45	45	137	138	137	137
43	57	1	female	l	89																																														